



<https://theses.gla.ac.uk/>

Theses Digitisation:

<https://www.gla.ac.uk/myglasgow/research/enlighten/theses/digitisation/>

This is a digitised version of the original print thesis.

Copyright and moral rights for this work are retained by the author

A copy can be downloaded for personal non-commercial research or study, without prior permission or charge

This work cannot be reproduced or quoted extensively from without first obtaining permission in writing from the author

The content must not be changed in any way or sold commercially in any format or medium without the formal permission of the author

When referring to this work, full bibliographic details including the author, title, awarding institution and date of the thesis must be given

Enlighten: Theses

<https://theses.gla.ac.uk/>
research-enlighten@glasgow.ac.uk

**MORPHOMETRIC STUDIES OF AXONAL RESPONSES AFTER
TRAUMATIC AXONAL INJURY (TAI)**

AHMED MOHAMMED SULAIMAN

**MORPHOMETRIC STUDIES OF AXONAL RESPONSES AFTER
TRAUMATIC AXONAL INJURY (TAI)**

By

Ahmed Mohammed Sulaiman M.B.B.Ch, M.Sc. (Med.Sci)

**A Thesis Presented in partial fulfilment of the regulations for the
Degree of Doctor of Philosophy
at the Institute of Biomedical and Life Sciences,
University of Glasgow**

October 2005

**Laboratory of Human Anatomy
Institute of Biomedical and life Sciences
University of Glasgow**

ProQuest Number: 10391082

All rights reserved

INFORMATION TO ALL USERS

The quality of this reproduction is dependent upon the quality of the copy submitted.

In the unlikely event that the author did not send a complete manuscript and there are missing pages, these will be noted. Also, if material had to be removed, a note will indicate the deletion.



ProQuest 10391082

Published by ProQuest LLC (2017). Copyright of the Dissertation is held by the Author.

All rights reserved.

This work is protected against unauthorized copying under Title 17, United States Code
Microform Edition © ProQuest LLC.

ProQuest LLC.
789 East Eisenhower Parkway
P.O. Box 1346
Ann Arbor, MI 48106 – 1346

GLASGOW
UNIVERSITY
LIBRARY

CONTENTS

	Page No
Contents	iii
ACKNOWLEDGEMENTS	viii
SUMMARY	ix
CHAPTER ONE – INTRODUCTION	1
1. Traumatic Brain Injury (TBI) as a cause of disability	2
2. Models of Traumatic Brain Injury.	3
2.1 Types and mechanisms	3
2.2 Use of stretch-injury to the optic nerve as a model of Traumatic Axonal Injury (TAI)	9
2.3 Organisation of the mammalian optic nerve and components of the cytoskeleton in control/uninjured axons	12
Neurofilaments	13
Microtubules	16
Microtubule associated Proteins (MAPS)	16
Table 1. Microtubule associated Proteins	17
Actin	18
2.4. Nomenclature, Spectrum, and Type DAI/TAI	19
2.5. Diffuse axonal injury (DAI)	21
2.6. Primary axotomy versus secondary axotomy and the calcium hypothesis	23
2.7. Injured axons demonstrate a spectrum of pathology after traumatic axonal injury	30
3. Axonal transport.	33
3.1 Patterns of axonal transport	33
3.2 Fast Axonal transport	34
Table 2. A summary of the Five Groups of Speed of Axonal Transport	37
3.3 Motor molecules	35
Kinesins	35
Dynein family	38
Myosin	39
3.4 Slow axonal transport	40
4. Wallerian degeneration.	41
4.1. Definition	41
4.2. Sequence of events	41
4.3. The Neuronal response and the cytoskeleton	42
4.3.1. The distal segment of an injured axon	43
4.3.2. The proximal segment of an injured axon	43
4.3.3. The neuronal cell soma	46
4.4. Non-Neuronal cellular response	49
4.4.1. Macrophages	53
4.4.2. Microglia	53
4.4.3. Astrocytes	56
	60

Table 3. Secretory products and molecular signals between astrocytes and microglia	61
4.4.4. Oligodendrocytes	64
Hypothesis	66
CHAPTER TWO - MATERIAL AND METHODS.	67
1. Animals	68
2. Operation	68
Fig. 16. Schema for Stretch-Injury Apparatus	105
3. Fixation and Dissection procedures for Transmission Electron Microscopy (TEM)	72
4. Tissue processing for TEM	72
A. <i>Tissue collection and postfixation</i>	72
B. <i>Dehydration and Araldite embedding</i>	73
C. <i>Semithin sections and staining</i>	74
D. <i>Transverse thin sections and staining</i>	74
E. <i>Calibration of the transmission electron microscope</i>	75
6. Sampling Procedure	76
7. The counting method	76
8. Estimation of the cross sectional area of the optic nerve	78
A. Estimation of the total cross sectional area using a stage Micrometer	78
Fig. 17. Axes for determination of the cross-sectional area	106
B. Estimation of the total cross sectional area using a modified point counting technique	78
9. Estimation of the total area sampled in thin sections	79
10. Estimation of total number of axons in the area sampled in thin sections	79
Fig. 18. Schema for unbiased sampling method	106
11. Estimation of the total number of axons	80
12. Estimation of the cross-sectional area of axons	81
12. Statistical analysis of raw number data	81
CHAPTER THREE - RESULTS.	83
1. The cross-sectional area of the right and left optic nerves	84
2. Low magnification transmission electron microscopy	84
3. The number of axons in control (uninjured) animals	86

4. The number of intact and injured axons in the right optic erve following injury.	86
5. The number of intact axons within 0.5 μm wide bins of control optic nerve.	87
Table 4. The numbers of axons within 0.5 μm wide bins in control animals	88
6. The number of axons within 0.5 μm wide bins after injury	88
Table 5: The mean number of intact axons in 0.5 μm wide bins at one, two and three weeks after injury	89
7. Changes in the summated cross-sectional area of intact axon	90
8. Changes in the morphology of astrocyte processes	91
Summary of the results	93
Hypothesis: supported or not supported by the Results	94

CHAPTER FOUR – ILLUSTRATIONS AND FIGURES 95

Fig. 1. Relationships of the number of neurofilaments (NF) and microtubules (MT) to the diameter of an axon in control guinea pig optic nerve	96
Fig. 2. Primary Axotomy	97
Fig. 3a. Spiral microtubules	97
Fig. 3b. Non-aligned neurofilaments at an internode at 4 hours	98
Fig. 4. Transverse section to show holes in the internodal axolemma	98
Fig. 5. Longitudinal and transverse sections of nodal blebs	99
Fig. 6. Thin sections of nodes of Ranvier labelled for p-NPPase activity	100
Fig. 7. Thin sections of nodes of Ranvier labelled for Ca^{2+} -ATPase activity	100
Fig. 8. Longitudinal section at the point of Secondary Axotomy	101
Fig. 9. Involution of the internodal axolemma at 4 hours	102
Fig.10. Low and high power transverse sections for loss of microtubules and the occurrence of "intramyelinic spaces"	102
Fig.11. Transverse section for enlarged "periaxonal space", reduced spacing between or compaction of neurofilaments and loss of microtubules	103
Fig.12. Schema for kinesins	103
Fig.13. Schema for dyneins	104
Fig.14. Schema for Wallerian degeneration	104
Fig.15. Transverse section at 14 days for amorphous axonal remnants	105
Fig.16. Schema of the stretch-injury apparatus	106
Fig.17. Axes for determination of the cross-sectional area of an optic nerve	107
Fig.18. Schema for unbiased sampling method for counting axons	107
Fig.19. Example of the structure of axons from a control animal within a single counting frame	108
Fig.20. Example of the appearance of axons at 1 week survival	109
Fig.21. Example of a counting field at the sampling magnification at 2 weeks	110
Fig.22. Two fields of detail to illustrate types of axonal pathology at 2 weeks	111
Fig.23. Example of a counting field at the sampling magnification at 3 weeks	112
Fig.24. A higher magnification area to show pathology at 3 weeks	113
Fig.25. Bar graph of the number of intact and injured axons in control, 1 week, 2 week and 3 weeks survivals	114
Fig.26. Line graph of the number of intact axons at different survival	114

Fig.27. Line graph of changes in number of intact axons within 0.5 μ m wide bins in controls and 1,2 and 3 week survivals	115
Fig.28. Changes in cross-sectional area of the number of intact axons within 0.5 μ m wide bins in controls and 1,2 and 3 week survivals	115
Fig.29. Changes in the proportion of intact axons within different bins in controls and 1, 2 and 3 week survivals	116
CHAPTER FIVE - DISCUSSION	117
1. Changes of Cross-Sectional Area of the Optic Nerve	118
a) Contribution by myelinated fibres to the cross-sectional area of control optic nerve	118
b) Evidence for glial activation	121
2. Novel information about axonal pathology	123
3. Numerical distribution of axons in control/sham animals	125
4. Changes in the Number of Intact Axons within Different Sized Bins after Injury	126
Table 6. Percentage of Control Numbers of Intact/Normal Axons after Injury	128
5. Consideration of Mechanisms of Axonal Cytoskeletal Responses	129
6. Evidence of Wallerian Degeneration	123
7. Hypothetical Mechanisms for Compaction of Neurofilaments	135
CHAPTER SIX - BIBLIOGRAPHY	140
CHAPTER SEVEN - APPENDIX	194
Table 7. Raw data for the total cross sectional area (μm^2) of optic nerves	195
Table 8. Sham-control, animal one	196
Table 9. Sham-control, animal two	197
Table 10. Sham-Control, animal three	198
Table 11. The mean estimated number (n = 3), total (\pm SEM) and subgroups of intact axons in sham-controls	199
Table 12. One week survival, animal one	200
Table 13. One week survival, animal two	201
Table 14. One week survival, animal three	202
Table 15. One week survival (n =3): Mean estimated number, total (\pm SEM) and subgroups or bins of intact axons	203
Table 16. Two weeks survival, animal one	204
Table 17. Two weeks survival, animal two	205
Table 18. Two weeks survival, animal three	206
Table 19. Two weeks survival (n =3): Mean estimated number, total (\pm SEM) and different number in subgroups or bins of intact axons	207
Table 20. Three weeks survival, animal one	208
Table 21. Three weeks survival, animal two	209
Table 22. Three weeks survival, animal three	210

Table 23. Three weeks survival (n = 3): Mean estimated number, total (\pm SEM) and subgroups or bins of intact axons	211
Table 24. The mean estimated (n = 3), total and sub-groups in sham-control and one week, two weeks, and three weeks survivals	211
Table 25. Number of axons (injured and intact) in each sample	212
Table 26. Total estimated number of axons (normal \div injured) (n = 3) at one, two and three weeks survivals	213
Table 27. Estimated mean cross-sectional area of the number of axons within 0.5 μ m wide bins in each experimental group	213

ACKNOWLEDGEMENTS

I am very grateful to William L Maxwell Ph.D., D.Sc. for acting as supervisor during the period of my studies. I should like to express my deep appreciation to him for his continued support, invaluable and constructive criticism and advice throughout the period of study and draft form of the manuscript of this thesis.

I am very grateful to Professor A.P. Payne of the Laboratory of Human Anatomy, IBLS, at the University of Glasgow for his support and help in solving many difficulties, and his encouragement during my period of study.

I am very grateful to Professor D.I. Graham of the Unit of Neuropathology, Southern General Hospital for his help.

I would like to express my deep appreciation of the technical help provided by Mr Andrew Lockhart, by Mr David Russell for his technical help and advice in cutting thin sections, and Ms Mary-Anne MacKinnon for her help .

I extend many thanks to all IBLS staff for their willingness to offer help and advice whenever required, and for providing a friendly environment within which to work.

I am very grateful to Mr David McLaughlin and staff of the Veterinary Research Facility at the Garscube Estate, University of Glasgow for the provision of operating theatre facilities and their help during operations.

Finally, I would like to appreciate the encouragement of all members of my family, with especial thanks to my mother, my wife and children Taha, Shahed, Yasin, Shada, and Mohammed.

SUMMARY

The optic nerve of adult guinea pigs contains $99,005 \pm 9,199$ ($n=3$) myelinated axons. Earlier studies have shown that axons of different diameters within $0.5\mu\text{m}$ wide numerical bins respond in different ways up to 7 days after traumatic axonal injury (TAI). The present study tested the hypothesis that such differential responses may continue over 3 weeks after TAI to result in a differential loss of intact or healthy axons. Stereological techniques were used to obtain estimates of the total number of intact axons, those lacking any morphological evidence of pathology. The number of intact axons fell from 99,005 to 74,845 at 1 week, to 66,744 at 2 weeks and to 55,696 at 3 weeks. However, statistically significant numerical differences and ultrastructural evidence for loss of axons via Wallerian degeneration were obtained only at 3 weeks after TAI.

A novel finding was that a few axons possessed intact cytoskeletal components within an electron dense axoplasm limited by an intact axolemma at 2 and 3 weeks after TAI. This finding was suggestive of a loss of axonal calibre. Estimates of the number of intact axons within different sizes of bin showed that the bin size containing the highest number of axons fell from a diameter of $1.5\text{-}2.0\mu\text{m}$ in controls to $1.0\text{-}1.5\mu\text{m}$ at 1 and 2 weeks, and to $0.5\text{-}1.0\mu\text{m}$ at 3 weeks after TAI.

It is concluded there is both a loss of number and a previously unreported loss of calibre of axons after TAI in the CNS. Moreover, morphological evidence for Wallerian degeneration occurred only at 3 weeks after injury. As a result, the time course of loss of axons after TAI differs markedly from that described either in the PNS or after crush injury in the CNS.

CHAPTER ONE
INTRODUCTION

1. Traumatic Brain Injury (TBI) as a Cause of Disability.

Neurotrauma is a major public health problem. The incidence varies from 67 to 317 per 100,000 world-wide in different countries. Mortality rates are approximately 1% after minor injury, 18% after moderate injury, and 48% after severe head injury (Armando et al., 2001).

According to the Center for Disease Control (CDC), Traumatic Brain Injury (TBI) is a "silent" epidemic. There are some 2 million cases of TBI per annum in the U.S.A., of which around 500,000 require hospital admission. TBI is the cause of death of 50,000 patients per annum and of non-lethal but significant disabling injuries in a further 70,000-90,000 patients each year (Laurer et al., 2000; Thurman et al., 1999; CDC 2001). In the European Union, brain injury accounts for one million hospital admissions per year. Within the United Kingdom there are 1,000,000 cases a year attending Accident and Emergency and 100,000 patients are admitted to hospital. Of those, some 10,000 patients a year are transferred to neurosurgical units for specialist attention. In the U.K., road traffic accidents (RTA) give rise to 50% of serious head injuries, falls 30% and assaults 10% (Andrew et al., 2001).

But TBI is not a problem limited to the developed world. In economically fast developing countries, TBI is a growing problem. For example, in India 1.5 to 2 million persons are injured and 1 million succumb to death every year. Again, road traffic accidents are the leading cause (60%) of TBI followed by falls (20-25%) and violence (10%), (Gururaj, 2002). In those countries of the world in which increased economic development provides improved transport and personal or individual mobility the requirement for rehabilitation of brain-injured patients is high and is increasing from year to year. Developed and developing countries face major

challenges in prevention, pre-hospital care and rehabilitation in their rapidly changing environments to reduce the socio-economic burden of TBIs.

Moreover, evidence is beginning to accumulate that the types of injury currently referred to as mild traumatic brain injuries (mTBI) where a patient may not even lose consciousness at the time of injury, may result in long term deterioration, a reduced performance in the work environment and problems in interpersonal interactions (Hellawell et al., 1991; Hawley, 2003).

Finally, distinction should be made between injuries to patients that either give rise to space occupying lesions that may be readily identified using computerised tomography (CT) and develop over a short time scale, for example development of either extra-cerebral or intra-cerebral haemorrhage. And injuries that do not form space-occupying lesions and provide no evidence of injury using CT but are indicated by a Glasgow Coma Score of 8 or less. The clinical syndrome of diffuse axonal injury (DAI) is used to refer to such a condition. However, a definitive diagnosis may only be made post mortem upon neuropathological examination.

2. Models of Traumatic Brain Injury

2.1. Types and mechanisms

Good experimental design should be directed toward standardization to minimize variability and obtain maximal consistency. Within animals, major problems may result from variation in the level of injury, strain, different responses related to the gender of a subject and the anaesthetic agents used. Using animal models for study of pathology in humans is not without risk and any potential pitfalls should always be recognised and care taken to reproduce clinically relevant injury

responses that, as closely as possible, parallel what happens to and in the human brain after trauma. Traumatic brain injury (TAI) is now the preferred term used to refer to injuries in animal models (Maxwell et al., 1997). TBI is a result of both direct, immediate mechanical disruption of brain tissue, the primary injury; and indirect, delayed or secondary injury mechanisms. The primary damage occurs at the time of injury or mechanical insult and takes the form of surface contusions, lacerations or diffuse vascular and/or axonal injury (DAI). The latter is wide spread or diffuse mechanical damage to axons in the central white matter of the brain that may result in tearing, or in biomechanical terms shearing, of a number of axons scattered widely among a larger population of uninjured, morphologically intact axons. The overall incidence of primary injury in humans has been somewhat reduced in recent years by the use of preventive measures, such as advances in safety education, use of safety equipment (airbags, helmets), and the enforcement of laws enhancing individual and public safety.

Secondary mechanisms, on the other hand, have a delayed onset and progress over hours to days and months after the initial trauma. Examples include intracranial haemorrhage, brain swelling, raised intracranial pressure (ICP), hypoxic brain damage among other types of pathology (Adams, 1980; Lighthall et al., 1989; Povlishock et al., 1994; Gennarelli, 1994; Teasdale et al., 1999; Laurer and McIntosh, 1999; Graham et al., 1993, 2000; Thompson et al., 2005). In addition, due to the time course indicated above, secondary injuries are potentially amenable to post-injury therapeutic intervention.

The present experimental models of traumatic brain injury may be classified into three general groups: mechanical impact to the head, head acceleration and direct deformation of the brain. The characteristics of TBI are associated with complex

processes including, but not limited to, static and dynamic loading. Static loading occurs when gradual forces are applied to the head, usually through a slow process (Gennarelli, 1994). This mechanism of TBI is quite uncommon in the clinical setting, but may occur when the head is exposed to a heavy weight (such as the head being trapped underneath a wheel of a car). The more common type of mechanical input causing TBI, dynamic loading, is associated with a rapid acceleration/deceleration of the brain and the duration of this loading has proven to be a significant factor in determining the severity of TBI (Stalhammer, 1986; Gennarelli et al., 1993). Dynamic loading can be classified into two types, a) impulsive or b) impact loading. The former occurs when the head is set into motion impulsively or when the head is brought to a sudden rapid stop without being struck, leading to inertial forces within the brain, which produce the injury. Impact injury occurs when a blunt object strikes the head (or *vice versa*) and is usually associated with both contact and inertial forces (Smith et al., 2000). Both types of TBI produce tissue strain (the amount of deformation experienced by the tissue due to the forces applied against it) and the amount of this strain is a relevant biomechanical factor that influences outcome (Graham et al., 1995). Penetrating TBI is associated with armed combat and/or inner city violence and is most commonly caused by gunshots (missile wounds). Injury severity in these cases depends on several factors, such as the mass, shape, direction of travel through the head and velocity of the missiles as well as the different properties of the human skull at the location of impact.

Further to the above, any experimental model designed to reliably reproduce the clinical sequelae of TBI should fulfil a number of criteria. These include an ability to precisely modify the severity of injury and the response must be quantifiable and reproducible between different investigators and laboratories (Povlishock et al., 1994;

Teasdale et al., 1999) and replicate the type(s) of severity and injury in man. Ideally, the damage produced should be part of a continuum, increasing in severity as the mechanical forces applied are increased (Lighthall et al., 1989; Povlishock et al., 1994; Teasdale et al., 1999; Graham et al., 2000).

Most experimental TBI models currently employ standardized experimental protocols including the use of sham (uninjured) animals, which undergo identical surgical treatment without receiving TBI, and allow for the control of systemic variables such as the influence of the anaesthesia, operative procedure, head restraint, and physiological parameters. Additionally, most but not all trauma devices designed to produce TBI in rodents now employ computer-based measurements of the applied load (pressure gradients, impact or velocity, etc.), which allow the investigator(s) to make precise adjustments to the device to achieve a controlled range of severity of injury within a particular study. Further, in an attempt to mimic the range of severity of human TBI, injury models must be capable of producing brain trauma over a wide spectrum of severity, a task typically accomplished by adjusting the mechanical parameters of the injury device (Lighthall et al., 1989). A number of studies have revealed a close relationship between severity of injury, posttraumatic responses, induction of coma and the rate of recovery of brain-injured animals (Gennarelli, 1994; Laurer et al., 1999; Smith et al 2000). As a result, a classification for severity of experimental TBI comparable to the clinical categories of mild, moderate, and severe human TBI. But the mechanical, physiological and environmental conditions that result in human TBI are much more variable than are obtained in laboratory models where, generally, the insult is a single one and the conditions under which the insult is delivered is carefully controlled. Therefore, different injury models need to be employed to reproduce the spectrum of characteristics seen in human TBI, including

focal and/or diffuse damage since no animal model, except, perhaps, the primate head acceleration model (Gennarelli et al., 1982), reproduces the combinations of types of injury that occur in human TBI.

Focal injury due to impact injuries, skull fractures, or following penetrating TBI (Graham et al., 1995) has been observed in patients and include extradural haematoma, subdural haematoma, intracerebral haematoma, cerebral contusions, and coup contrecoup damage. In human TBI focal injuries and/or pathology usually occur in the direct vicinity of the mechanical impact to the head and, at relatively mild levels of injury involves primarily the cortical mantle. Injuries are surface contusions (when the pia mater remains intact) and lacerations (when the pia is torn). These may or may not be accompanied by skull fracture or development of a haematoma (McIntosh et al., 1989; Laurer et al., 1999). At injuries of greater severity damage to subcortical structures, for example the underlying white matter, thalamus and basal ganglia may result in multi-focal injuries (Laurer et al., 2002).

On the contrary, diffuse axonal injury (DAI) is believed to occur from widespread tissue distortion, or shear, resulting from inertial forces acting at the time of injury (Gennarelli, 1993; Pettus et al., 1994; Graham et al., 2000). However, DAI is only one of four main pathologies induced by the above biomechanical conditions, the other three being diffuse vascular injury, diffuse hypoxic brain damage, and diffuse brain swelling due to an increase in the cerebral blood volume or the water content of the tissue of the brain. Diffuse vascular injury has the worst outcome of the four with the occurrence of multiple small haemorrhages within the white matter that often result in the immediate death of the patient (Tomlinson, 1970; Graham and Gennarelli, 2002). DAI often does not result in death in the short term, but wide spread destruction of white matter tracts during the post-traumatic episode is an important contributor to the

disabilities that patients who survive DAI experience (Hurley et al., 2004). Traumatic axonal injury is identified by morphological change in axons after injury only able to be seen by immunolabelling microscopy. There is a progressive occurrence of swellings and axonal bulbs over hours to days, and many studies have allowed generation of the hypothesis that development of this pathology is an ongoing process (Maxwell et al., 1997; Hurley et al., 2004).

It is generally believed that the number of injured axons occurring in DAI/TAI is a critical determinant as to whether patients die, remain vegetative, are severely or moderately disabled following blunt head-injury (Adams et al., 1999, 2000, 2001, 2003; Meythaler et al., 2001; Graham and Gennarelli, 2002). Both experimental and clinical studies have shown that initial mechanical forces applied over a short time scale may injure axons and lead to a focal impairment of axonal transport over several hours. This leads to the formation of axonal swellings, followed over hours or days by axonal disconnection (Maxwell et al., 1997; Povlishock, 2000). However, not all traumatically injured axons necessarily go on to swell and/or disconnect (Stone et al., 1999).

2.2 Use of Stretch-injury to the optic nerve as a model of traumatic axonal injury (TAI)

Since the first pathological characterization of TBI in the middle of the last century (Strich, 1956; Peckless and Rewcastle, 1967), investigators have attempted to establish and characterize clinically relevant laboratory models of TBI using primates, dogs, sheep, rabbits, cats, and, in particular, rodents. However, due to the marked heterogeneity of human TBI, no one model has yet reproduced the entire spectrum of injuries that occur in DAI as originally defined (Adams et al., 1989). In addition, in patients, injuries to the brain are never "identical". Injuries vary as to their cause, location within the brain, and severity. As a result, diagnosis and treatment is difficult. Several animal models have been developed, but each only replicate specific distinct characteristics of human TBI.

In human head injury where a space occupying lesion does not occur, widespread or diffuse damage to nerve fibres in central white matter is often the major type of injury and is, for example, diagnostic for diffuse axonal injury (DAI) (Adams et al., 1989). The optic nerve stretch-injury model was developed in the later 1980's to allow study of the development of pathology after injury in pure white matter where axons alone are damaged since the majority of animal models –*vide supra* include mechanical injury to both cortical grey matter and white matter in the medulla.

The optic nerve was selected because it is the only part of the CNS where central, myelinated nerve fibres may be accessed without also injuring overlying grey matter. The model was designed to improve understanding of the initial responses of axons in central white matter after transient loading such as occurs in acceleration/deceleration injuries where impact to the head does not happen, for example DAI. In this model, transient (19-21 msec duration) mechanical loading is applied to the mobilized optic

nerve by placing a sling around the globe and applying a load of 200-250g to the nerve along the longitudinal axis of the optic canal (Gennarelli et al., 1989). This model was initially developed using guinea pig but has more recently been refined to allow use in mice (Saatman et al., 2003).

At the loadings indicated above, early quantitative analyses demonstrated that only 17% of the total number of axons within the optic nerve (Gennarelli et al., 1989) is injured. The damaged axons increased in diameter and there was metabolic derangement in the soma of retinal ganglion cells (RGC) over the 12-24 hours following injury. This model also provided, first, evidence for post-traumatic depolarization in the entire optic nerve that extended over 24 hours in more than 60% of experimental animals, and up to one week in over 40% of animals (Tomei et al., 1990). Loss of RGC was later shown to occur between 7 and 14 days after injury (Maxwell et al., 1994).

Importantly, however, ultrastructural analysis of the development of pathology within injured axons has been key in the development of the concept of secondary axotomy (Maxwell et al., 1993, 1995, 1997; Jafari et al. 1997,1998). Secondary axotomy is now accepted as the mechanism whereby injured axons undergo disconnection over hours after injury (Blumberg, 1995), the de-afferentation of these neurons (Povlishock, 1992, 2000; Povlishock et al 1983; Povlishock and Christman 1995) and provides an explanation as to why head-injured patients may only be confused or disorientated immediately following injury but descend into coma over the following 72-96 hours.

A variety of ultrastructural techniques has been applied to the stretch-injury model. These studies have provided quantitative evidence for structural and functional alterations at the axolemma at nodes of Ranvier and internodes (Maxwell, 1996;

Maxwell et al., 1990, 2003), an abnormal accumulation of free calcium in the axoplasm of injured fibres (Maxwell et al., 1995, 1999), and a widespread swelling of mitochondria with loss of their cristae (Maxwell et al., 1995). Within ten to fifteen minutes, there was also loss of axonal microtubules (Maxwell and Graham, 1997). Later, there was development of foci of an increased packing density of neurofilaments (Jafari et al., 1997; 1998; Maxwell et al., 2003), also termed neurofilaments compaction (Pettus and Povlishock, 1996), and a loss of organization of the myelin sheath. Finally, foci of dissolution of the axolemma and compaction of neurofilaments occurred at the site at which an injured axon had disconnected or undergone secondary axotomy (Jafari et al., 1997, 1998; Maxwell et al., 1997, 2003). However, perhaps most importantly, together with the fluid percussion model (Thompson et al., 2005), the stretch-injury model has provided incontrovertible evidence for a time course extending to a minimum of several hours in experimental animal models and 12 hours in humans (Christman et al., 1994) before axonal disconnection occurs after TAI.

The optic nerve stretch injury model is unique because the force applied and the time course is precisely measured during injury; is delivered only to central white matter and force is applied only along the longitudinal axis of the axons. A major advantage is that the model is "clean" in the sense that the only part of a neuron injured is the axon. It thereby eliminates complications such as excitotoxic post-traumatic insults. Further, the guinea pig optic nerve does not possess a central artery so that the influence of toxic components of blood following haemorrhage is eliminated. It is hypothesised that the resulting axonal damage is similar to that which occurs early in diffuse, central white matter injury in humans but may not be shown since the axonal damage happens prior to patient arrival at hospital. Moreover, the

model offers the possibility of improving our understanding of traumatic damage in central nervous system axons as it generates reproducible axonal injury at a well-defined anatomical location where the extent and the type of the damage may be easily identified. The model thus eliminates many problems associated with studying damaged axons within the complex structure of the brain. However, secondary effects such as hypoxia still need to be addressed.

2.3 The Organisation of the Mammalian Optic Nerve and the components of the Axonal Cytoskeleton in Control/Uninjured Axons.

The optic nerve is formed by the axons of retinal ganglion cells and by glial cells. It is enveloped by a connective tissue sheath that is a continuation of the meningeal membranes that surround the brain within the cranium and capillaries from the ciliary arteries.

The optic nerve has postchiasmatic, chiasmatic and prechiasmatic parts. The prechiasmatic segment lies between the posterior of the globe and the chiasm and according to its location, is subdivided into intra-ocular, intra-orbital and intracanalicular parts. In the guinea pig optic nerve the prechiasmatic portion is about 12-15mm in length (Gennarelli et al., 1989; Jafari et al., 1997).

The human optic nerve contains about 1 million nerve fibres. The number of axons in the optic nerve of horse (*Equus equus*) is 481,000 (Guo et al., 2001), that of buffaloes (*Bos bubalis*) is 1.5 million (Kassab et al., 2002), that of rabbit (*Oryctolagus cuniculus*) is 294,000 (Robinson et. al., 1987), for cat (*Felix domestica*) is 112,000 (Stone and Campion, 1978), for monkey (*Macaca papio*) is 1.2 million (Sanchez et al., 1986) and for the guinea-pig (*Cava*) about 97,000 (Guy et al., 1989).

Most CNS axons with a diameter greater than $0.2\mu\text{m}$ are myelinated (Bunge et al., 1967). All axons of the guinea-pig optic nerve are myelinated (Guy et al., 1989) and surrounded by compact lamellae formed from the plasmalemma of oligodendrocytes that is helically wound, tightly around the axons. At the most basic level the structure of the myelinated axon in both central (CNS) and peripheral nervous systems (PNS) is similar. The thickness of the myelin sheath increases with the diameter of the axon (Guy et al., 1989), and provides optimal insulation to keep current leakage to a minimum that allows saltatory conduction of the action potential.

The ratio of the diameter of the axon to the diameter of the myelin sheath is expressed as the g ratio. The g ratio for guinea pig optic nerve is 0.81 (Guy et al., 1989). In the internode region of fibres in the optic nerve the cross-sectional profile of an axon is nearly circular when cut in perpendicular transverse section. The circularity of an axon is determined by the parameter \varnothing . This is defined as the ratio of the axonal area to the area of the circle having the same circumference as that axon (Arbuthnott et al., 1980). When \varnothing has a maximum value of 1.0 the axon is truly circular and the value of \varnothing decreases as circularity is reduced.

The morphology of individual axons is strongly associated or linked to the structure of its axonal cytoskeleton that consists principally of neurofilaments, microtubules, actin, and fodrin (Bryan et al., 1976; Heidermann et al., 1984; Bretcher et al., 1991; Chen et al., 1999; Gallant et al., 2000; Yang et al., 2004). Microtubules and neurofilaments are organised into an interacting network that extends from the cell body at the axon hillock to the tips of the axon to provide the structural framework that defines the axon's three-dimensional shape.

Neurofilaments are a type of intermediate filament that occurs only within neurons. They are 10nm thick, un-branched, and run longitudinally in the axons and

form bundles that play a role in the maintenance of the shape and integrity of the axon (Griffith and Pollard, 1982; Hoffman et al., 1984). Neurofilaments are primarily composed of three subunits, (NF-H, NF-M and NF-L) and each has a different molecular weight (NF-L = 60 kDa, NF-M (100 kDa and NF-H (115-120 kDa) (Hisanaga et al., 1991; Shaw 1991). The above are formed by complexes of some five or six neurofilaments subunits of which six have been sequenced for their amino acid content (vimentin, peripherin, α -internexin, NF-L, NF-M and NF-H) (Shaw, 1991; Fliegner et al., 1990). Each filament visible at intermediate to high magnification in thin sections, however, is composed of a complex of NF-L, NF-M and NF-H which form a central core 10-12nm in width (Gotow et al., 1994) possessing an intrinsic axial periodicity of 22nm (Brown et al. 1997). From the central core project thinner filaments, composed of the C-terminal domains of NF-M and NF-H and termed "side-arms". Side-arms extend regularly and bilaterally from the core and are thought to help to maintain a constant spacing between core filaments of between 40 and 60 nm by forming the so-called "cross bridges". The mechanisms whereby interneurofilament spacing is maintained, however, are still controversial (Kumar et al., 2002a, b). In addition, larger myelinated fibres contain a higher number of neurofilaments than microtubules and even within the same axon they are not uniformly distributed throughout the axoplasm (Reles and Friede, 1991). Maxwell (1996) and Jafari et al. (1998) provided specific evidence for nerve fibres of the guinea pig optic nerve. The number of neurofilaments in control axons increases more rapidly (slope = 117.57; $r^2 = 0.94$) with increasing axonal size than does the number of microtubules (slope = 29.68; $r^2 = 0.86$) (Fig. 1, page 96).

There are three, current hypotheses for the nature of the interactions between neurofilaments: - there is either

(a) An interaction between side-arms through binding or cross-bridges mediated either by the side-arms themselves or by accessory factors

Or

(b) The side-arms of neurofilaments are negatively charged. As a result they repel one another through direct, colloidal electrostatic forces

Or

(c) The side-arms form a polymer brush-like layer around the core of a neurofilament and repulsion between neighbouring filaments occurs through mutual steric exclusion.

Current thinking centres on a mutual repulsive mechanism that may, in part, be related to the intrinsic charge within neurofilament side-arms that are unstructured polyelectrolyte chains (Kumar et al., 2002b). These are thought to have a fractional charge, the ratio of anionic to cationic residues, of 0.067 in normal axons. The fractional charge results from maximal phosphorylation of the side-arms which occurs upon myelination through, at least in part, the direct influence of myelin associated glycoprotein (MAG) that is localized at the glial-axolemma interface (Trapp et al., 1989; Kumar et al., 2002a). Dephosphorylation of NF side-arms has been promulgated (Povlishock et al., 1997) as a mechanism for NF compaction following TBI. Such dephosphorylation may result in a loss of fractional charge by individual NFs, a correlated reduction of the repulsive forces between NFs and result in reduction in NF spacing. Since NFs are phosphorylated within the internode (Mata et al., 1992) it might be expected that dephosphorylation/NF compaction occurs principally within the internode. Stereology provides strong support for that hypothesis (Jafari et al., 1997, 1998; Maxwell et al., 2003). However, the controversy about the precise mechanism of the control of spacing between

neurofilaments in normal, uninjured axons makes detailed consideration of changes under conditions of pathology currently unrewarding.

Microtubules (MTs) are another important element of the cytoskeleton that provides a system for transport of membrane bound organelles either toward the axon terminus (anterograde) or cell soma (retrograde). Microtubules are composed of proteins, α and β tubulins, which form a tube. The protein assemblies resemble strings of beads wrapped in a spiral around an invisible core. The tubes are 25 nanometers(nm) in diameter with a 15nm diameter hollow core. Tubules range in length from 200 nm to 25 micrometers. Within axons, MTs are strictly orientated with the tyrosinated portion of α tubulin located at the so-called plus end. This is the site of microtubule assembly and elongation, through interaction of monomers and oligomers of tubulin (Bass et al., 1993; Simon et al., 1998). In axons, the plus end is always more distant from the cell body than the so-called negative end at which MTs may undergo disassembly. MTs are longitudinally orientated within the axoplasm either singly or in groups termed bundles. Early work showed that microtubules in neurons and other types of cells differ in their behaviour and physiology being subdivided into cold and or drug labile and stable subtypes (Olmsted and Borisy, 1975; Weisenberg, 1972).

Microtubule associated proteins (MAP) are a group of high molecular weight > 200 kDa, (Francon et al., 1982) and a lower molecular weight proteins (55-65 kDa in CNS, 110 kDa in PNS) (Cleveland et al., 1977; Goedert et al., 1992; Couchie et al., 1992). A variety of MAPs (MAPs 1-5 and tau) have been described, the isomers, localisation and functions of these proteins are summarised in Table 1.

Table 1: Microtubule Associated Proteins (MAPs)

Type	Isomers and molecular weight	Function and/or Location
MAP1	MAP1A 350kDa	Phosphorylated during neurite outgrowth and glia; major component of MT sidearms in axons
	MAP1B 320kDa	Neurons (phosphorylated form in axons and unphosphorylated in dendrites) (Sato-Yoshitake et al. 1989) and glia. Major component of MT sidearms in axons
	MAP1C/cytoplasmic dynein 310kDa	retrograde axonal transport
MAP2	MAP2a, MAP2b 280kDa	Microtubule assembly and stabilization in dendrites
	MAP2c 70kDa	Present in (developing) axons (Tucker et al 1988)
Tau	55-62kDa	Axons and glia
MAP3	180kDa	Microtubule assembly in NF rich axons (Huber et al. 1985, 1986) and glia during development
MAP4	210kDa	Astrocytes and oligodendrocytes (Parysek et al, 1985)
MAP5	320kDa	Microtubule assembly in immature brain

MAP2 is normally restricted to the somatodendritic parts of neurons (reviewed in Brandt, 1996) while tau is restricted to axons. Tau is composed of proteins closely related to MAP and forms periodic arm like projections from the surface of microtubules where it may be a component of the short cross-bridges that link bundles of microtubules within axons. It is thought that tau promotes polymerization of tubulin, formation of bundles of microtubules by cross-bridges, has a role in growing and maintaining nerve cell axonal processes *in vivo* (Hirokawa, 1991; Mandelkow and Mandelkow, 2002; Mandelkow et al., 2003) and can regulate the transport of cell components by molecular motors along microtubules (Ebner et al. 1998).

Experimentally, when levels of tau are increased above normal cellular levels, for example by transfection, anterograde transport along microtubules is inhibited while retrograde transport is maintained. This results in accumulation of vesicles and membranous organelles within the cell soma of a transfected cell (Mandelkow et al., 2003). Thus, the axonally located MAP tau is intrinsic to the maintenance of anterograde axonal transport.

Conventional **Actin** is a self-assembling 43 kDa protein with a single nucleotide binding site and one high affinity divalent metal, usually Mg^{2+} , ion binding site. Members of the actin family have well-characterised cytoskeletal functions but in the early 1990's it was realised that conventional actin is a member of a much larger group of **actin-related proteins** that have roles in actin polymerization, dynein motor activity, and remodelling of chromatin and/or transcription (Goodson and Hawsc, 2002). The present discussion will refer only to the cytoskeletal Actins currently recognised in axons of myelinated, mammalian nerve fibres. Actin exists in two forms in an equilibrium governed by the interaction of G-and F-actin with profilin and gelsolin in most animal cells. All of these have been documented in neurons (Blikstad et al., 1980; Nishida et al., 1984; Yin et al., 1981). Actins filaments are essential for maintaining the structural integrity of bundles of MT's since actin can provide bridges from one MT to another (Fath et al., 1994; Bearer et al., 1999) and when actin is depolymerised movement of organelles decreases (Hasaka et al., 2004).

Actin also contributes to the subaxolemmal cytoskeletal network. It interacts with other cytoskeleton proteins to form the spectrin-ankyrin-actin network. This network is thought to play an important role in maintaining the integrity of certain specialised regions of the axolemma such as nodes of Ranvier, paranodes and juxta-paranodes

where the spectrin/fodrin complex participates in anchoring a variety of ion channels and membrane pumps (Ichimura et al., 1991).

2.4. The Nomenclature, Spectrum, and Types of DAI/TAI.

Since the first observation of neuropathology in non-impact head injury (Strich, 1956) several different names have been used to refer to the clinico-pathological scenario now referred to as Diffuse Axonal Injury (DAI), (Adams et al., 1989). For example, shearing injury (Strich, 1961), diffuse damage to white matter of immediate impact type (Adams et al., 1977), and diffuse white matter shearing injury (Zimmerman and Gennarelli, 1978). However, Adams et al., (1989) used a number of criteria to define Diffuse Axonal Injury and that name has received worldwide recognition and acceptance. Three grades of DAI have been characterised. Grade 1 in which there is widespread damage to axons in the white matter of the cerebral hemispheres. Grade 2 where, in addition to the above, focal haematogenous lesions occur in the splenium of the corpus callosum. And Grade 3 in which, in addition to the above, there are haemorrhagic lesions in the rostral portion of the brain stem (Adams et al., 1989), most frequently in the corticospinal and medial lemniscus tracts.

At the level of individual axons within the central white matter, the severity of such trauma varies from the most severe with immediate tearing or fragmentation, or in biomechanical terms shearing, of axons, to a mild type in which there is diffuse damage but not immediate loss of continuity of axons. However, there is now wide acceptance of the hypothesis that those axons enter a pathological cascade of events stimulated by the loss of ionic homeostasis. The latter results in the uncontrolled influx of Na^+ and Ca^{2+} which allows development of the ensuing pathology to result in axonal disconnection over, perhaps, tens of hours following the initial mechanical

insult. This type of injury is now accepted to be the commonest pathology in patients with brain trauma ranging from mild concussion to DAI (Medana and Esiri, 2003). However, pure DAI are not encountered very often in patients and is frequently associated with coup/contra-coup contusions. In its mildest form, there is no visible macroscopic evidence of injury, for example a space-occupying lesion such as an intracranial or petechial haematoma, and evidence for axonal injury may only be obtained through microscopic examination post-mortem.

Recently, it has been suggested that non-disruptive axonal injury may occur even when a patient does not lose consciousness but may only be confused for a short period, for example, after a sports injury (Biasca et al., 2005). Under the above conditions non-disruptive damage to central white matter axons may be the key, initial step in the development of post-traumatic deterioration resulting in behavioural and social problems in survivors of mild TBI (Hawley, 2003; Hellowell et al., 1999).

A widely used, clinical criterion for the classification of severity of head-injury in Accident and Emergency Departments is the Glasgow Coma Scale (GCS) (Teasdale and Jennett, 1974). However, the GCS is only a measure of whole organ function of the brain and does not serve to indicate which type of injury or insult to axons has occurred. The GCS requires assessment of a patient's response to tests for 1) motor response 2) verbal response and 3) opening of the eyes. If a patient achieves a GCS score of 13-15 without a history of loss of consciousness, a mild head injury has been experienced. When a GCS of 9-12 is found the patient has experienced a moderate head injury, and with a GCS of 8 or less a severe head injury.

2.5. Diffuse axonal injury

The concept of diffuse brain damage is not new. It has been recognised since the early work of Denny-Brown and Russell (1941). Before the application of immunocytochemistry, numerous reports of diffuse abnormalities of axons with an irregular profile were demonstrated using the Palmgren silver staining technique and allowed identification of so-called 'retraction balls or bulbs' in paraffin embedded material obtained systematically from the brain (Adams et al., 1989). The clinical term diffuse axonal injury (DAI) has been recognized and established since the early 1990's (Adams et al., 1989).

More recently, use of immunocytochemical markers for axonal injury –*vide infra*– identifies or labels damaged axons within 35 minutes (Gorrie et al., 2002) and shows that damaged axons occur in the internal capsule, parasagittal white matter, corpus callosum, corona radiata, cortical medulla and the brain stem (Gorrie et al., 2002; Wilson et al., 2004). But, diagnosis of DAI may only be achieved post-mortem, and *in vivo* is based on exclusion criteria alone where its occurrence is inferred in post-traumatic coma patients that have no evidence of a detectable intracranial lesion in CAT scans (Niess et al., 2002). It is now accepted that DAI is the most common cause of post-traumatic coma in the absence of intracranial mass lesions.

Recently, more sensitive, immunocytochemical techniques have been developed and widely accepted for diagnosis. For example, damaged axons are labelled with antibodies against light neurofilaments (NF-L/SMI 32) (Grady et al., 1993; Christman et al., 1994; Saatman et al., 2003), compacted neurofilaments (RMO-14) (Stone et al., 1999, 2001) or ubiquitin (Gultekin and Smith, 1994). However, the use of antibodies labelling beta amyloid precursor protein (β -APP) seems to have been the most widely adopted for diagnostic or clinical purposes. Moreover, importantly,

immunocytochemical techniques have demonstrated that damaged axons are probably far more widespread and numerous in patients than the use of the Palmgren Silver technique ever indicated. When axonal damage was first recognised or accepted as being a direct result of trauma to the brain, the understanding was that axotomy occurred at the time of injury and the observed pathology occurred in separated fragments of nerve fibres following axotomy (Povlishock, 1983). The early finding of swollen, terminal axonal profiles in the early or short posttraumatic period, that is to say one to several hours after injury, gave the impression that all damage was inflicted upon the axon at the time of the biomechanical insult and an immediate loss of axonal continuity resulted. Continued axonal transport on either side of the site of fragmentation lead to swelling of the adjacent parts of the injured axon and resulted in the formation of so-called retraction balls (Adams, 1973) comparable to those observed after a penetrating wound injury to the cortex and corpus callosum (Maxwell et al., 1990). It must be remembered, however, that the development of these ideas was based upon observations of an on-going process seen in static, fixed, embedded material.

However, within the last few years, studies of animal models (Maxwell et al., 1997; 2003) and humans (Gorrie et al., 2002) at very short post-traumatic survivals has clarified the picture about what is happening in an injured but contiguous axon after traumatic brain injury. These studies have revealed that the pathogenesis of axonal damage is more complex than originally thought (Povlishock et al., 1983; Gennarelli et al., 1989; Tomei et al., 1990; Grady et al., 1993; Christman et al., 1994; Christman and Povlishock, 1997; Maxwell et al., 1988, 1995, 1997, 1999, 2003; Smith and Meany, 2000). Among these studies, those conducted using a model in which transient, mechanical loading was applied to an isolated central tract of myelinated

axons, the optic nerve (Gennarelli et al., 1989; Maxwell et al., 1997) has probably given the greatest insight into the pathobiology of an axon after non-disruptive TAI where primary axotomy is not the immediate effect of that loading.

2.6. Primary axotomy versus secondary axotomy and the calcium hypothesis.

The phenomenon of delayed or secondary axotomy was first unmasked in 1993 by Maxwell et al. Prior to that time, the sequences of pathology in experimental animals subjected to mild traumatic brain injury (Povlishock et al., 1983) where an experimental tracer, horseradish peroxidase (HRP) was used to identify damaged axons, was thought to reflect fragmentation of axons at the time of injury. The associated disruption of the integrity of the axolemma was hypothesised to have allowed post-traumatic influx of HRP into the axoplasmic remnants. However, no direct evidence was found which supported the idea that primary axotomy has occurred in the mild injury model since the axolemma was always intact around foci of intra-axonal HRP.

The only direct, ultrastructural evidence for primary axotomy has been obtained from the lateral head acceleration model of DAI in the non-human primate (Gennarelli et al., 1982; Maxwell et al., 1993). In this model, direct evidence for fragmentation of the axolemma was obtained at 20 and 35 minutes after injury. At such sites (Fig. 2, page 97) complete loss of any recognizable axoplasmic, cytoskeletal organelle occurs. Instead, only a flocculent precipitate was present between and around membranous organelles like mitochondria (Fig. 2) and is interpreted as remnants of the autolysis of the axonal cytoskeleton upon shearing of the axolemma (Maxwell et al., 1993). Such ultrastructure has never been obtained in any other model of traumatic axonal injury (TAI).

At milder levels of mechanical loading foci of abnormal ultrastructure of the injured axon, termed perturbations (Pettus and Povlishock, 1994, 1996), occurred at points along the axons (Povlishock et al., 1983; Maxwell et al., 1995; Pettus and Povlishock, 1996). Perturbation consists of regions along the length of an axon where the normal, linear, longitudinal arrangement of microtubules and neurofilaments is lost and is replaced by a spiral orientation (Fig. 3 a, page 97) or a transverse orientation of neurofilaments (Fig. 3b, page 98).

However, careful observation indicates that a spectrum of pathologies may be encountered in thin sections: - for example loss of the usual number of microtubules and neurofilaments with the occurrence of gaps or holes in the axolemma (Fig. 4, page 98).

As already indicated, no evidence has been obtained in support of the old hypothesis that axonal bulbs develop at the moment of injury as a result of disconnection of axons leading to direct escape of axoplasm into the brain parenchyma (Cajal, 1928) to generate the so-called reactive swelling obtained in the great majority of animal models of TAI. Instead the traumatic episode triggers a perturbation at foci along the length of an axon (Maxwell et al., 1991; Pettus et al., 1994) at which an impairment of axonal transport has occurred, and led to an accumulation of axonal organelles to form axonal swellings (Jafari et al., 1997; Adams et al., 1982; Povlishock, 1983, 1994). Maxwell et al., (1997) suggested that a distinction should be made between zones of increased calibre where the axon is in continuity on both sides - **axonal swellings** - and increases in calibre where axonal disconnection has occurred on one side of the enlargement - **degeneration bulb** - when axonal disconnection or secondary axotomy had occurred. This terminology has since been accepted.

However, the initial mechanism(s) leading to secondary axotomy has been a topic of debate over the last decade especially with regard to the role of the axolemma. On one hand, in the early 1990's Povlishock and colleagues concentrated upon the direct effect of trauma upon the cytoskeleton as being the key factor responsible for the sequence of events which leads to secondary axotomy (Povlishock et al., 1983; Povlishock, 1992) and this was promulgated in later work from the same group (Pettus et al., 1994; Pettus and Povlishock, 1996; Povlishock et al., 1997). Povlishock and co-workers utilised the phenomenon of a reduction in interneurofilament spacing at foci in injured nerve fibres. These foci are termed zones of neurofilaments compaction (Pettus and Povlishock, 1996). The basis of their argument was that damage to the axolemma was not crucial to the development of pathology. In a series of experiments, horseradish peroxidase (HRP) was injected into the cerebrospinal fluid before axons were injured. However, HRP did not penetrate the axoplasm of all axons within which compaction of NFs occurred (Pettus et al., 1994; Pettus and Povlishock, 1996). The axolemma therefore remained intact and did not become permeable. Rather, the hypothesis that mechanical injury via the fluid percussion experimental paradigm caused direct damage to NFs and led to their misalignment and compaction was developed. Damage to NFs was therefore hypothesised to be the initiating event for the development of pathology leading to secondary axotomy (Pettus and Povlishock, 1996).

An alternative hypothesis was that the key event was damage to the axolemma resulting from mechanical shear injury. This damage compromised the normal function of the membrane and led to a rapid influx of calcium (Maxwell et al., 1995; Fitzpatrick et al., 1998) down the normal concentration gradient of intact axons where the concentration of Ca^{2+} is 10,000 greater in the periaxonal space than in the

axoplasm (Goldman, 1982). Evidence for focal axonal injury was provided as early as 5 min post-trauma in the occurrence of so-called nodal blebs at nodes of Ranvier (Fig. 5, page 99). The associated loss of the characteristic subaxolemmal density or dense undercoating (red arrows in Fig. 5) indicated that some degree of damage to the structural integrity of the nodal axolemma had occurred very early after trauma (Maxwell et al., 1991).

Further support for the concept of damage to the axolemma is provided by two types of evidence. First, cytochemical evidence for an altered distribution of Na^+/K^+ -ATPase activity (Fig. 6, page 100) and membrane pump Ca^{2+} -ATPase activity (Fig. 7, page 100) (Maxwell et al., 1995, 1999). Second, loss of intramembranous particles in freeze fracture replicas of the nodal axolemma (Maxwell, 1996; Maxwell et al., 1999) where that loss of particles is thought to represent loss of transmembrane proteins such as ion channels and ATP dependent pumps. These changes occur over a period of several hours after stretch-injury to the axons (Maxwell et al., 1995, 1999). Overall, there is now strong evidence that damage to or perturbation of the axolemma as a result of transient mechanical loading is key to the initiation of pathology culminating in secondary axotomy over tens of hours after TBI and this hypothesis is now widely accepted (Smith, 2005). According to the hypothesis, damage to the axolemma leads to sudden loss of ionic haemostasis inside axons, and the resultant calcium influx activates calcium activated neutral proteases (Calpains) which in turn leads to loss or collapse of the side-arms of NF and their compaction. At the same time, there is loss of microtubules (Maxwell and Graham, 1997) that depolymerise spontaneously at elevated, intra-axoplasmic concentrations of calcium (Weisenberg, 1972; Gaskin et al., 1975; Olmsted and Borisy, 1975; Nishida and Sakai, 1977; Maxwell and Graham, 1997). This latter change leads to impairment of axonal

transport at the site of axolemmal damage, and because such axonal transport is still functioning elsewhere along the length of the axon, both anterograde and retrograde transport continues to deliver material to the site of loss of microtubules where it accumulates to form an axonal swelling. Further evidence that supports the calcium hypothesis in TAI is the direct, ultrastructural demonstration of calpain-mediated spectrin proteolysis (CMSP) using antibodies targeting CMSP and neurofilaments (NF) (Buki et al., 1999). The localisation of spectrin breakdown products first occurs at the under surface of the axolemma but then expands toward the centre of the axoplasm over a period of about an hour (Buki et al., 1999). Calcium activated neurofilament proteases have been hypothesised to result in removal and/or collapse of neurofilaments side-arms and result in neurofilament compaction and/or degradation (Buki et al., 1999).

Immunocytochemical labelling for low molecular weight neurofilaments (NF-L) or beta amyloid precursor protein (β -APP) allows identification of focal enlargements of axons as early as 35 minutes to an hour or two after injury. This has been observed in both animal models of TAI and human DAI (Grady et al., 1993; Christman et al., 1994; Blumbergs et al., 1995; McKenzie et al., 1996; Gorrie et al., 2002). It is now clear that development of axonal swellings has an extended time-course of a minimum of 3-4hours in experimental TAI and 12 hours in human DAI. Further, the process may continue over a long period after the initial injury since β -APP labelled axonal swellings have been visualised up to 99 days following human, mild head-injury (Blumbergs et al., 1994). Overall, the findings described support the hypothesis that injured axons demonstrate a continuous and progressive pathology that is initiated at the time of an insult and has a time course consisting of a "pathological cascade of events" rather than being a single event. As mentioned earlier, disconnection of an

injured axon occurs at least 2-4 hours in laboratory animals and 12-24 hours in humans after the initial insult to the head. Despite the differences in the extent and distribution of axonal swellings within the central white matter between patients and experimental animals there is now good evidence that the interlinking mechanisms in the development of axonal pathology are the same. However, it is also widely acknowledged that the time course for axonal responses is shorter in smaller animals than in larger ones (Maxwell et al., 1997). At the site of axonal disconnection, an early observation made by Povlishock et al. (1983) was the apparent involution of part of the axolemma within the swelling and the hypothesised fusion of the axolemmae from opposite sides of the swelling to separate the axon into two fragments.

Ultrastructural analysis, however, has extended that observation by showing that the dark centre within an axonal swelling seen by light microscopy (Povlishock et al., 1983) is, in fact, a region of marked compaction of NFs (Jafari et al., 1997, 1998) (Fig. 8, page 101). Importantly, the latter studies provided evidence that rather than fusion of the axolemmae from opposite sides of the axonal swelling, the membrane is destroyed leaving the compacted NFs directly exposed to the extracellular space. There is therefore elimination of any barrier to influx of Ca^{2+} and the terminal proteolysis of NFs results (Fig. 8, page 101).

In summary then, primary axotomy occurs only at very high mechanical loadings to axons. It is probable that secondary axotomy occurs much more frequently and in a more widespread distribution within the central white matter of the brain of a patient exposed to TBI. It may be suggested that primary axotomy probably occurs only in patients who either enter coma at the site of an accident or die at the scene. On the other hand, labelling of injured axons using, for example using antibodies for β -APP, has been documented up to 99 days after mild head injury (Blumbergs et al., 1994)

where the cause of death was not directly associated with the episode of TBI. Use of the β -APP marker has demonstrated that a time course is required for the development of abnormal axonal profiles (McKenzie et al., 1996) and profiles both before and following axonal disconnection or secondary axotomy may be obtained in the same brain area. Further, it has recently been questioned whether all injured axons label with β -APP. Use of the marker RM014 appears to label a different population of damaged axons (Stone et al., 1999, 2000; Maxwell et al., 2005; Marmarou et al., 2005). Thus, the hypothesis that at least two markers of injured axons may more completely indicate the total number of injured axons within central white matter after TBI has not yet been satisfactorily resolved.

A model of mild TAI has not yet been developed although labelling of damaged axons in patients following mild TBI was documented about ten years ago (Blumberg et al., 1994). There is a developing consensus that disrupted axonal transport as reflected by labelling with β -APP or RM014 probably occurs in less severe forms of TBI and, even, perhaps, in patients exposed to mild head injury who may not be either taken to hospital or admitted. There is good behavioural and sociopsychological evidence that at least a proportion of these patients experience behavioural or intellectual difficulties over a period of years after an initial insult (Hcllawell et al., 1999; Hawley, 2002, 2003; Hawley et al., 2003). It is highly likely that these patients have experience low levels of secondary axotomy (Biasca et al., 2005). It may therefore be hypothesised that the incidence of secondary axotomy is probably much more common than has been appreciated until the present time and is the principle form of axonal injury or response to injury following TBI.

2.7. Injured axons demonstrate a spectrum of pathology after traumatic axonal injury (TAI).

Immunohistochemical labelling with monoclonal antibodies directed either toward β -APP (Shcriff et al., 1994; Gentleman et al., 1993; McKenzie et al., 1996) or different subunits of NF (Grady et al., 1993; Christman et al., 1994) has allowed rapid identification of damaged axons for diagnosis. However, perhaps a greater insight into the cellular pathology and its time course has been obtained through the application of stereology to the study of the changes in the axon and its cytoskeleton (Jafari et al., 1997, 1998; Maxwell et al., 2003). There is now a consensus that loss of microtubules (MT) (Maxwell and Graham, 1997) and changes in the alignment and packing of neurofilaments occur early in traumatic injury and is a direct result of damage to the axolemma during transient loading (Maxwell et al., 1997). The resulting disturbance in axonal transport leads to the formation of axonal swellings between 35 minutes and 2 hours in both animals and humans, and development of foci of NF compaction (Pettus et al., 1994; Gentleman et al., 1995; McKenzie et al., 1996; Pettus and Povlishock, 1996; Povlishock et al., 1997; Gorrie et al., 2002). Moreover, stereology has provided incontrovertible evidence that different changes occur in the axonal cytoskeletal after TAI. These changes occur both (1) in subgroups of axons of different size and (2) between both the earliest and latest experimental time points examined; either at 15 min (Maxwell and Graham, 1997), 4 hours (Jafari et al., 1997, 1998), or up to 7 days (Maxwell et al., 2003) after injury.

There is loss of microtubules (MT) within 15 minutes of stretch-injury. This loss occurs at both nodes of Ranvier and at internodes (Maxwell and Graham, 1997). However, it is possible to make a clear distinction of pathology between nodes and internodes upon grounds of morphology. First, nodal ultrastructure differs between

controls and those in which nodal blebs occur (Fig 5, page 99). Second, in the latter, there is loss of MTs from injured nodes at both 15 min and 2 hours after injury, but only normal nodes occur at 4 hours after injury (Maxwell and Graham, 1997).

However, there is no loss of NFs from nodes with nodal blebs.

There are also two subtypes of damage at internodes. At injured internodes, there is loss of MTs up to at least 4 hours after injury (Maxwell and Graham, 1997). There is also a significant reduction of the number of both MTs and NFs within the axoplasm either within an axonal swelling or at a region of infolding/involution of the axolemma (Fig 9, page 102). However, the loss of NFs is greater at sites of infolding of the axolemma - (loss of some 90% of NFs) compared to axonal swellings - a loss of 50% of control numbers (Maxwell and Graham, 1997). Jafari et al., (1997, 1998) extended those findings in a detailed analysis of changes in the axonal cytoskeleton in internodes of damaged axons at 4 h after injury. This work provided the first evidence that axons of different size in terms of their transverse diameter differed with regard to the changes in organisation of the components of the axonal cytoskeleton. In summary, injured axons within optic nerve at 4 h after injury showed (a) an increased number of NFs in axons up to 1.00 μ m in diameter, (b) a reduced spacing between or compaction (Pettus and Povlishock, 1996) of NFs in axons up to 1.5 μ m in diameter, (c) no change of either number or spacing for MTs in axons up to 1.5 μ m diameter, (d) an increased spacing or "dispersion" of both NF and MTs in axons with a diameter greater than 1.5 μ m and within which intramyelinic spaces occurred (Fig. 10, page 102) and (e) compaction of NFs and loss of MTs in larger axons surrounded by an enlarged periaxonal space (Fig. 11, page 97) (Jafari et al, 1997).

A novel observation in this study, however, was that in the smallest axons in the optic nerve, those with a diameter < 1.0 μ m, there was an increase in the number of

neurofilaments at 4 hours after stretch injury compared to the number in control axons of the same diameter. Further, in those same fibres there was no change of either number or spacing between MTs. There is a dramatic loss of MTs (Maxwell and Graham, 1997) with a return to normal values by 4 hours and the development of two discrete pathologies in larger axons. This observation stimulated generation of the hypothesis that cytoskeletal changes obtained in thin sections in injured axons reflected a progression over time and that a greater number of axons may undergo pathology with increasing post-traumatic survival.

Increased confidence in this hypothesis was provided in a subsequent analysis at 24 hours and 7 days after injury (Maxwell et al., 2003) in three segments of the injured optic nerve: the juxtaglobal, middle and juxtachiasmatic segments. In summary, there was an increase in the number of small axons, less than 0.5 μm diameter, in all three segments at 4 h but only in the middle segment at 24 h and 7 days. In controls, in the middle segment of the nerve, these make up 1.6% of the total number of axons. However, at 4 hours after injury they form 6% of the total, at 24 hours 5.8% and at 7 days 4.3%. There was also loss in the number of axons of 0.5- 1.0 μm diameter at 4 h. At 24 h and 7 days there was an increased number of the smallest axons (<0.5 μm diameter) but no difference from control values for other sizes of axon; 0.5 – 1.0 μm , 1.0 – 1.5 μm and 1.5 – 2.0 μm . Within the axoplasm of axons of <0.5 μm diameter NFs were both increased in number and compacted in comparison to control axons of the same size. At 7 days after injury, NFs were still compacted in these small nerve fibres (Maxwell et al., 2003).

3. Axonal transport

3.1 Patterns of Axonal Transport:

At the simplest level axonal transport is composed of two types known as fast and slow transport ranging between 0.3-400mm/day and traditionally classified into five subgroups of differing speeds (Grafstein and Forman, 1980; Brady and Lasek, 1982; Baitinger et al., 1982). The fast component is formed by Groups I, II and III for membrane-bound structures. These are - I = 70-400 mm/day, II = 20-70 mm/d, III = 4-20 mm/d. Slow axonal transport, however, relates to cytoskeletal and other proteins and consists of group IV or Scb = 1-4mm/day for certain glycolytic enzymes and cytoskeletal proteins not included in V, and Group V or SCa = 0.2-1.2mm/day for neurofilament proteins and tubulins. Membranous organelles such as mitochondria and the axoplasmic reticulum move most rapidly (in Groups I – III), whereas cytoskeletal propolymers and protein neurofilaments (NF) complexes move more slowly (in Groups IV and V). But there has, recently, been a major change in the interpretation of experimental results obtained over the last fifty years since axonal transport was first recognised. Until recently, it had been assumed that the difference in rates of transport of material by fast and slow components indicated that membranous and non-membranous components or cargoes were moved in anterograde (away from the cell soma) and retrograde (toward the cell soma) directions by fundamentally discrete or distinct mechanisms (Allan et al., 1991; Nixon, 1991). Within the last five years, however, direct observation of movement of organelles in living cells has indicated that all cellular components, membranous and non-membranous, may be transported by fast motors and that the major difference between fast and slow transport is not the mechanism of movement *per se* but the manner in which the movement is regulated (Brown, 2003).

3.2 Fast axonal transport

Membranous organelles or membrane limited aliquots of proteins, lipids and polysaccharides synaptic vesicles, vesicle-associated proteins such as synapsin, kinesin (Morris et al., 1993), neurotransmitter receptors trophic factors including nerve growth factor (NGF), as well as amyloid precursor protein (Koo et al., 1990; Morris et al., 1995) move rapidly along an axon via fast axonal transport.

Membranous organelles and membrane-limited vesicles may move either in the anterograde or retrograde direction but predominantly in the former in the intact axon. A summary of information contained in the relevant literature is provided in Table 2 (page 37) and has led to a marked change in our interpretation and/or understanding of mechanisms and rates of axonal transport. In this context, it is also notable that the identity of the hypothetical slow motors has remained elusive for the last 25 years (Brown, 2003). On the contrary the identity of the anterograde fast motor proteins in the kinesin family and the retrograde motor proteins in the dynein family have been established since the middle 1980's (Brady, 1985; Vale et al., 1985; Lye et al., 1987; Paschal et al., 1987). So, rather than there being fast and slow mechanisms of axonal transport, it is presently thought that all cytoskeletal components and or precursors are transported by fast motors but that the relative differences in apparent rates of transport arise because the proportion of time that different components move or are moved varies. This has given rise to the "duty hypothesis" or duty ratio (Brown, 2003) which is the proportion of time that an entity or cargo actually spends moving. For example if a membranous organelle binds to a fast motor for 50 out of 60 seconds it will move a greater distance over a period of direct observation than a NF protein that binds to a fast motor for only 10 out of every 60 seconds. That is to say, items

that move slowly along an axon spend more time paused than moving when attached to a motor.

3.3 Motor molecules:

Fast axonal transport depends upon the integrity of the microtubules and other proteins that work as molecular motors for axonal transport. The motor molecules are the kinesin superfamily, the dynein family, dynactin and myosin.

Kinesins (Fig. 12, page 103) are a superfamily of microtubule-based motor proteins that perform many different functions in all cells. Examples of the diversity of kinesin functions are transport of vesicles, organelles (both membranous and increasingly within the literature non-membranous), chromosomes, protein complexes, enzyme systems and ribonucleic proteins (Lawrence et al., 2004). In addition, kinesins are involved in the regulation of dynamic changes in function and/or activity of MTs (Hirokawa et al., 1998). In overview, kinesins are an elongated molecule about 80nm in length (Fig. 12, page 103). At one end is a pair of globular heads about 10nm in diameter; at the other end is a fan shaped tail (Allan et al., 1991). The pair of globular heads contain microtubule activated ATPases. A newly established convention classifies the kinesins into 14 families (Lawrence et al., 2004). All family members bear the name kinesin and different groups are designated by use of an Arabic numeral, thus kinesin-1 denotes conventional kinesin, kinesin-13 denotes M-kinesin and kinesin-14 denotes C-kinesin. Earlier, kinesins had been classified using the location of their motor domains along the length of the molecule. Terminal motor N-Kinesin or Kinesin-1 has the motor domain close to the N-terminal of the molecule, M-Kinesin or Kinesin-13 a middle motor domain and C-Kinesin or Kinesin-14 a C-terminal motor domain (Hirokawa and Reiko, 2004; Lawrence et al., 2004). The conventional kinesin or kinesin-1, the first member of the kinesin superfamily,

consists of two heavy chains, each of 120 kDa, and two light chains each of 64kDa (Bloom, 1992; Brady, 1993; Muresan, 2000; Weiss et al., 1991). When examined by transmission electron microscopy, after low-angle rotary shadowing, it has a rod like stem of 80nm length and two globular heads at the amino-terminal end. The heads are the sites of binding to microtubules and each also contains one ATPase binding site. The latter may be inhibited by calmodulin binding to the light chains and thus the light chain may have a regulatory role in kinesin function (Matthies et al., 1993). The light chains also possess a fan-like tail that binds to plasma membranes and is the site of attachment for membranous organelles (Hirokawa, 1998). In conclusion, this motor system utilizes microtubules as rails and is involved in transport of a wide variety of intracellular cargoes the great majority of which are transported anterogradely and include precursors of synaptic vesicles, other vesicles containing amyloid precursor protein (APP), or are associated with spectrin/fodrin, mitochondria, lysosomes and tubulin oligomers (Table 2, page 37). However, recent, *in vitro*, evidence has shown that both neurofilaments up to 15.8 μ m long (Wang et al., 2000) and non-filamentous neurofilament protein (Prahlad et al., 2000) can move along microtubules at speeds of 0.5-1.0 μ m/s and that this movement involves kinesin. Thus, perhaps all axonal, anterograde transport utilizes fast motors but the period of time over which movement occurs varies widely. However, the mechanism controlling or regulating the period over which transport occurs is still obscure.

Table 2: A summary of the Five Groups of Speed of Axonal Transport, the Entities transported in each Group, the known Motors operating in each group, the Overall and Instantaneous rates and the Direction of Movement.

Cytoplasmic organelle	Overall Rate (pulse labelling)	Instantaneous rate (light microscopy)	Direction
FAST			
Golgi-derived vesicles (synaptic vesicle proteins, kinesin, enzymes for neurotransmitter metabolism)	200-400mm/d ^a 2-5µm/s	1-5µm/s ^d	Anterograde
Endocytotic vesicles (internalised membrane receptors, neurotrophins)	100-250 mm/d ^a 1-3µm/s	1-3µm/s ^g	Retrograde
Lysosomes (active lysosomal hydrolases)	100-250 mm/d 1-3µm/s	1-3µm/s ^g	Retrograde
Autophagosomes	100-250 mm/d 1-3µm/s	1-3µm/s ^g	Retrograde
Mitochondria (cytochromes, enzymes of oxidative phosphorylation)	< 70 mm/d ^b (< 0.8µm/s)	0.3-0.7µm/s ^c	Bidirectional
(SCa) neurofilaments		0.3-1µm/s ^f	Bidirectional
Tubulin in CNS		0.3-1µm/s ^f	Bidirectional
α-spectrin, actin, calmodulin		0.22 – 3.3µm/s ^k	Bidirectional
SLOW			
(SCc) MAP1 phosph	7-9 mm/d ^h	unknown	Anterograde
(SCb) Actin, clathrin, dynein, dynactin	2-8 mm/d (0.02-0.09µm/s) ^g		
Cytosolic protein complexes (glycolytic enzymes, creatin kinase, aldolase, enolase)	2-8 mm/d (0.02-0.09µm/s) ^g	unknown	unknown
MAP1 dephosp	1-6 mm/d ^h	unknown	Anterograde
(SCa) neurofilaments	0.3-3 mm/d (0.004-0.04µm/s) ^g	0.3-1µm/s ^f	Bidirectional
Tubulin in CNS		0.3-1µm/s ^f	Bidirectional
α-spectrin, actin, calmodulin		0.22 – 3.3µm/s ^k	Bidirectional
Spectrin, tau proteins	0.3-3 mm/d (0.004-0.04µm/s) ^g		

References: ^a Grafstein and Forman, 1980, ^b Lorenz and Willard, 1978; ^c Morris and Hollenbeck, 1993, 1995; Ligon and Stewart, 2000; ^d Breuer et al., 1987; Viancour and Kreiter, 1993; Nakata et al., 1998; Kaether et al., 2000; ^f Roy et al., 2000; Prahlad et al., 2000; Wang et al., 2000; Wang and Brown, 2001, 2002; ^g Brown, 2000; ^h Ma et al., 2000; ^k Koenig et al., 1985).

The **dynein** family (Fig. 13, page 104) is another widespread group of motor proteins that is usually subdivided into axonemal and cytoplasmic groups. The axonemal group contains 18 members that are motor for the activity of cilia and flagella and are not relevant to the present discussion. The nine members of the cytoplasmic dynein group are thought to contribute to retrograde axonal transport. One type of cytoplasmic dynein has been isolated from bovine brain, has a microtubule activated ATPase and promotes *in vitro* gliding of microtubules (Paschal et al., 1987). Within axons it is present in two forms, major and minor. Major dynein is a huge macromolecular complex of 1000-2000 kDa (Susalka and Pfister, 2000; Vale et al., 2003) and it is composed of four types of subunits, two identical heavy chains (HC), two intermediate chains (IC), two light intermediate chains (LIC) and a small but variable number of light chains (LC) (Vallee et al., 1988). The HCs are approximately 350kDa each consisting of a globular head from which protrudes a slender stalk 10-15 nm in length. This contains an ATPase activated microtubule binding site that generates power for movements along a microtubule (King, 2000; Gee et al., 1997) where each dynein motor domain is formed of six subunits arranged in a hexameric ring (Gee et al., 1997). Also extending from the head is a long cargo-binding stem containing an intermediate chain of 74kDa, a light intermediate chain (Habura et al., 1999; Tynan et al., 2000a) all of which bind to the heavy chains of the globular head. These three subunits (light, light intermediate and intermediate) are involved in cargo binding when the descriptor "cargo" is applied to the membranous or non-membranous organelle that is to be transported along a track of MTs. However, for linkage of dynein to membranous organelles and movement along tubules an interaction between dynein and the dynactin complex p150^{glued} is necessary (Shah et al., 2000; Deacon et al., 2003). The latter also allows movement of non-membranous

organelles, for example neurofilaments, along MTs (Shah et al., 2000). Dynactin links to membranes derived from the Golgi complex via β III-spectrin to establish the dynactin-mediated dynein endomembrane binding system (King et al., 2003). However, understanding of the mechanism for linkage of membrane-limited organelles to axonal MTs is still incomplete; at least in part, because it seems that different types of endomembrane may utilise discrete and specific binding molecules (King et al., 2003) where the amino-acid sequence of the stem varies between dyneins and allows binding to different cargoes (Tynan et al., 2000a, b). Further, the linker molecule between MTs and non-membranous organelles is, presently, unknown. However, it is becoming accepted that the fast motors kinesin and dynein bind both membranous and non-membranous organelles and use the same track of microtubules but move in opposite directions, kinesin to the plus end away from the cell body in axons, dynein to the minus end of MTs. The overall rate of movement, however, differs with the proportion of time that an organelle is linked to the motors. Finally, biochemical cross-linking experiments and image analysis has revealed that both dynein and kinesin compete for tubulin isomers α and β which form a microtubule binding site 80Å in length (Mizuno et al., 2004). However, our present understanding of these complex interactions is not great enough to allow a simple explanation of changes under conditions of axonal pathology.

Myosin is a member of a superfamily of filamentous molecules which interact with members of another filamentous protein family, the actins. Within the myosin superfamily the present classification is into seventeen classes each of which is denoted by a Roman numeral. Myosins occur in a huge range of types of cells, over plants, prokaryotes and eukaryotes. However most classes are restricted to particular

types of cell, particular groups of organisms or to cells specialized for specific functions (Sellers, 2000). Within nervous tissue myosin V and myosin VI have both been implicated in transport of vesicles and/or transport of mRNA. Myosin V has been recognized recently as an organelle motor in the axoplasm of the giant axon of squid (Bearer et al., 1993; Tabb et al., 1998) and homogenates of chicken brain (Evans et al., 1998). It is involved in transport of vesicles in both mature (Espreafico et al., 1992) and cultured (Evans et al., 1997) neurons and with release of neurotransmitters from rat cerebrocortical synaptosomes (Perkeris and Terrian, 1997) and Purkinje cells (Takagishi et al., 1996; Dekker-Ohno et al., 1996). Myosin has been hypothesised to be a motor molecule for the final delivery of membrane limited organelles into parts of the neuronal cytoplasm where tubulin content is low but actin content is high; for example, growth cones in the developing nervous system, mature dendritic spines and synapses (Tabb et al., 1998) or the plasma membrane (Gallant, 2000). An investigation of the role of myosin, and in particular myosin-V, in any model of TBI is currently lacking. However, the association of myosin-V with axonal transport of vesicles and its interaction with the actin subaxolemma cytoskeleton may be of interest with regard to damage and or repair of cell membranes.

3.3. Slow axonal transport

When axonal transport was first investigated and described two subcomponents were described, subcomponent SCa constituting the microtubule-neurofilament cytoskeleton and SCb representing the microfilament network (Black and Lasek, 1980; Brady and Lasek, 1982). But, as discussed earlier (page 32-34) visualization of NF movement in real time in living neurons after transfection with green fluorescent protein (GFP) -tagged NF subunits in superior cervical ganglion neurons has revealed

that both NF-M and NF-H move at a rate of 0.3 -1 μ m /s (Table 2, page 37) (Roy et al., 2000; Wang et al., 2000). However, the movement occurs only for short periods during any one observation and that movement is not continuous but interrupted by prolonged pauses. The result is that most NFs are stationary at any one time. It is presently thought that NFs are transported for short periods by the two fast motor transport molecules kinesin and dynein-dynactin (Brown, 2003). It may therefore be suggested that the concept of slow axonal transport is outmoded and should be discarded.

4. Wallerian Degeneration

4.1 Definition

The phenomenon of the degeneration of the distal segment of a nerve after axotomy was described first by Augustus Waller (1850) as he described changes in the distal segment of the glossopharyngeal and hypoglossal nerves of frog (*Rana*) after the nerves had been transected. The degenerative changes in the distal part of an axon following disconnection from the cell soma are now termed Wallerian degeneration after him. However, Wallerian degeneration *in senso stricto* occurs in the distal segment of peripheral nerve fibres.

Similar changes occur in the distal portion of axons in the CNS although the supporting or glial cells involved differ, astrocytes and oligodendrocytes rather than Schwann cells (Fig. 14, page 104). A basic conclusion, however, is that the time course of axonal degeneration and loss in CNS tracts is considerably longer (Avellino et al., 1995; George and Griffin, 1994a, b), particularly in humans (Bung et al., 1993), than in the PNS.

The events and time course of Wallerian degeneration has been widely investigated in the PNS and there is now a very extensive literature (reviewed Griffin et al., 1995). The responses by different types of cell may be summarized as follows. In the PNS, there is no morphological change in the axon for the first 12 to 24 hours. An active, enzymatic proteolysis of the axonal cytoskeleton then occurs between 24 and 48 hours after axotomy and progresses rapidly throughout the length of the axon that has been disconnected from its cell soma (Griffin et al., 1995; George and Griffin, 1994a). There is a correlated opening of the blood-nerve barrier. However, opening of the blood-brain barrier in the CNS may not occur (Griffin et al., 1995). As a consequence, the rapid accumulation of macrophages noted in PNS Wallerian degeneration occurs much more slowly in the CNS where reactive cells are derived from intrinsic microglia rather than from the circulation (reviewed in Griffin et al., 1995). Consequently, the time course for removal of myelin in the CNS is greatly prolonged compared to that in the PNS. In the PNS Schwann cells down regulate the production of myelin markers and form the classic “bands of Bügner”. In the CNS, however, myelin debris is “walled off” by astrocyte processes (Stoll et al., 1989) and oligodendrocytes have been associated with clearance of myelin (Ludwin, 1990).

4.2. Sequence of events

In TAI, the trigger for degeneration is damage to the axon following different forms of and degrees of trauma. In the majority of experimental models of axonal injury such as crush in development of a haematoma or transection as in a penetrating injury to the head large numbers of spatially closely related axons are injured (Barron et al., 1983) or as the result of an ischaemic insult. However, in TAI models of DAI, injured axons are relatively few in number and scattered among a larger population of intact or uninjured axons (Povlishock and Christman, 1995; Maxwell et al., 1997). In

addition, trauma in most cases of blunt head injury does not result in severance or primary axotomy at the time of injury. Rather, there is the initiation of a chain of events leading to axonal disconnection or secondary axotomy 3-4 hours later in experimental animals and 12 hours in patients. As a result, initiation of Wallerian degeneration may only follow TBI once axons have undergone secondary axotomy, some 72-96 hours after the initial insult to the head.

4.3. The Neuronal response and the Cytoskeleton

4.3.1. The Distal Segment of an Axon (See schema, Fig. 14, page 104)

The vast majority of the literature documenting responses in axons in Wallerian degeneration describes changes after axotomy in the PNS. The highly authoritative review by Griffin et al., (1995) allows the following summary to be made. First, there is little detectable change in the organisation of the components of the axonal cytoskeleton over the first 24 hours after axotomy. Then a rapid breakdown of the cytoskeleton, termed granular disintegration (Griffin et al., 1995), occurs over only a few hours along the whole length of the distal axonal segment. Correlated with loss of the integrity of the distal part of the axon there is stripping of synaptic contacts with the postsynaptic cell/tissue (reviewed Mack et al., 2001). Upon loss of the axon, responses by the myelin sheath and its associated glial cells are initiated. In the PNS there is proliferation of Schwann cells with peak numbers of dividing cells at 4 days after axotomy. Over the same time frame, monocytes invade the region of injury, differentiate into activated macrophages and removal of remnants of the myelin sheath occurs.

After axotomy via transection the axolemma rapidly reseals and "reactive axonal swellings" develop. These are characterised by a high content of mitochondria, dense

or lysosomal bodies, vesicular elements and increased numbers of neurofilaments. In the CNS the occurrence of reactive axonal swellings was first described almost forty years ago in dorsal ascending tracts of the spinal cord (Lampert, 1967) and the numerous studies in the intervening years have only provided some extra detail but not necessitated re-appraisal of the initial observations and conclusions. However, the occurrence and development of axonal swellings filled with large numbers of membranous organelles has stimulated the concept that axonal transport continues within the distal segment following axotomy even though electrical conductivity is lost. Additional evidence is the occurrence of aggregates of membranous organelles at nodes or Ranvier and Schmidt-Lanterman incisures (Ballin and Thomas, 1969; Maxwell et al., 2003) which are now recognised by some workers as a marker that an axon has undergone axotomy and has entered the early stages of Wallerian degeneration.

The next step in Wallerian degeneration is the pivotal, rapid loss of an organised, recognisable axonal cytoskeleton throughout the distal segment of an axon (George and Griffin, 1994a). The time course of these changes was documented quantitatively following injury to a peripheral nerve, the phrenic nerve, almost thirty years ago (Lubinska, 1977) where complete loss of the axoplasm occurs over only a few hours between 24 and 30 hours after injury. Different changes have been described in CNS axons within the opossum optic nerve after crush injury (Narciso et al., 2001). Here axons undergo focal degeneration of the cytoskeleton but two types of degeneration have been described. Either there is almost complete loss of cytoskeletal elements that has been termed "watery degeneration" (Narciso et al., 2001). Or the axoplasm is replaced by an amorphous, granular and dark material termed "dark degeneration"

(Narciso et al., 2001). Both types of change occur between 24 and 72 hours after crush injury.

However, Narciso et al (2001) did not provide any quantitative evidence in support of the use of these novel descriptors. A detailed analysis in TAI of optic nerve confirmed the hypothesis that microtubules and neurofilaments within injured axons respond in different ways. The first post-traumatic time point at which examples suggestive of Wallerian degeneration were recognised was 24 hours (Maxwell et al., 2003) and axons were designated as "degenerating fibres". Here the axolemma is still intact and closely related to the internal aspect of the myelin sheath. Thus, the calibre of these axons does not differ from control values. However, the number of neurofilaments within the axoplasm is reduced by 60% and of microtubules by 70% (Maxwell et al., 2003) with an increase in their spacing. Thus, degeneration of components of the axonal cytoskeleton occurs relatively slowly compared with the precipitous loss in PNS axons. Indeed, evidence for an incomplete or partial loss of neurofilaments and microtubules is obtained at 7 days post-trauma. In addition, between the remaining microtubules and neurofilaments an amorphous material, suggestive of proteolysis, occurs. Although the changes described above mirror those earlier described in nerve fibres after injury in the PNS (George and Griffin, 1994) and crush injury to optic nerve (Narciso et al., 2001), the time course for loss of NFs and MTs in central axons after TAI is much longer, that is about 160 hours compared to 48-72. Finally, there is complete loss of a recognisable cytoskeleton where cytoskeletal elements are replaced by an amorphous electron dense deposit inside the remnants of the myelin sheath (Fig.15, page 105). Within these fibers there is also dissociation of myelin lamellae, the myelin remnant has an irregular profile and a reduced calibre (Fig. 15). Similar ultrastructural changes has been seen in Wallerian

degeneration in the PNS, although, again, it is notable that the time course in the PNS is shorter than in the optic nerve after TAI.

4.3.2. The Proximal Segment of an Axon

After axotomy, the proximal part of the axon is the only part that remains connected to the cell soma. When axotomy occurs close to the cell body the effect of the injury is more severe and often results in the axon reaction and the death of the neuron (Lieberman, 1971; Barron, 1983). When a considerable proportion of the full length of the axon is retained the consensus is that the cell does not die and the axonal remnant does not degenerate. Rather, the axonal remnant undergoes a series of pathological changes over 8 – 10 weeks after axotomy (Barron et al., 1983; Hoffman et al., 1984; Kreutzberg, 1995). However, present understanding and interpretation of experimental results is complicated by a number of factors. For example, neuronal responses to axotomy differ between species with (1) the age of the animal when axotomy occurred, (2) the type of injury to the axon (crush, section or avulsion), (3) whether contact is retained with the distal stump as for example in incomplete crush, (4) the distance between the cell soma and the point of axotomy and (5) the type of neuron according to its function within the nervous system (Kreutzberg, 1995).

In the proximal stump of peripheral nerve after crush injury there is a series of changes in calibre of the axon and of the axonal cytoskeleton (Hoffman et al., 1984). These are dependent upon continued axonal transport and the possibility of reconnection with the periphery. After crush-injury to the sciatic nerve of adult rats (Hoffman et al., 1984) there is a reduction in the calibre of axons in large motor neurons over the next four weeks. This reduction is initiated at the cell soma and proceeds toward the degeneration bulb over time. Thus, the reduction in axonal

calibre occurs within the proximal part of the L5 motor root of the sciatic nerve at two weeks, at the middle part of the axonal remnant at three weeks and only occurs at the distal part by four weeks after injury. The rate of proximo-distal movement was 1.7mm/day and considered, at that time, identical to the speed of axonal transport of neurofilaments (Hoffman and Lasek, 1975; Hoffman et al., 1984). However, in the light of recent re-appraisal of rates of axonal transport (Brown, 2003), it would be of interest to re-assess rates of transport of axonal components within the proximal segment of a peripheral nerve following injury.

In addition to changes in the calibre of the proximal stump, a number of other morphometric changes are now recognised. First, there is loss of axonal circularity (the ratio $[\Phi]$ of axonal cross-sectional area to the area of a circle having the same circumference as the axon). In control, guinea pig optic nerves Φ is 0.78 in small axons and 0.90 in large axons. In an injured animal, however, the value for Φ varies between 0.25 and 0.90 (Jafari et al., 1997, 1998). Second, there is an increase in the thickness of the myelin sheath in internodes of axons with an altered value for Φ . In control animals, the number of myelin lamellae is directly axonal cross-sectional area, except in axons with an area of more than $20 \mu\text{m}^2$ (Hoffman et al., 1984). After crush injury to the sciatic nerve the number of myelin lamellae in the myelin sheath do not change. But when the calibre of axons is reduced there is an apparent increase in the number of lamellae within the associated myelin sheath. Further, with a reduction in axonal calibre, the circumference of the myelin sheath is inappropriately large and the profile becomes less regular, often convoluted, in shape – see also Fig. 15, page 105. Third, there is a reduction in the number of neurofilaments in axons with a reduced calibre. In axons of control rat sciatic nerve the number of neurofilaments increases linearly with the increase in axonal cross-sectional area (Hoffman et al., 1984) with

the result that their packing density does not change being 107 neurofilaments/ μm^2 . However, the same value for the density of neurofilaments is obtained in axons with a reduced calibre 3 weeks after injury. There must, therefore be a loss of *circa* 60% of NFs in axons of reduced calibre. On the contrary, however, within those same axons the packing density of microtubules was increased: 26 microtubules/ μm^2 in control animals compared with 35 microtubules/ μm^2 at 3 weeks after injury. Thus, the reduction in cross-sectional area of the proximal stump of sciatic nerve axons after crush-injury is correlated with a proportionate decrease in the number of neurofilaments but not of microtubules (Hoffman et al., 1984) by three weeks after injury. At greater survivals when there is recovery of motor function between 4 and 10 weeks after crush injury, however, there is a significant increase in the calibre of axons within both proximal and distal levels. Therefore, the mean axonal cross-sectional area in nerves that had regenerated was comparable to that in control, uninjured animals. Moreover, with recovery of motor function following crush injury to a sciatic nerve root there was no evidence for loss of axons in that the number in control nerves was not different from the number present at either 3 or 10 weeks after injury. Overall, Hoffman et al. (1984), provide good, quantitative evidence that axons within the proximal segment of a peripheral nerve do not degenerate following crush injury distant from the cell soma. Rather, axons undergo a series of responses over 6 to 8 weeks until end organ reconnection is achieved and there is then recovery of normal axonal structure as functional recovery is established.

It is not presently possible to make a direct, temporal comparison of responses by axons after central TAI because no experimental investigation has yet followed axonal responses for a period of greater than 7 days after TBI. There is, however, presently a consensus that Wallerian degeneration occurs more slowly in the CNS than in the

PNS (*vide supra*). This allows generation of the hypothesis that response(s) in the proximal segment of a central axon after secondary axotomy may have a longer time course than in the PNS outlined above.

4.3.3. The Neuronal Cell Soma

The great majority of experimental studies of axonal injury and/or Wallerian degeneration have investigated neuronal responses to a focal and often relatively severe insult such as transection or crush injury to a large proportion of axons within a peripheral nerve and close to the cell body. This elicits responses by the neuronal cell body of the injured axon to primary axotomy and results in loss of or degeneration of motoneurons within a week (Lieberman, 1971; Barron, 1983; Kreutzberg, 1995). The neurons enter the so-called "axon reaction" (Lieberman, 1971) characterised by the following overview.

The first morphological change is the peripheral displacement of the nucleus toward one side of the cell and the loss its normal smooth profile. This results in a scalloped profile facing the centre of the cell. A large Nissl body with a high density of free ribosomes and polysomes is often located within the cytoplasm of this nuclear indentation and there is a reduced number and length of cisternae of the rough endoplasmic reticulum. This has been suggested to reflect a change from synthesis of extrinsic to intrinsic proteins that are required for replacement of cell components that have been lost or proteins necessary for repair. There is good evidence that this process is stimulated by the **immediate early genes** (IEG) and transcription factors such as *c-fos*, *c-jun* and *jun-B* which are known to bind to DNA at sites known to regulate gene expression. However, there is also increasing evidence that different types of neuron respond differently to axotomy. For example, after peripheral

axotomy in rat sciatic nerve there is rapid up-regulation of *c-jun* mRNA in dorsal root ganglia neurons within hours and this remains elevated throughout the chronic phase of neurite sprouting (Kenney and Kocsis, 1998). Expression of IEGs in neurons with axons in the medial forebrain bundle (Leah et al., 1993) and rubrospinal tract (Jenkins et al., 1993), however, does not achieve maximal levels until 48 hours in the former and 10 days after injury in the latter. Recent data, (Cavalli et al., 2005), suggests that retrograde transport of a complex formed by activated c-Jun NH₂-terminal kinase and the scaffolding protein Sunday Driver (*syd*) interacts with a subunit of kinesin-1 to form a transport-dependent axonal damage surveillance system. However, there is only limited knowledge of such macromolecular interactions and the suggestion that that the IEG response in CNS neurons is slower than after PNS injury still has strong support.

Changes occur in the organisation of neurofilaments within the proximal segment of an axon after axotomy, *vide supra*. All cytoskeletal components of axons are synthesised in the cell soma of a neuron and it may be hypothesised that changes in the biosynthesis of cytoskeletal proteins will be altered following axotomy. Good evidence for such changes was documented more than a decade ago in both optic nerve (Hoffman et al., 1993) and sensory neurons (Greenberg and Lasek, 1988). A marked decrease to half of control values of the low molecular weight (NF68) and intermediate molecular weight (NF145) neurofilaments between 1 and 5 days after transection was reported after use of radiolabelling techniques (Hoffman et al., 1993). Levels of the above neurofilaments were reduced until 10 days after injury, only returning to control levels between 20 and 40 days. In parallel, the content of mRNA for NF-L (NF68) was decreased in retina (Hoffman et al., 1993) and dorsal root ganglia neurons (Moskowitz et al., 1993) until 14 days after injury.

But an opposite result was obtained for both actin and tubulin where radiolabelling showed that the somal content was one third greater between 1 and 5 days after injury with a return to control levels by 10 days. In parallel, the content of beta-tubulin mRNAs increased over the same time frame in DRGs (Moskowitz et al., 1993), but, notably, not in the retina (Hoffman et al., 1993).

The enhanced content of RNA necessary for increased protein synthesis requires increased numbers of ribosomes. It has been suggested that an increase in glucose uptake one day after facial and hypoglossal nerve transection (Kreutzberg, 1995) reflects up-regulation of the hexose monophosphate shunt and this allows increased synthesis of nucleotides and ribosomes. Other evidence for increased utilization of glucose after injury to axons has been documented in neurons from both the hypoglossal nucleus (Smith et al., 1984) and, in a model of TAI, retinal ganglion cells of the guinea pig retina (Gennarelli et al., 1989).

Only two studies have examined neuronal soma responses with respect specifically to TAI. A quantitative analysis of retinal ganglion cell responses over 14 days after stretch-injury to the guinea-pig optic nerve (Maxwell et al., 1994) and a combined immunocytochemical and ultrastructural analysis of neuronal responses in the parietal and temporal cortices, the thalamus and the hippocampus of rat up to one week after central fluid percussion injury (Singleton et al., 2002). In the former study, only a third of retinal ganglion cells demonstrate classic chromatolysis at 3 days after injury. There is no increase in the number of chromatolytic or degenerating neurons at either 7 or 14 days after injury. Within chromatolytic neurons there is overt evidence for nuclear eccentricity, dispersal and degranulation of Nissl substance, loss of the Golgi apparatus, all of which are indicators of neuronal degeneration by 3 days after injury (Maxwell et al., 1994). In the latter study (Singleton et al., 2002), neuronal somata

demonstrate increased APP immunoreactivity at 6 hours after TAI. But evidence for dispersal and degranulation of the RER and dispersal of the Golgi apparatus, was not obtained until 24 hours after TAI when tubular and vesicular profiles filled with APP electron dense reaction product occurred throughout the cytoplasm of the cell soma. Importantly, however, in the latter study, evidence for nuclear eccentricity and loss of cytoplasmic organelles comparable to that described in the axon reaction (Lieberman, 1971) and retinal ganglion cells after TAI (Maxwell et al., 1994) was not obtained until 7 days after injury (Singleton et al., 2002). Moreover, at 7 days, use of the antibody RMO-42 that labels phosphorylated neurofilaments identified some neuronal cell bodies in the mediodorsal cortex. On the other hand, in control or intact neurons, phosphorylated NFs occur only within axons.

An important conclusion to be drawn from the above is that neurons, after TAI compared to primary axotomy, do not show pathological progression to cell death when only diffuse white matter injury occurs. Rather, both Maxwell et al. (1994) and Singleton et al. (2002) suggest a potential neuronal attempt at reorganization for recovery and repair. Early evidence in support of this hypothesis was provided by stereological evidence of an increase in size of the nucleolus in regenerating RGC at 7 and 14 days after axonal injury (Maxwell et al., 1994). Further support is provided by expression of markers associated with axonal elongation or regeneration, for example microtubule-associated protein 1B (MAP1B and MAP1B-P), growth-associated protein (GAP-43) and the polysialylated neural cell-adhesion molecule (PSA-NCAM), in the cerebral cortex and hippocampus of rats after lateral fluid-percussion injury (Emery et al., 2000). This, together with the results of Singleton et al. (2002), provide evidence that neurons, after TAI in which only relatively small numbers of axons are injured, enter a transient state of repair rather than undergoing immediate

degeneration. It is also now recognised that the concept that central neurons are incapable of a regenerative response is incorrect. Rather, the inhibition of this response probably arises within the microenvironment in the region where injury has occurred. However, the factors involved are still undefined.

4.4. Non-Neuronal Cellular responses in Wallerian degeneration

As indicated earlier (page 43-44), the cells removing myelin debris during Wallerian degeneration in the PNS and CNS differ. In the PNS there is opening of the blood-nerve barrier and ingress by numerous monocytes that differentiate into macrophages. In the CNS, however, the blood-brain barrier does not open unless there is also mechanical damage to blood vessels within the neuropil as might occur, for example, in diffuse vascular or a penetrating injury. In TBI, however, opening of the blood-brain barrier has not been demonstrated unless petechial haemorrhages occur. Thus, except in the latter, only intrinsic microglia, oligodendrocytes and astrocytes may respond after TAI.

4.4.1 Macrophages

The source of macrophages after injury to the PNS or CNS differs in particular when the blood-brain barrier remains intact. In the PNS, although some macrophages are present locally within the endoneurium (Monaco et al., 1992), there is a rapid and abundant infiltration by haematogenous monocytes when the blood-nerve barrier is opened and these cells quickly differentiate into cluster domain (CD) activated macrophages (Griffin et al., 1993; reviewed in Stoll et al., 2004). However, CD macrophages have been subdivided in a wide variety of sub-types, for example cluster domain CD68, CD34+, CD8+, CD5+, CD4+ that are subtypes of the external domain (ED1+) macrophages. Different cell surface molecules are expressed by monocytes,

macrophages and activated microglia. The cell surface molecules vary with different subtypes of tissue growth factors (TGF- β 2 or TGF- β 1); the precise role being undertaken by the cells within damaged tissue; or the type of insult to the CNS, for example activation of cyclooxygenase (COX-1) expression by microglia and COX-2 by neurons in Alzheimer's disease (Fiala et al., 2002). Recent evidence, for example, has indicated that bone marrow derived cells, for example, CD34+ cells, migrate into adult brain and differentiate into both perivascular and ramified microglia (Asheuer et al., 2004). A detailed review of the vast literature on this topic is beyond the remit of the current thesis. Clearly, however, use of a single type of antibody as a marker for these cells in any study will provide only limited information.

There has not yet been an investigation of the involvement of haematogenous macrophages (the CD8+, CD5+ and CD4+ cells above) or the intrinsic microglia in studies of TBI. However, Jander et al (2001) have compared entry by macrophage subtypes the CD8 +, CD4+, and ED1+ variants of these MHC class II- cells into either sciatic (PNS) or optic nerve (CNS) after crush injury. In sciatic nerve there was strong expression for ED1, CD4 and CD8 cells at the crush site at 2 days. In the distal nerve stump, however, CD4 expression increased continuously up to 14 days and then declined. On the other hand, CD8+ cells were limited to the perineurium and declined from peak values at 2 days to low numbers between 4 and 7 days. The most marked change, however, was the number of CD8+ cell within the degenerating nerve parenchyma. Until day 7, their number was low. However, between 7 and 14 days there was a massive increase of large, round CD8+ cells which filled the entire degenerating nerve parenchyma. Activated macrophages removing myelin debris were spread throughout the length of the peripheral/distal part of the degenerating nerve with peak numbers occurring at 14 days after the injury followed by a decline

(Jander et al., 2001). It is noteworthy that in the PNS macrophages are not only involved in myelin clearance but also in the stimulation of proliferation of Schwann cells (Fernandez-Vallc et al., 1995).

After crush injury to the optic nerve, however, the timescale and the spatial extent of penetration of the damaged tissue by MHC class II cells differed (Jander et al., 2001). Infiltration by CD8⁺ cells occurred at the crush site with peak numbers at 4 rather than 2 days. Thereafter, there was a continuous fall in the number of CD8⁺ cells. Notably, CD8 cells did not enter the region of degenerating nerve fibres distal to the site of crush injury. Rather, unlike in the PNS, the number of CD4⁺ cells increased within the distal stump of degenerating nerve fibres and peak numbers were obtained at 2 to 4 weeks after injury. Lawson et al. (1994) also reported a four-fold increase in the number of macrophages and microglia in the distal segment of the optic nerve and the superior colliculus by 7 days after crush injury to mouse optic nerve. However, a different marker, the monoclonal anti-mouse macrophage marker (F4/80) expressed at all levels of activity by these cells was used (Lawson et al., 1992) and direct comparison of the two different experimental paradigms is therefore not possible. Although, the increased number of macrophages is comparable to that noted in the PNS, there is, importantly, a difference in the time scale over which peak numbers occur between the PNS and CNS as well as differences in subtypes of these cells as indicated by their differential expression of cell surface antigens. Lawson et al., (1994) obtained maximum numbers of macrophages at 3 days in the saphenous nerve, 5 days in the sciatic nerve but only at 7 days in the optic nerve after crush-injury.

The above discussion illustrates the present lack of understanding of the role and/or effect of the presence and/or activity of macrophages within the CNS after injury. It is

also suggested that in any forthcoming immunocytochemical analysis a spectrum of antibodies for substages in the life span or subtypes of monocytes, macrophages and microglia will need to be undertaken. It is also clear that those macrophages that do enter areas of CNS damage probably differ in their role or function, as indicated by the different components of the cluster domain (CD complex) expressed by the cells entering a site of injury in the PNS or CNS. In the mature CNS, macrophage-like cells are generally absent apart from the presence of perivascular cells (Graeber and Streit, 1990; Liu et al., 1994) that may be regarded as an intermediate stage derived from CD34+ cells (Asheuer et al., 2004) and that have a significant turnover throughout life (Lawson et al., 1992). Macrophages may invade the neuropil particularly at sites where the blood-brain barrier is opened or in young animals in which the blood-brain barrier is not yet established. There is little evidence that large, rounded CD8 cells derived from haematogenous monocytes enter the CNS, particularly in TAI, where evidence for disruption of the blood-brain barrier is lacking (Maxwell et al 1988). However, perivascular macrophages can appear in the brain in cerebrovascular accidents when these cells are generally limited to the vicinity of a lesion and do not enter the neuropil but remain, perhaps for years, within the perivascular space (Kida et al., 1993; Bechmann et al., 2001).

4.4.2. Microglia

These cells form a network of immunocompetent cells in the CNS that differentiate from cluster domain 45 (CD45) and CD34+ bone marrow precursors that colonise the foetal brain (Santambrogio et al., 2001; Asheuer et al., 2004). CD4, and leukocyte common antigens, are expressed by different microglial subpopulations (Streit and Graeber, 1993). Microglia are subdivided into two groups in adult animals (Hickey

and Kimura, 1988): perivascular microglia and ramified microglia, also termed resting microglia, because the latter have been regarded as quiescent cells possessing only a small number of relatively short, branching cell processes. The two subtypes of microglia differ, however, immunologically since perivascular microglia express high levels of CD4 (Engel et al., 2000) and CD45 while parenchymal microglia express only low levels. Macrophages and perivascular cells express peptide loaded MHC class II molecules, for example macrophage-related protein (MRP) 8 and MRP14. But intrinsic microglia do not. Rather the latter express “empty” or peptide-receptive class II MHC. Intrinsic microglia express cathepsin S and L but not F. Cathepsin F occurs only on resident, mature macrophages, while cathepsin S is expressed by undifferentiated or immature cells. One, current view is that intrinsic microglia are immature, relatively undifferentiated cells that are well placed to provide a “graded” response and are capable of great morphological plasticity under degenerative, inflammatory and autoimmune conditions (Santambrogio et al., 2001). Following injury to the CNS, the concept of microglia activation involves differentiation from ramified microglia to amoeboid macrophages. This process involves a stereotypical sequence of steps (Stence et al., 2001). First, in the so-called withdrawl phase, the existing ramified processes retract back into and are completely absorbed into the cell body. Second, in the motility stage, a new set of active processes, that show cycles of rapid extension and retraction, extend from the cell body. Third, in the locomotory stage, and only once new motile processes have developed, cells start to relocate within the tissue and may be identified by immunocytochemical markers for cell surface receptors of which some 60 have been documented (Guillemin and Brew, 2003). Examples of routinely used labels for microglia are histochemical labelling by isolectin-B4 from *Griffonia simplicifolia*, and immunocytochemical labelling against

a multitude of proteins within the MHC complexes I and II, moreover, expression of these change throughout activation and the precise conditions prevailing at the site of that activation. For example, complement receptor type 3 (OX42), is the only immunocytochemical marker for quiescent microglia. Activated microglia may be localised using murine clone (MUC 101 and 102), MHC class I (OX18) within 1 day of injury. Between 3 and 7 days, however, reactive microglia may be labelled with MHC class II (OX6, MRP8 and MRP14) and rat macrophage marker ED1. In addition, an antibody against complement receptor 3 (CR3/43) has allowed identification of microglia in human CNS tissue (Graeber et al., 1988, 1994; Gehrmann and Kreutzberg, 1991, 1995; Svensson and Aldskogius, 1992; Kato et al., 1995) or cytoplasmic labelling for the amyloid precursor protein (APP) (Banati et al., 1993). Indeed, microglia share several antigens with different cell types including macrophages (CD11b, CD68), endothelial cells (VAM-1 = vascular cell adhesion molecule 1), lymphocytes (LFA – lymphocyte function-associated antigen, LCA = leucocyte common antigen), laminin I (LN-1) and oligodendrocytes (GD3) (Guillemin and Brew, 2003). Furthermore, the expression of surface markers changes with, for example, the period that has elapsed from the onset of activation (Kato et al., 1995, Engel et al., 2000). With expression of the major histocompatibility complex class I and II molecules the activated microglia become the antigen-presenting cells of the CNS parenchyma. They are also the primary source of brain macrophages (Streit W. et al., 1988; Lawson et al, 1994). In addition, when microglia are activated the cells become interconnected by intercellular gap junctions (connexin 43, Cx43) to allow for improved communication and possible integration of their response to a CNS insult (Eugenin et al., 2001). But, perhaps more importantly, over the last couple of decades it has become recognised that microglia respond to tissue insult with a

complex array of inflammatory cytokines and actions, and that these actions transcend the historical view of only phagocytosis and physical support enshrined in the earlier concept of “reactive gliosis”. Therefore, the concept of “glial activation” now implies a more aggressive role in responding to activating stimuli. When the blood-brain barrier is compromised or opened activation of microglia is characterized by major changes affecting cell number, cell morphology, and cell surface antigens which act on and engender responses in target cells analogous to the responses of activated immune cells in the body out with the CNS. In the absence of blood-brain barrier breakdown, however, there is a subtler response of the brain’s own immune system reflected largely in rapid activation of glial cells (Streit, 2004). Thus the role of brain macrophages and microglia after CNS injury is not just to clean up but also to reconstruct the site of injury involving production of extracellular matrix molecules, for example thrombospondin and laminin, which are substrates for growing neurites (Rabchevsky et al., 1998). It must therefore be recognised that caution should be exercised in drawing conclusions from experimental results from the vast literature related to macrophages and microglia. There is not a single marker for only microglia, or only macrophages or only pericytes in terms of immunocytochemical cell surface antibodies. Perhaps the most specific marker for microglia is labelling by isolectin-B4 from *Griffonia simplicifolia*. In summary, different subtypes of macrophages enter an injured area of the CNS than in the PNS. Also the rate of penetration of the area of injury varies with the subtype of macrophage. However, in general terms, in Wallerian degeneration within the CNS, macrophages are derived from intrinsic microglia rather than from haematogenous monocyte/macrophage precursors. Removal of axonal debris occurs more slowly in CNS tracts than in peripheral nerve. However, once removal of axonal and myelin debris has been accomplished the

microglia/macrophages are themselves removed via apoptosis in patients that survive diffuse traumatic axonal injury by 12 months or more (Wilson et al., 2004). However, requisite experiments in an animal model have not yet been undertaken.

It is also now clear that no cell type within the CNS operates in isolation either under normal or pathological conditions. There is a wide range of chemical messengers synthesised and released by or acting upon the groups of cells conventionally described within the CNS. An attempt to summarise these is provided in Table 3 (page 63).

4.3.3. Astrocytes After insult to the CNS reactive astrocytosis is by far is the commonest finding associated with injury. Astrocytes normally occupy about one third of the volume of the cerebral cortex (Norenberg, 1994) and out number neurons by ten to one. Astrocytes are organized into a syncytium mediated by gap junctions that are vital for intercellular communication and cellular homeostasis (Kettenmann et al., 1983; Norenberg, 1994). Astrocytes are involved in activities that are critical to brain function such as neuronal migration, neurite outgrowth, maintenance of the blood brain barrier and provide protection of the brain from toxicity. However a major role is that of regulation of water content via aquaporin-4 channels (APQ4), electrolyte balance and re-uptake of excess amino acid neurotransmitter content, together with modulation of immune/inflammatory responses (Norenberg, 1994) and see Table 3. Astrocytes have also been suggested to play a minor role in phagocytosis in Wallerian degeneration where astrocytes “wall off” myelin debris and have been suggested to participate in slow breakdown and removal of myelin figures (Stoll et al., 1989; Narciso et al., 2001).

Table 3: Secretory products and molecular signals between astrocytes and microglia

Factor or signal	Astrocytes	Microglia
Cytokines	IL-1 α , IL-1 β , IL-3, IL-5, IL-6, IL-8 CSF-1, G & GM-CSF, TNF- α , Monocyte Chemoattractant protein 1 Macrophage Inflammatory protein-1 α	IL-1 α , IL-1 β , IL-3, IL-5, IL-6, IL-8 INF- α , TNF- α
Growth factors	Nerve Growth factor, Transforming Growth factor β , Basic Fibroblast Growth Factor, Ciliary Neurotrophic factor, Insulin-like Growth factor, Glial Derived Growth Factor, S100 β	Nerve Growth Factor, Transforming Growth Factor α and β , Basic Fibroblast Growth Factor, S100 β
Complement Proteins	C3, C4, C6, C7, C8, C9, Factor B, Factor I, Membrane Cofactor Protein, CD46, CD11b, CD68, Clusterin, Vitrosectin	C1, C3, C4, CD11b, CD68
Coagulation Factors	Tissue Plasminogen & Urokinase Type, Plasminogen Activator	Tissue Plasminogen & Urokinase Type, Plasminogen Activator
Eicosanoides		Prostaglandin D2, Leucotrine C4
Proteases	Protease Nexia 1, α -1-Antichymotrypsin, α -2	Metalloproteinase Inhib TIMP-1 & TIMP-2
Protease Inhibitors	Macroglobulin, Cathepsin G	Cathepsin S & L
Matrix Proteins	Laminin, Fibronectin, Tenascin, Heparan sulphate, Chondroitin sulphate, Dermatan sulphate Proteoglycans	
Transport Proteins	Apolipoprotein D, Apolipoprotein B	
Adhesion Factors	VCAM-1, NCAM, ICAM-1, ICAM-2	VAM-1
Reactive N ₂ Intermediaries	Nitric Oxide	Nitric Oxide
Reactive O ₂ Intermediaries		Superoxide ions
Neurotransmitter Receptors	GABA,	GABA, purinergic receptors
Communication molecules	ATP < [Ca] _i	ATP < [Ca] _i

Early morphological studies (Norenberg, 1994) indicated two phases of response by astrocytes after an insult to the brain. First, transient swelling and development of electron lucency occurs within hours of injury. This is most notable in perivascular astrocyte foot processes where the concentration of ion pumps and receptors is high compared to the rest of the plasmalemma of the cells. There is also a high

concentration of aquaporin 4 (AQP4) water channels on these foot processes (Rash et al., 1998; Wen et al., 1999). Transport of water is important in multiple physiological processes of the brain and spinal cord, including secretion and absorption of cerebrospinal fluid, movement of fluid across the blood–brain barrier, osmosensation, and regulation of renal water conservation. In the brain, precise control of cell volume is critical, because the brain is encased within the rigid cranium, and thus, even minor changes in water metabolism may result in fatal compressive cerebral edema.

Aggregates of AQP4 subunits form square arrays in freeze-fracture preparations of astrocyte and ependymocyte plasma membranes (Rash et al., 1998). The observation of similar square arrays in renal collecting duct cells predated the discovery of AQPs but the hypothesis that AQPs are involved in cellular water transport appears to be correct. The co-ordination of the activities of separate AQP4 and potassium leak channels may facilitate “potassium-siphoning” at astrocyte end-feet (Orkand et al., 1966; Newman, 1986) during osmoregulatory activity that follows both synaptic transmission and repetitive nerve firing.

Astrocytes take up excess glutamate after nerve firing. Both glutamate stimulation and mechanical stimulation of the astrocyte plasmamembrane can cause a local increase of cytoplasmic Ca^{2+} , depolarize the cells and may initiate oscillating changes of membrane potential. Depolarization passes to neighbouring cells as a Ca^{2+} wave that spreads at a rate of $\sim 100 \mu\text{ms}^{-1}$ and results in release of adenosine triphosphate (ATP). The ATP signal promotes astrocytes and microglia to release several trophic factors (see Table 3), for example basic fibroblast growth factor, ciliary neuronotrophic factor and nerve growth factor.

The ionic disequilibrium across the astrocyte cell membrane, together with change in the activity of AQP4 channels in the perivascular plasmalemma is suggested to result

in the observed transient swelling and assumption of a lucent cytoplasm demonstrable by 24 hours after TBI in rats, and which reaches a maximum response by 3- 4 days and then subsides over the next 2-3 weeks (Arnaducci et al., 1981; Maxwell et al., 1990b). The situation in trauma is probably exacerbated by the uncontrolled release of excess neurotransmitters by injured neurons as almost all neurotransmitters induce transient, increased levels of internal $[Ca^{2+}]_i$ in astrocytes (reviewed in Hansson and Rönnbäck, 2003).

Transient swelling is followed by reactive astrogliosis manifested by accumulation of glial fibrillary acidic protein intermediate filaments within the cytoplasm of these cells. The technique used to detect this response in sections of the CNS is immunocytochemical labelling for GFAP. Application to human tissue indicates that increased content of GFAP is not evident until 4 days after injury, peaks at 2-3 weeks and then regresses over subsequent weeks although GFAP labelling may be upregulated in central white matter 5-8 years after severe head injury (Maxwell et al., 2006). The release of ATP by astrocytes, indicated above, triggers both the release of chemical neurotransmitters by neighbouring astrocytes and a delayed $[Ca^{2+}]_i$ in microglia. However, ATP release by an astrocyte also acts upon neighbouring, interconnected astrocytes to result in a number of responses. ATP acts upon an astrocyte through purinergic receptors to (1) increase synthesis of DNA and stimulate mitosis, (2) stimulate formation of cell processes and their elongation and (3) increased synthesis of glial fibrillary acidic protein (Neary et al., 1999; Hansson and Rönnbäck, 2003). There is only limited evidence at present concerning astrocyte and other glial responses in experimental TAI at least, in part, because no study has investigated more than 7 days after injury. However, one publication has provided ultrastructural evidence of mitosis by astrocytes within the parenchyma of the stretch-

injured nerve (Sharpe et al., 1996). However, evidence indicates that there is only a very limited response in tracts undergoing Wallerian degeneration where linearly organised, spindle shaped cells (isomorphic gliosis) occurs, possibly as a result of loss of nerve fibres (Kimelberg and Norenberg, 1994) and the associated reduction in volume of white matter.

4.4.4. Oligodendrocytes

The myelinating cells of the central nervous system respond only slowly during Wallerian degeneration and their response only follows loss of the axon for which they provide segments of the myelin sheath. Thus oligodendrocytes do not proliferate but instead undergo apoptosis or programmed cell death. Loss of oligodendrocytes occurs during the first week after spinal cord injury in rats and monkeys (Crowe et al., 1997) and their number may be reduced by as much as 50% in a white matter tract undergoing Wallerian degeneration (Warden et al., 2002). The loss of oligodendrocytes is associated with sequential loss of myelin associated proteins (MAPs) – for example myelin basic protein = MBP; myelin oligodendrocyte glycoprotein = MOG; NOGO-A an inhibitory molecule originating from oligodendrocyte myelin sheath of degenerating axons. These MAPs are differentially located at different areas in relation to the myelin sheath. Myelin-associated glycoprotein (MAG) occurs at the periaxonal myelin ring, myelin proteolipid protein (PLP) in compact myelin and MOG at the outer myelin membrane (Buss and Schwab, 2003; Buss et al., 2005) while NOGO is widely distributed at both inner and outer myelin membranes and in the oligodendrocyte cell body. MAG is lost first, when axonal markers are also lost, in human spinal cord at 14 days after an insult (Buss et al., 2005) and in rats between 1 and 3 days after dorsal cordotomy (Buss and Schwab, 2003). Proteins located within compact myelin (PLP) or the outer myelin membrane

(MOG) may still be detected up to 3 years after injury in humans, long after loss of the associated axon in degenerating tracts (Buss et al., 2005). However, the loss of myelin is not correlated with a total loss of oligodendrocytes since NOGO-A labelling showed that oligodendrocyte cell bodies were present in degenerated tracts between 26 and 30 years after injury although their number was reduced to 40-50% of control values (Buss et al., 2005). Another study using correlated terminal de-oxynucleotidyl transferase-mediated dUTP nick end labelling (TUNEL) and immunocytochemical identification of three types of glial cell and macrophages has identified oligodendrocytes as a cell type undergoing apoptosis 28 days after dorsal column cordotomy (Warden et al., 2001). Oligodendrocytes (RIP labelled) are dying through apoptosis rather than necrosis at sites distant from the site of injury at 28 days after injury to a rat spinal cord. Microglial activity peaks at a week and then rapidly declines (Koshinaga and Whittemore, 1995) and no OX-42+ (microglia) or GFAP+ (astrocytes) cells were TUNEL positive at 28 days after injury in rat spinal cord (Warden et al., 2001).

HYPOTHESIS

The Hypothesis that will be tested is that there is continuing loss and degeneration of central myelinated axons at survivals greater than one week after Traumatic Axonal Injury (TAI) in the right optic nerve of adult guinea-pigs.

However, in regard to the current literature reviewed in the Introduction, the following secondary hypotheses will be tested:

- that the cross-sectional area of the injured optic nerve will fall with increasing post-traumatic survival
- or the null hypothesis that there is no change in the cross-sectional area of the injured optic nerve with increasing post-traumatic survival
- that the number of intact or normal axons will fall between one, two and three weeks following TAI
- the alternative null hypothesis is that the number of intact axons is unchanged with increasing post-traumatic survival
- that there is a differential loss of intact axons between axons of different size or cross-sectional diameter with increasing post-traumatic survival
- or the null hypothesis that all sizes of axon are lost at the same rate with increasing post-traumatic survival
- that pathology comparable to that in the established literature for Wallerian degeneration will be obtained
- or the null hypothesis that no evidence of Wallerian degeneration will be obtained
- that there is no response by glial and/or non-neuronal cells following TAI in CNS white matter

CHAPTER TWO

MATERIAL AND METHODS

1. Animals

Material was obtained from 12 adult, albino Duncan Hartley guinea pigs (Harlan UK) the range of the weights of animals used was 525 - 617 grams, the mean was 571 ± 46 grams. Three animals were used as controls (sham-operated), and the other nine animals were the experimental group. This group of animals was subdivided at random into three experimental subgroups for different periods of survival after injury: one week ($n=3$), two weeks ($n=3$) and three weeks ($n=3$) survival.

Animals were deeply anaesthetised with an intraperitoneal injection of Hyponorm/Hypnovel: 2 parts water (6ml kg^{-1}) body weight. The depth of anaesthesia was confirmed by the absence of a withdrawal reflex when pressing the operator's thumbnail into the sole just proximal to the origin of the phalanges, or whether a blink reflex occurred when the tip of a pair of forceps touched an eyelid squeezed one hind foot. Topical application of xylocaine was used to provide additional, local anaesthesia prior to canthotomy and to minimise discomfort during the early postoperative period.

2. Operation

All animals were anaesthetized with an intraperitoneal injection of Hypnorm/Hypnovel: 2 parts water (6 mL kg^{-1}) and under experimental conditions the whole body of animals was placed on a heated blanket to maintain body temperature at 38.5°C , normal core temperature for guinea-pigs (Wegner and Manner, 1976). The rate of respiration was carefully monitored throughout the operation to check that the rate did not differ from normal values (mean $35\text{ breaths/min} \pm 4.2$) and that there was no change in the colour of the pinna, snout, the soles of the feet or the iris from the usual pale pink colour that might

indicate respiratory or circulatory distress. Under Home Office license and with the approval of the University of Glasgow Ethical Review Committee, the right palpebral fissure was flooded with local anaesthetic (1% xylocaine) before the eyelids were retracted using 4/0 silk sutures. Sutures were passed through each eyelid close to its free margin and the eyelids retracted to provide full exposure of the area of attachment between the conjunctiva and the surface of the globe. Using miniature scissors, the conjunctiva was excised through 360° peripheral to the limbus to allow exposure of the muscular cone formed by the extraocular muscles and the optic nerve.

A sling fashioned from sterile umbilical tape and moistened with (1% xylocain) was placed around the posterior pole of the globe and secured in front of the globe by passing sutures through the sling at least 3mm in front of the cornea, in order to avoid damage to the latter, and tying it there. A length of at least 30mm of suture thread was left free from the knot used to appose the ends of the sling.

The sutures used to retract the eyelids were removed before animals were placed in a custom-built stereotactic frame, and the animal's head secured by means of ears bars. The loose end of the suture attached to the umbilical tape sling was then attached to a pulley on a custom-built stretch-injury apparatus (Generalli et al., 1989). (Fig. 16, page 106).

At the beginning of each experiment the output from the force transducer in the stretch-injury apparatus is calibrated using a 100 g weight and recorded on the pen recorder. The head of each anaesthetised, experimental animal is placed in the stereotactic head holder and secured by use of ear canal pins. The loose end of the suture tied to the sling was threaded through the pulley on the injury apparatus before being tied about 10 mm in front of the eye. The pulley is firmly attached to an inertially compensated force

transducer (Fig. 16, page 106). The head holder has three degrees of freedom of motion and was manoeuvred horizontally and vertically until the pulley, sling and optic nerve were aligned along the longitudinal axis of the optic canal. Precise alignment is necessary to ensure that (a) the line of force applied to the optic nerve is exactly axial to the optic canal to prevent any risk of bending of the nerve around the lip of the canal to eliminate any risk of undesired, localised injury to the outer margin of the nerve and (b) to ensure that all the applied tensile loading was applied to the nerve fibres and the meningeal sheath of the nerve.

The optic nerve possesses enough inherent, mechanical flexibility or anatomical slack to allow for movement of the eyeball within the orbit *in vivo*. To achieve a standard initial state of the nerve where this anatomical slack has been overcome a pre-load of 30-40 g needs to be placed on the nerve (Gennarelli et al., 1989) This is accomplished by advancing a screw thread until the force transducer output begins to change as mechanical loading is applied to the nerve. Experimental displacement of the globe is achieved by activation of a pulse generator that moves a solenoid piston (Fig. 16). Movement of the solenoid piston provides a controlled mechanical force that results in elongation of the nerve to about 130% of its original length. This results in injury to 17-20% of axons in the optic nerve of a 740-760 gm adult guinea pig (Gennarelli et al., 1989; Jafari et al., 1997; 1998). The movement of the solenoid piston generates loading between 150 and 180 g (plus the pre-load giving a total load of 180-220 g) over periods ranging from 19 to 21 ms. (Gennarelli et al., 1989). At this force level, there have been no instances of optic nerve avulsion or of traumatic vascular injury, as assessed by noting any change in the colour of the retina, which may result from tearing of blood vessels that

supply the optic nerve or retina (Jafari et al., 1997, 1998; Maxwell et al., 1991, 1995, 1999, 2003). Throughout the operation the eye was moistened with isotonic saline and xylocaine at frequent intervals. Just before injury the pen recorder is switched on with trace paper moving at a rate of 30cmsec^{-1} , and then the trigger on the control box (Fig. 13) pressed once. A permanent record of the profile of the time course of changes in the mechanical load applied is obtained using a polygraph pen recorder. An example of record obtained from one of the experimental animals is provided in Appendix 1.

The time taken for preparation, placement of the sling around the globe, placement of the animal on the apparatus and generation of stretch-injury to the right optic nerve is 45 ± 3 seconds. In order to minimise post-operative discomfort the sling is rapidly and immediately, carefully removed, the eyelids replaced over the globe and xylocaine applied. Within 30 seconds of injury the local anaesthetic xylocaine is applied and the animal laid within an incubator where the temperature is kept at 37°C . At regular intervals regularity of breathing and any variation in skin colour is monitored during recovery from anaesthesia and the return of animals to their pens. Normal locomotion and feeding behaviour resumed within 60 minutes of operation. The Home Office in the UK and the Research Ethics Committee of the University of Glasgow approved all animal procedures.

The experiments described below and in Chapter 3 – RESULTS – utilise analysis of resin embedded material using transmission electron microscopy (TEM).

3. Fixation and Dissection for TEM.

Animals were randomly assigned to one of the three experimental groups indicated above. At a selected post-traumatic survival animals were terminally anaesthetised with intraperitoneal barbiturate and, once all respiratory movement had ceased, animals underwent thoracotomy as quickly as possible followed by transcardiac perfusion through the left ventricle. Blood was flushed from the systemic vasculature with a mammalian Ringer lactate solution for about one minute as assessed by the change in colour of the liver following opening of the superior vena cava. Clearance of blood was followed by perfusion with 2.5% glutaraldehyde in 0.2M PIPES buffer (pH 7.6, 360 mOs), (Baur and Stacey, 1977) for 30 min.

Animals were then decapitated, the skull opened, the brain removed and the optic nerves identified. The floor of the cranium and the area of the orbits were immediately flooded with fixative (2.5 glutaraldehyde in 0.2 M PIPES buffer), the optic chiasm was sectioned longitudinally to allow the entire length of the optic nerve to be dissected out and both right and left nerves removed with globe still attached. This facilitated identification of the retinal end of the nerve. The whole length, from chiasm to globe, of each left (control) and right (injured) optic nerve was then re-immersed and kept in fixative for another 48 hours at 4°C.

4. Tissue processing for TEM

A. Tissue Collection and Post-fixation.

Under a binocular, dissecting microscope each of the optic nerves was cleaned of any remnants of attached tissue but leaving the dural sheath intact. Then, using a fresh

scalpel blade, each nerve was divided into three segments of equal length and each segment placed in separate, labelled flasks.

The total length of the optic nerve of the adult guinea pig is 12-15 cm (Jafari et al., 1997) and each segment was therefore between 4 and 5mm in length. Segment 1 was defined as being adjacent to the globe, segment 2 intermediate and segment 3 adjacent to the optic chiasm. After separation, individual segments were washed in 2% sucrose in 0.2M PIPES buffer three times every 20 minutes and post-fixed in 1% osmium tetroxide in 0.2M PIPES buffer for one hour. They were then quickly rinsed three times with 0.2M PIPES.

B. Dehydration and Embedding in Araldite.

Specimens were dehydrated through 50%, 70%, 90%, and three changes of 100% ethanol for 30 minutes at each change of solute toward processing for embedding in Araldite as follows:-

Cleared in propylene oxide (2 changes) of 20 minutes each

Propylene oxide/ Araldite 753 mixtures (2:1) 12 hours

Propylene oxide/ Araldite 753 mixtures (1:2) 12 hours

100% Araldite 753 (2 changes) for a minimum of 12 hours each

Polymerization in fresh Araldite over 24 hours at 70° C.

The recipe for Araldite resin within every 26 ml of embedding medium used was:

Araldite (resin)	12.5g
DDSA (hardener)	12.5g
DMP 30 (accelerator)	0.38g
Dibutyl phthalate (plasticizer)	0.68g

After embedding and curing of resin to provide the blocks for sectioning, Dr Maxwell took all of the blocks away and coded them. I was then given coded groups of blocks to cut semi-thin and ultra-thin sections for microscopy. I was ignorant of the code used and therefore the precise identity of the animal from which any particular block had been obtained. This was done to ensure that all future treatments of blocks and gathering of data were without bias. All further processing, sectioning, examination and collection of micrographs was done using the coded identifying label.

C. Semi-thin Sections and Staining.

The blocks containing the embedded optic nerve segments were mounted onto cured resin stubs with Rapid Araldite. The blocks were trimmed to a suitable size to allow semi-thin sectioning from one randomly selected end of a middle segment of each optic nerve. Semi-thin sections were cut with glass knives until a complete transverse section of the optic nerve was obtained for the purpose of orientation of the block. These sections were stretched, dried and adhered to glass slides on a hot plate. They were stained with Toluidine blue and viewed under the light microscope in order to determine the optimal orientation for the cutting of axonal transverse sections for transmission electron microscopy. Also these sections were used later to determine the total cross sectional area of the optic nerve.

D. Transverse Thin Sections and Staining.

Serial ultra-thin sections, $\approx 75\text{nm}$ thick as judged by colour of refracted light (silver-gold) from the section, were cut on a Reichert-Jung Ultracut E ultramicrotome using a

Diatome 45 diamond knife. Sections were stretched with chloroform vapour and collected on 300 thin mesh uncoated copper grids (Agar Aids, Berkhamstead, U.K.).

A series of ten, transverse thin sections were cut from the middle segment of the right, uninjured, control optic nerves (n=3), and from the middle segment of the right optic nerve at one (n=3), two (n=3) and three weeks (n=3) survival animals after stretch-injury. Each separate section was collected on a separate grid. All thin sections were stained with fresh 12.5% methanolic uranyl acetate for 5 minutes, washed in distilled water for 1 minute and air-dried. All sections were then stained with lead citrate (2.5%) for 5 minutes (Donaghy et al., 1988). The sections were then washed in distilled water for 1 minute before being air dried in a dust free area. In order to achieve a representative but unbiased sample of transverse sections of the optic nerves, a random number generator was used to choose a number between one and ten from the set of TEM grids obtained from each animal and the appropriate numbered section was selected. Each of the ten sections obtained from each animal therefore had the same chance of being selected for examination in a Philips 300 TEM. This procedure served to minimise bias during examination of all experimental material (Jafari et al., 1997).

E. Calibration of the Transmission Electron Microscope

For each set of micrographs obtained within a single operating session, a micrograph of a calibration plate was included. An indicated X 2800 magnification micrograph of an S 104-line grating (2160 lines /mm Agar Aids, Berkhamstead, UK) was taken. When all of the plates within a cassette had been developed that photomicrograph was used to calculate the actual magnification provided by the TEM during that session. The actual magnification was $X 2400 \pm 24$.

6. Sampling Procedure.

In this type of analysis it is essential that a standard and unbiased starting point be used for the collection of raw data (Williams and Rakic, 1988; Benes and Lange, 2001; Mouton, 2002). In the present analysis the top left hand corner of the thin section was chosen (Fig. 17 and 18, page 101). Having found that reference point the first sample was taken from the first grid square that was completely covered by the optic nerve. The sections were collected on 300 mesh fine, uncoated grids (Agar Aids, Berkhamstead, UK) and this resulted in the transverse section of the whole optic nerve covering 25-30 grid squares.

The first grid square completely covered by the section was taken as the reference point and the starting point for gathering data. After photographing the top, left hand corner at an indicated magnification of X 2800, each third successive grid square completely covered by the section was photographed, moving horizontally from left to right, then right to left until micrographs had been gathered across the whole transverse section of the optic nerve. This usually resulted in 10 micrographs in each transverse section of each optic nerve. All the images collected from the segments of the control and experimental groups were used to estimate the total number of intact axons.

7. The Counting Method

The number of intact axons present in each micrograph was counted using an X-ray box. Each electron micrograph negative was placed on the illuminated screen of the X-ray box to help visualization of axons. Before counting was started a counting reference scale was

made using a correction factor derived from the calibration grid (*vide supra*) for each set of micrographs.

Use of the above correction factor allowed the subdivision of axons into seven subgroups by size or bins. Axons were grouped into seven bins, those with an axonal diameter between 0.0-0.5 μm , 0.51-1.0 μm , 1.01-1.5 μm , 1.51-2.0 μm , 2.01-2.5 μm , 2.51-3.0 μm and those of greater diameter than 3.01 μm . During counting of axons within each size range or bin – (*vide supra*) - a transparent paper was laid over the micrograph and each axon counted was marked. This prevented any double counting of axons and gave a reference of progress. Any damaged axon – was excluded. Criteria for exclusion were evidence of damage to the myelin sheath where separation of myelin lamellae had occurred, the presence of myelin intrusions, the presence of an unusually thick or thin myelin sheath, and the occurrence of an irregular myelin profile (Jafari et al., 1997, 1998). Thus, only axons that provided no morphological evidence of pathology were counted. The criteria for the latter were

- the presence of a smooth, circular transverse profile with a value for Φ greater than 0.9,
- a regular and closely packed myelin sheath within which lamellae were visible in at least 60% of the circumference,
- the axolemma was closely apposed to the internal aspect of the myelin sheath,
- there was lack of any distorted or lucent mitochondria and
- discrete cytoskeletal components were present.

The numbers obtained were plotted in tables – see appendix - according to their size and the data used to estimate the total number of axons within the section- *vide infra*.

8. Estimation of the cross-sectional area of the optic nerve.

Two methods were used:-

A. Estimation of total cross sectional area using a stage micrometer.

The total cross sectional area of each optic nerve of control and experimental animals was determined using Toluidine blue stained semi-thin sections. The cross section of the optic nerve is approximately circular. The diameter was measured along two perpendicular transverse axes passing through the centre of the axon using a stage micrometer (Fig. 17, page 101). The calculated mean was taken as the actual length of the diameter; the radius was determined from that value and the cross sectional area calculated as that of an equivalent circle ($A = \pi r^2$) with the same radius.

B. Estimation of total nerve cross sectional area using a modified point counting technique.

The semi-thin section was examined under a light microscope at x 40 and a 0.5mm graticule (Agar Scientific, Stanstead, U.K.) was placed in the eyepiece of the microscope. The cross-sectional area was estimated by placing the grid over the section and the profile of the nerve drawn onto a prepared grid of 1 cm squares. The number of point intersections between adjacent squares overlying the section was counted. This provided a value for the number of points overlying the section. The length of the sides of the squares on the graticule were then measured on a micrometer at the same magnification and provided a value for the distance between points. Multiplication of that value by the total number of points and the distances between them then gave the cross-sectional area of the nerve in square micrometers.

9. Estimation of the total area sampled in thin sections.

A S104 grating plate with 2160 lines/1mm was used to determine the actual magnification on the TEM in each set of micrographs. The true area sampled in each negative was then calculated. The value obtained was then multiplied by the number of negatives contained within each set of images for each animal and this provided the area sampled by electron microscopy for that animal.

10. Estimation of total number of axons in the area sampled in thin sections:

Using the randomized ultra-thin section (see section 3 above) used for each animal/sample a grid was placed in the TEM.

At the indicated magnification of X 2,800, the reference point (*see 6*) was found and the frame on the screen indicating the area covered by photographic negatives in the TEM was placed as closely as possible to that corner. This meant that the sample obtained was unbiased in that the only criterion for selecting the area for photography was the position of the specimen on the grid. Thus no bias for the occurrence of pathology or structural changes in the specimen was involved. The section was then systematically photographed. The top left hand corner of every successive third grid square completely covered by the section of the optic nerve working from left to right and in successive rows of grid squares were found and photographed until the entire section had been sampled (Fig. 18, page 101). The sampling method resulted in 10 ± 0.5 negatives for each animal.

These micrographs were examined by placing them on an X ray screen in order to enhance visualization of their content for easy counting (see section 6 above). In order to determine the number of each subgroup of axons in each nerve (section 6) a circle was

drawn around each axon on transparent paper as it was counted. Every axon within each bin was counted in turn and the circles on each overlay recorded progress during counts.

Axons were classed or grouped within 0.5 μ m wide bins (Section 6 above). The smallest axons (diameter between 0.0 and 0.5 μ m) were counted first in all negatives across the entire section of the nerve. Counting was then done for the next subgroup 0.51-1.0 μ m axonal diameter, and for succeeding subgroups in the series: 1.01-1.5 μ m, 1.51-2.0 μ m, 2.01-2.5 μ m, 2.51-3.0 μ m and 3.01-3.5 μ m in turn. The total count of axons in each axonal bin/subgroup in each complete transverse section was calculated. Using the magnification obtained from calibration of the TEM for that particular session, the area of each plate was calculated and multiplied by the number of plates obtained across the section. This provided a value for the sampled area (SA) or proportion of the total cross-sectional area of the nerve – for example in Fig. 15 this was 14 x the Mean Area of the EM negatives. That sum value was then divided into the total cross-sectional area of the nerve to provide a result which represented the proportion of the whole nerve that was sampled and the count results assembled into tables – see Appendix, Chapter Seven.

11. Estimation of the total number of axons:

After the total cross sectional area of each optic nerve had been measured (TA), the area of the sample (SA) was calculated, and the total number of axons (N) within each bin or subgroup in the sampled area estimated. Values were combined in the equation:

$$X = (TA/SA) \times N$$

that allowed calculation of the estimated number of axons (X) in an optic nerve. This provides an estimate of the total number of axons in the optic nerve in each animal, and, by summation, an estimate of the total number of axons within each and all bins.

12. Estimation of the cross-sectional area of axons

Late in the collection of the data for the total number of axons, it was observed that some axons occurred in relatively low numbers while others occurred in numbers that were greater by a factor of 10^2 or 10^3 . This stimulated the hypothesis that the loss of the axon's contribution to the total cross-sectional area of myelinated axons may be significant in the changes of relationships between groups of axons and the cross-sectional area of the entire optic nerve. The median value for the diameter of axons within each $0.5\mu\text{m}$ wide bin was calculated. That value was used to calculate the area of a circle of equal diameter. The area of the circle was multiplied by the number of axons within each bin at the different experimental time points. Data between experimental groups and relative cross-sectional areas were compared using standardised statistical tests.

13. Statistical analysis of raw numerical data.

Only after all counts from all experimental blocks had been completed did Dr Maxwell break the code to reveal the identity of the animals from which the blocks had been taken. The data obtained from each of the three animals in each experimental group could then be combined and the mean values and standard error of the mean (SEM) calculated. Analysis of Variance (ANOVA) was used to determine whether the differences in the number of axons were statistically significant across all experimental groups for the

cross-sectional area of the optic nerve, the total number of intact axons within optic nerves, or for the number of intact axons within each of the seven subgroups of axons/bins across groups. Comparison of differences in total number of intact axons and differences in the number of intact axons within different size groups was carried out by comparison of pairs of sets of data. However, since there is only one set of control animals, use of the *Student's t test* would have been inappropriate. Rather the *Bonferoni t* or the *Dunnnett t* test was used as appropriate.

CHAPTER THREE

RESULTS

1. The cross-sectional area of the right and left optic nerves

The cross-sectional area of control right and left optic nerves, the right optic nerve in stretch-injured animals and the corresponding left optic nerves were all measured across two discrete, perpendicular diameters. After calculation of the radius of each nerve, the cross-sectional area in μm^2 was calculated as the area of a circle ($A=\pi r^2$). The mean cross-sectional area in each experimental group (Control, 1 Week, 2 Week and 3 Week) was calculated together with the Standard Error of the Mean (SEM) for each group. The raw data is provided in the Appendix, Table 7, page 195.

The data for the experimental animals (Week 1, Week 2 and Week 3) were compared with the Controls (ANOVA, Dunnett Multiple Comparisons Test). There was no difference between controls or any of the injured right optic nerves ($p = 0.286$). Neither was there any difference overall across all control, injured right and left nerves (ANOVA, Bonferoni Multiple Comparisons Test) $p = 0.4$.

The conclusion may thus be drawn that survival up to 3 Weeks after stretch-injury to the right optic nerve does not result in either any change of size of that nerve or its relationship to the left, uninjured nerve.

2. Low magnification transmission electron microscopy:

A total of 120 micrographs were taken for the quantitative analysis described below. A small sample of these is provided as reference for the criteria of inclusion of fibres as intact and excluded as demonstrating pathology. In controls the transverse profile of axons of all sizes was regular and close to circular (Fig. 19, page 108). The myelin sheath of the axons was compact with regularly organised myelin lamellae. Both microtubules and neurofilaments are present and regularly spaced within the axoplasm as described by Jafari et al (1997, 1998). Following injury, damage reflects changes in both the myelin sheath, the relation of the myelin to the oligodendrocyte cytoplasm, a reduction in the circularity factor Φ of the axon to less than 0.8 and changes in the organisation of the components of the axonal cytoskeleton either reflecting lucency as the result of loss of a proportion of their total content of formed

axoplasmic components or an increased electron density which probably reflects compaction of NFs. The micrographs also indicate that there is possibly a time course for the changes. At 1 week (Fig. 20, page 109) the great majority of axons have a smooth profile and the myelin sheath is formed by closely packed myelin lamellae. But it is also apparent that a few axons have a reduced content of axoplasmic components, are electron lucent and possess myelin intrusions into the axon.

At two weeks, however, most notably the vast majority of nerve fibres now have an irregular or non-circular profile (Fig. 21, page 110). It may be suggested on looking at one picture that the plane of section of the fibres was not transverse. However, the irregular shape illustrated occurred throughout the optic nerve from one side to the other. Thus the organisation of the fibres within the nerves was grossly abnormal. Axoplasmic electron lucency is more discrete or marked in a proportion of nerve fibres. Moreover, in the same fibres the separation of lamellae within the myelin sheath is increased and the fibre profile is less regular or circular (Fig. 22, page 111). Within the same region or area small numbers of small diameter axons with an increasingly electron dense axoplasm occur (Fig. 21 and 22). Notably, however, the thickness of the myelin sheath in these fibres appears to be increased when compared to axons of the same diameter in control animals. Such a form is suggestive of a shrinkage or reduction in calibre on the part of the axon. In addition, at 2 weeks, there is an increased spacing between nerve fibres and the extra-axonal space contains both lucent and dense profiles of astrocytes (Fig 21, page 110).

At 3 weeks after injury there is widespread evidence for axonal loss obtained in that myelin figures occur and these frequently lack any evidence of remnants of the axon (Fig. 23, page 112). But, importantly, at 3 weeks, numbers of myelin sheaths occur which contain only foci of electron-dense material lacking any content of recognisable membranous organelles, microtubules or neurofilaments. These are thought to be nerve fibres in which the axon has degenerated but its remnants not yet removed (Fig 23 and 24, page 112 and 113). Rather the remnant remains within a sleeve formed by the myelin sheath and a well-defined periaxonal space occurs between the inner aspect of the myelin sheath and the remnants of the axon (Δ in

Fig 24). No evidence was obtained for microglia in thin sections so the mechanism or mechanisms of removal of axonal and myelin debris is presently obscure. Clearly, however, the time course of such changes is greater than three weeks after TAI.

3. The number of axons in control (un-injured) animals (n = 3):

The estimate of the total number of axons in the three, control or un-injured animals overall was $99,005 \pm 9,199.28$ (Appendix: Tables 8, 9, 10 and 11, pages 196-199). The percentage difference between control animals was $\pm 9.29\%$ and the variance was $p = 0.999$ (ANOVA). Thus there was no overall difference in the number of axons present in the three control animals.

4. The number of intact and injured axons in the right optic nerve following injury (n=9):

The estimate for the total number of axons, both intact and injured, was $92,480 \pm 944.1$ at one week after injury, $87,202 \pm 2904.57$ at two weeks and $80,427 \pm 3666.62$ at 3 weeks (Tables 25 and 26, pages 212 and 213). ANOVA showed that the differences between groups overall were not quite significant with $p = 0.086$. However, when comparison of the three experimental groups was compared with controls (Dunnett Multiple Comparisons test) there was a small but significant loss of axons by three weeks after stretch-injury where $p < 0.05$, and $q = 2.952$ for Controls against 3 Weeks survival. There was no difference between Controls and either 1 Week survivors ($p > 0.05$, $q = 1.037$) or 2 Weeks survivors ($p > 0.05$, $q = 1.87$). The hypothesis was then tested that loss occurred between 2 and 3 weeks after injury by comparing the numbers of axons between 1, 2 and 3 Weeks survivors. Use of both the Tukey-Kramer and the Dunnett multiple comparison tests confirmed that there was a significant reduction of the number of intact and damaged axons at 3 Weeks (Tukey-Kramer $p < 0.05$, $q = 4.37$; Dunnett $p < 0.05$, $q = 3.09$). But there was not loss at 2 weeks $p > 0.05$, $q = 1.91$ for Tukey-Kramer, $q = 1.35$ for Dunnett. Thus despite the fact that ICC techniques (McKenzie et al., 1996) suggest that axonal transport is disrupted within minutes or hours

after TAI and axons undergo secondary axotomy within several hours (see Introduction, sections 2.6 and 2.7) there is not a significant change in the total number of axons until between 2 and 3 weeks after injury.

A different result was obtained when only the number of intact axons was considered (Fig. 26, page 114). The total number of intact axons in the right optic nerve at one week after stretch-injury was $74,734 \pm 1,451$ (Tables 12-15, pages 200-203); at two weeks was $66,774.67 \pm 3,563.0$ (Tables 16-19, pages 204-207); and at three weeks was $55,696.33 \pm 2,496.47$ (Tables 20-23, pages 208-211), (Fig. 26, page 114). ANOVA showed that there was a loss of intact axons overall ($p = 0.0007$, Dunnett Multiple Comparisons test). Comparison between groups demonstrated a difference in the number of intact axons between control and one-week survival animals ($p < 0.05$, $q = 3.89$; Dunnett). There was also a significant loss of the number of intact axons at both 2 weeks ($p < 0.01$, $q = 5.20$; Dunnett test) and 3 weeks after injury ($p = 0.01$, $q = 6.99$). However, loss of intact axons between 1 and 2 weeks, and between 2 and 3 weeks after injury did not achieve statistical significance.

5. The number of intact axons within 0.5 μm wide bins of control optic nerve ($n = 3$).

The estimated number of axons within bins 0.5 μm wide in control animals ($n = 3$) is shown in Table 4. The raw data for each animal is provided in the Appendix, Tables 8,9 and 10, pages 196-198. Overall there was significant difference in the number of intact axons within the above bin sizes ($p < 0.0001$) (ANOVA, Tukey multiple comparisons test). The great majority of axons in the uninjured optic nerve fall between 0.5 and 2.5 μm overall diameter. The largest group of nerve fibres are between 1.5 and 2.0 μm in diameter but these are less than one third (27.78%) of the total. On the other hand less than one twentieth of the total number of axons is either of greater than 2.5 μm or less than 0.5 μm diameter (Table 4)

Table 4. The numbers of axons within 0.5 μm wide bins in control animals (n = 3)

Bin size	Mean number	SEM	% of total
0.00 – 0.5 μm	2118.66	863.5	2.2
0.51 – 1.0 μm	25030.66	4335.28	26.2
1.01 – 1.5 μm	26558.0	1239.57	27.78
1.51 – 2.0 μm	24763.0	290	25.9
2.01 – 2.5 μm	15277.33	3973.23	15.9
2.51 – 3.0 μm	1288.0	662.0	1.35
3.01 – 3.5 μm	502.33	140.47	0.52

6. The number of axons within 0.5 μm wide bins after injury (n=9)

At one, two and three weeks after the application of transient tensile strain (mean load 235.6 ± 37.2 g, n = 9) over a mean period of 19.9 ± 0.35 msecs the number of intact axons, those with a circular profile and a regularly organised myelin sheath, provided the mean values (n = 3) in table 5. The raw data for all experimental animals is provided in the Appendix, Tables 12-23, pages 200-211.

Comparison of differences of the number of intact axons within each bin between all experimental groups showed that there was loss of axons with a diameter between 0 and 0.5 μm (ANOVA, $p = 0.039$, $F = 4.5$), between 1.01 and 1.5 μm ($p = 0.038$, $F = 4.5$), of axons with a diameter between 1.51 and 2.0 μm ($p = 0.0005$, $F = 19.36$) and of axons of a diameter greater than 3 μm ($p = 0.012$, $F = 7.0$) over the experimental period. But there was no change in the number of axons with a diameter between 0.51 and 1.0 μm ($p = 0.10$, $F = 2.81$), or between 2.01 and 2.5 μm ($p = 0.32$, $F = 1.3$) or between 2.51 and 3.0 μm ($p = 0.67$, $F = 0.52$).

When comparison was carried out between Controls and the experimental groups the following results were obtained. For axons with diameter between 0.0 and 0.5 μm there was

no difference between control and one week survival animals but there was loss of axons at 2 weeks ($p < 0.05$, $q = 3.09$) and at 3 weeks ($p < 0.05$, $q = 3.26$) (Dunnett test). For axons between 0.51 and 1.0 μm , there was no change in their number from control values ($p = 0.107$, Dunnett test) throughout the whole experimental period. For axons between 1.01 and 1.5 μm there was a significant loss of axons only between 2 and 3 weeks after injury ($p < 0.05$, $q = 3.56$). There was loss of axons within the bin size 1.51-2.0 μm at 1 week ($p < 0.05$, $q = 2.94$), 2 weeks ($p < 0.01$, $q = 4.5$) and 3 weeks ($p < 0.01$, $q = 7.45$). There was no loss of axons within the bins 2.01- 2.5 μm and 2.51 – 3.0 μm . But there is loss of the largest axons occurring in the adult guinea pig optic nerve, those with a diameter between 3.01 – 3.5 μm with complete loss by 2 weeks after injury ($p < 0.05$, $q = 3.9$) (ANOVA, Dunnett).

Table 5. The mean number (\pm SEM) of intact axons in 0.5 μm wide bins at one, two and three weeks after injury. $\Delta\%$ is the percentage change from control values.

Bin size	0.0-0.5 μm	0.51 – 1.0 μm	1.01 – 1.5 μm	1.51 – 2.0 μm	2.01 – 2.5 μm	2.51 – 3.0 μm	3.01 – 3.5 μm
1 Week	754 ± 114.5	20858.5 \pm 1231.1	21005.5 ± 1781.2	20152.0 \pm 459.6	9296 \pm 3746.3	2508.5 \pm 2100.8	159.5 \pm 111.0
% $\Delta\%$	1.0 - 64.4	27.9 - 16.6	28.10 - 20.9	26.96 - 18.6	12.43 - 39.2	3.35 + 63.1	0.21 - 68.27
2 Weeks	208.7 \pm 15.5	16620.3 \pm 805.0	18927 \pm 2426.4	17723 \pm 2053.2	12841 \pm 1399.7	486.3 \pm 574.1	0 \pm 0
% $\Delta\%$	3.1 - 90.1	24.9 - 33.6	28.3 - 28.7	26.5 - 28.4	19.2 - 15.9	0.7 - 62.2	0 - 100
3 Weeks	105.0 \pm 52.3	16871 \pm 1180.8	16313.3 ± 2439.1	13096.6 \pm 614.4	8001.3 \pm 1108.5	1308.3 \pm 366.4	0.0 \pm 0
% $\Delta\%$	0.2 - 95.0	30.3 - 32.5	29.3 - 38.6	23.5 - 47.1	14.4 - 47.6	2.3 + 1.6	0 - 100

The results were also expressed graphically (Fig. 27, page 115)

Examination of Fig. 27, however, reveals that intact axons within different bin sizes are not all lost at the same rate; that is the slope of each graph is different. For example, axons with a diameter greater than 3 μm disappear completely between one and two weeks after injury

($p < 0.0001$); axons between 2.5 and 3.0 μm diameter increase in number at one week ($p < 0.05$) and then fall away; axons between 2.0 and 2.5 μm diameter fall in number at week one but then increase in number at two weeks ($p = 0.03$) before again falling at 3 weeks. The number of axons between 1.5 and 2.0 μm ($p = 0.003$) and between 1.0 and 1.5 μm ($p = 0.003$) both fall over the 3 weeks of the experimental period. However, the slope for the former group is steeper than for the latter suggesting a faster rate of change (Fig.27, page 115). Finally, the number of axons between 0.5 and 1.0 μm diameter falls in the first 2 weeks ($p = 0.032$) after injury but then is unchanged at 3 weeks ($p = 0.7$). Jafari et al. (1997, 1998) and Maxwell et al. (2003) have suggested, in shorter-term survivals, that different sized axons respond in different ways or that, possibly, axons change their calibre to the extent that they fall into different bin sizes with survival. The results in the present study provide novel evidence in support of that hypothesis and, importantly, indicate that although the axon appears structurally normal or intact at the low magnifications used in the current study there is an ongoing, slow pathology occurring that may not be Wallerian degeneration.

7. Changes in the summated cross-sectional area of axons

The finding that there was a numerical loss of axons suggested testing of the hypothesis that the total cross-sectional area of all intact axons changed over the experimental period. The median value of axonal diameter within each 0.5 μm wide bin was used to calculate the area of a circle of that diameter. That value was multiplied by the number of axons within each bin and the sum of all bins provided an estimate of the cross-sectional area of axons in the optic nerve. A literature search indicated that such an estimate has not been made previously either in a peripheral nerve, the optic nerve or any central tract. The sum total of areas of axons within all of the bins provided an estimate of the contribution made by the total cross-sectional area of the axons to the value obtained for the cross-sectional area of the whole nerve. The result was expressed as a percentage of the observed cross-section of the whole nerve. In control animals, the result demonstrated that the myelinated axons occupied 49.8% of the total cross-sectional area of the optic nerve. In terms of numbers of axons, there is a

loss of 24.40% at 1 week, 32.5% at 2 weeks and 43.74 % by 3 weeks (Fig. 28, page 115). The loss in terms of the reduced cross-sectional area of myelinated, intact axons between controls and 1 week survivals was -24.5%, by 2 weeks was -30.9% and by 3 weeks survival was -46.6%. The reduction in cross-sectional area of all intact myelinated axons is highly significant where $p=0.0001$ (ANOVA). There are also significant differences between controls and 1 week ($p < 0.01$, $q = 6.47$; Dunnett multiple comparison for differences from Control values), 2 weeks ($p < 0.01$, $q = 8.17$) and 3 weeks ($p < 0.01$, $q = 12.29$) survivals. A comparison of changes of cross-sectional area within $0.5\mu\text{m}$ wide bins provided corroborative evidence for loss of axons and for a differential rate of loss between axons of different size (Table 28, page 115) but did not add greatly to the conclusion that there is loss of axons over at least 3 weeks following TAI. Support for the hypothesis was therefore provided. Because myelinated axons contribute less than half of the total cross-sectional area of the uninjured nerve, however, their loss ought to result in a reduction in the cross-sectional area of the optic nerve by 4.3% at 3 weeks. However, no evidence was obtained in support of that idea. This generated the hypothesis that some other component of the optic nerve increases to compensate for the loss of axons.

8. Changes in morphology of astrocyte processes

During the procedure of counting axons within electron micrographs it became apparent that a variety of changes in the morphology of related astrocyte processes were occurring.

In control/sham animals, at the outer limits of myelinated axons (Fig 19, page 108), small regions of cytoplasm occur over about a tenth of the circumference of the myelin sheath. These processes represent the juxta-axonal portion of the oligodendrocyte process forming a segment of the myelin sheath. The processes of the oligodendrocytes are characterised by their high, relative content of microtubules (Fig. 19). Around these oligodendrocytes processes occur apparently empty spaces which *in vivo* contain cerebrospinal fluid. But, very infrequently, there occur thin, cell processes that insinuate between groups of axons and contain groups or bundles of fine filaments 10nm in diameter. These are the glial fibrillary

acid protein (GFAP) intermediate filaments characteristic of and unique to astrocytes. However, their number is low and astrocyte processes are widely separated in control optic nerves, although typical gap junctions may be observed between adjacent astrocyte processes (Fig. 19, gp). The routinely used marker for astrocytes is immunolabelling for GFAP intermediate filaments. But, as discussed in the Introduction, pages 60-64, immunolabelling does not identify either quiescent astrocytes or the first stage of an astrocyte reaction after injury, that of swelling by astrocytes. Moreover, the identification of changes or responses by astrocytes was not the central topic of the current investigation. The comments contained within this section therefore refer only to observations obtained in the thin sections used to estimate the number of intact axons.

One week after injury (Fig. 20, page 109) astrocyte processes appear swollen or enlarged and contain discrete bundles of intermediate filaments (Fig. 20, f). The impression is gained in Fig. 20 that astrocyte processes occupy an increased proportion of the total area illustrated. In addition, discrete gap junctions, a characteristic finding in astrocytes, may be observed (Fig. 20, g). At two and three weeks astrocyte processes progress to form more evident or discrete septae between groups of nerve fibres and appear to occupy a larger proportion of the cross-sectional area of any field used for counting of axons (Figs. 21 and 23, pages 110, 112). This qualitative evidence provides some support for the hypothesis that hypertrophy of astrocytes compensates for the loss of axons and maintains the cross-sectional area of the optic nerve.

SUMMARY OF THE RESULTS

The results demonstrate, for the first time, there is a continuous, development of pathology in axons over three weeks after stretch-injury (TAI) to the guinea pig optic nerve.

- 1) There is no measurable change in the cross-sectional area of the entire optic nerve.
- 2) The total number of intact axons falls from $99,005 \pm 7511$ in sham operated animals to $74,845 \pm 1194$ at 1 week, to $66,774 \pm 3563$ at 2 weeks and to $55,696 \pm 2496$ axons at 3 weeks after TAI.
- 3) There is a differential rate of loss between axons of different diameter. There is complete loss of the small number of the largest axons by 2 weeks. There is loss of 64% of the smallest axons by 1 week and 95% by 3 weeks. Axons with a diameter between 2.0 and $2.5\mu\text{m}$ increase in number at 1 week and their number then falls.
- 4) Morphological evidence for Wallerian degeneration is only obtained at 3 weeks.
- 5) No evidence is obtained for recruitment of monocytes or macrophages to remove cellular debris.
- 6) Qualitative evidence for hypertrophy of astrocytes is obtained.

HYPOTHESIS: SUPPORTED OR NOT SUPPORTED BY THE RESULTS

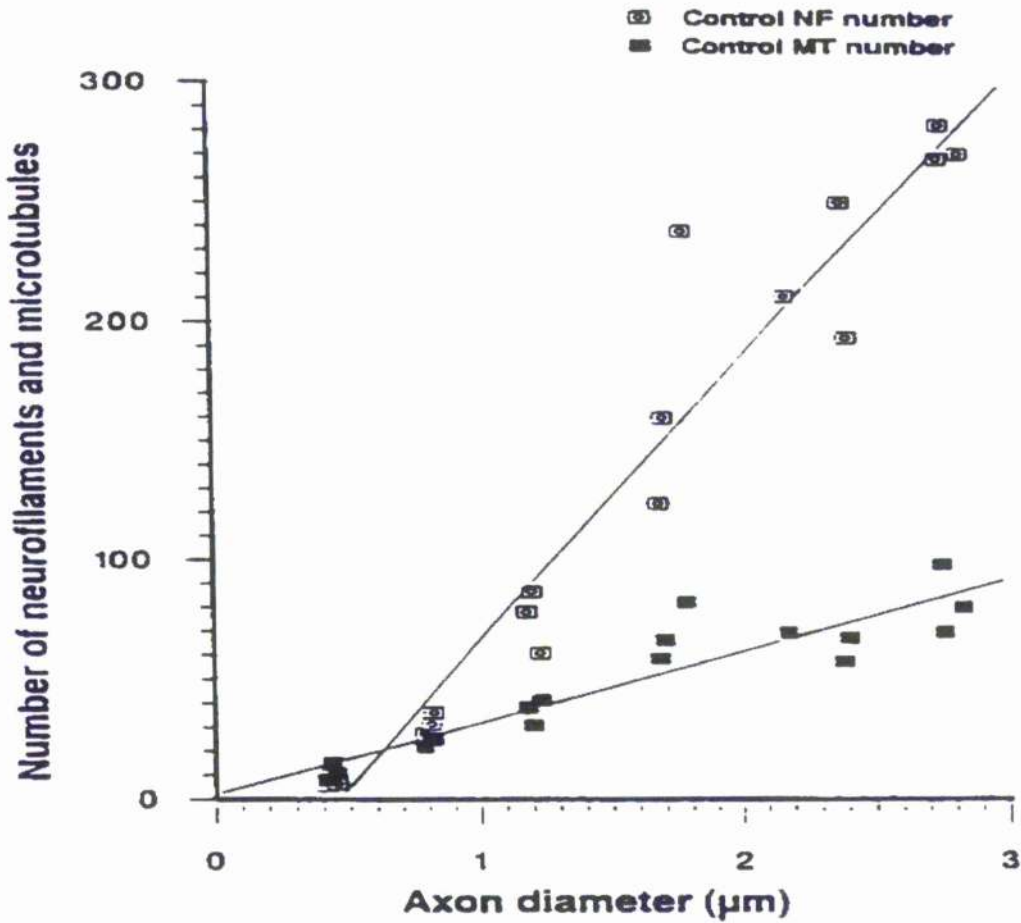
The Hypothesis tested is that there is continuing loss and degeneration of central myelinated axons at survivals greater than one week after Traumatic Axonal Injury (TAI) in the right optic nerve of adult guinea-pigs. The Results provide support for the above.

However, in regard to the current literature reviewed in the Introduction, the following secondary hypotheses will be tested:

- that the cross-sectional area of the injured optic nerve will fall with increasing post-traumatic survival. The Results do not provide support for the above.
- or the null hypothesis that there is no change in the cross-sectional area of the injured optic nerve with increasing post-traumatic survival. This hypothesis is proven.
- that the number of intact or normal axons will fall between one, two and three weeks following TAI. The Results provide strong support for this Hypothesis.
- the alternative null hypothesis is that the number of intact axons is unchanged with increasing post-traumatic survival. This hypothesis is unsupported.
- that there is a differential loss of intact axons between axons of different size or cross-sectional diameter with increasing post-traumatic survival. This hypothesis is supported.
- or the null hypothesis that all sizes of axon are lost at the same rate with increasing post-traumatic survival. This hypothesis is not supported.
- that pathology comparable to that in the established literature for Wallerian degeneration will be obtained. This hypothesis is supported.
- or the null hypothesis that no evidence of Wallerian degeneration will be obtained. This hypothesis is not supported.
- that there is no response by glial and/or non-neuronal cells following TAI in CNS white matter. This hypothesis is not supported.

CHAPTER FOUR
ILLUSTRATIONS AND FIGURES

Fig.1. Relationships of the number of neurofilaments (NF) and microtubules (MT) to the diameter of an axon in control/sham operated guinea pig optic nerve. (After Jafari et al., 1998, J. Neurotrauma 15, pp958)



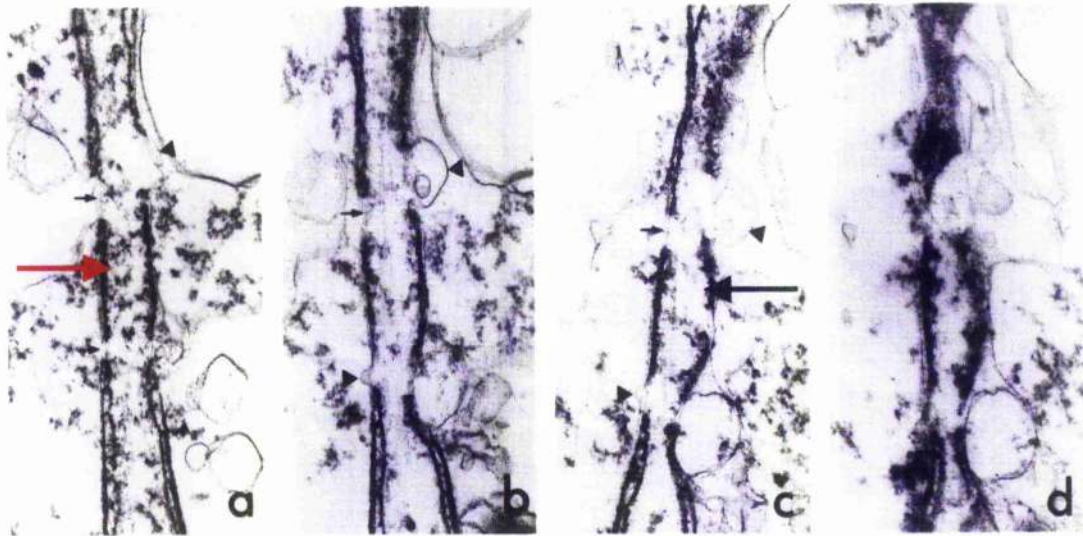


Fig. 2. Serial sections from an animal 20 min after lateral head acceleration through a node of Ranvier in an axon that has undergone primary axotomy. Holes occur in the axolemma (arrowhead). The most marked pathology is the replacement of the axonal cytoskeleton by a flocculent precipitate (red arrow) indicating rapid dissolution of the cytoskeleton. The characteristic dense undercoating of the nodal axolemma is retained (black arrow) (Courtesy of Maxwell et al., 1993). *Acta Neuropathol.* **86**: 136-144.

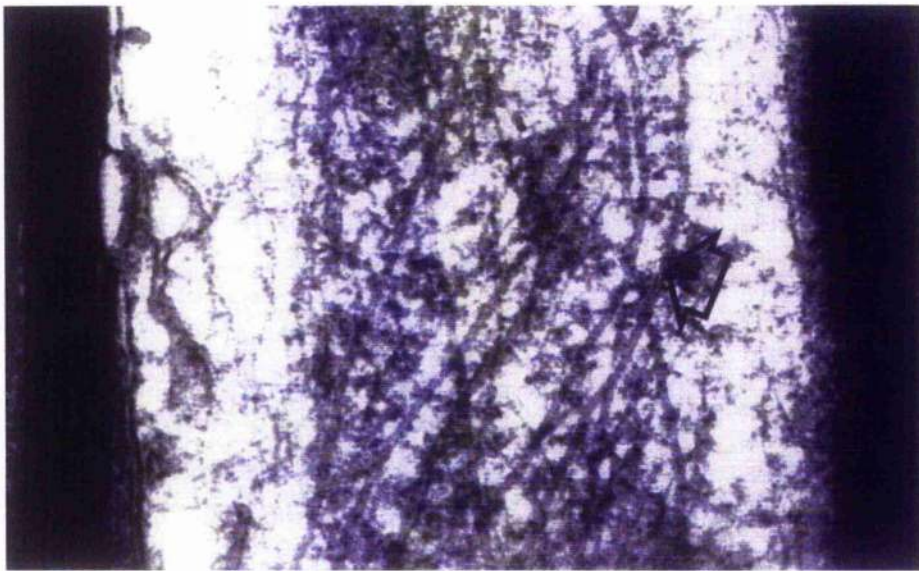


Fig. 3a. A longitudinal section of the internode of an injured axon at 4hrs after injury. The microtubules, one is indicated by the black arrow, of the cytoskeleton have a spiral rather than linear orientation.

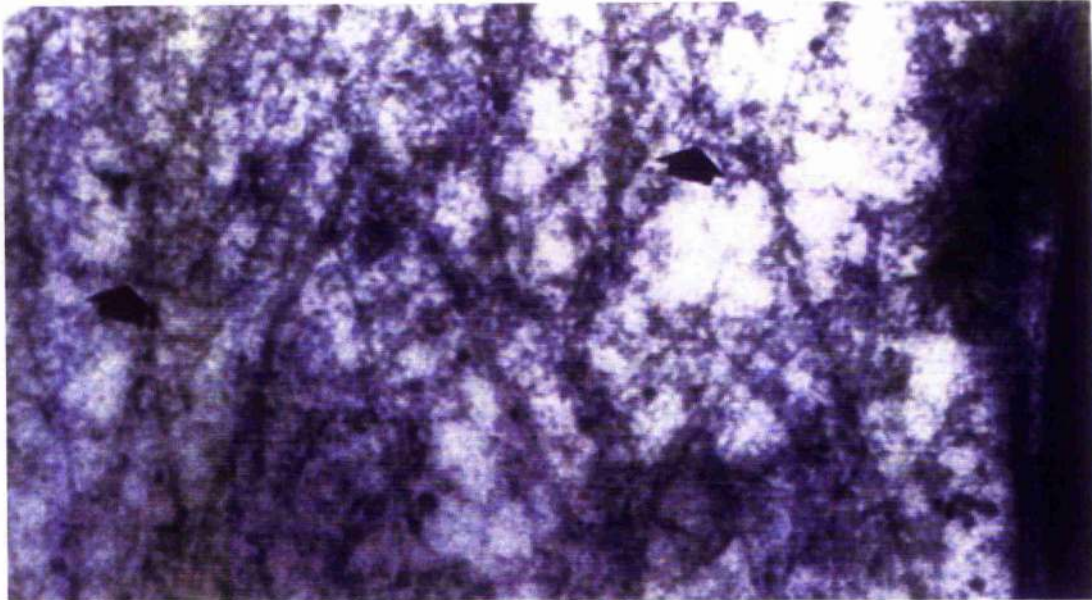


Fig. 3b. A field of axoplasm taken from a longitudinal section of an internode of a nerve fibre at 4 hours after injury. The orientation of NFs is no longer parallel to the longitudinal axis of the fibre. Black arrows indicate two NFs with a transverse orientation. But close examination reveals that NFs have a wide variety of orientations within the axoplasm. (Courtesy of Jafari et al., 1997) *J. Neurocytol.* **26**: 207-221.

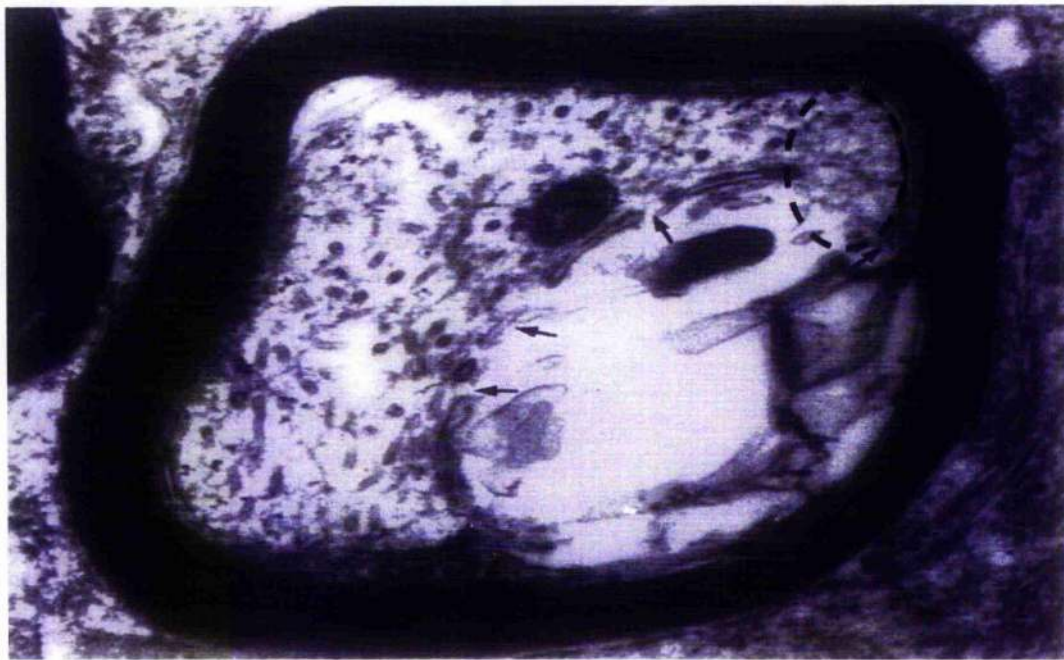


Fig. 4. A medium power transverse section of an internode from a nerve fibre 4 hours after injury. The axon has an irregular profile and the axolemma is incomplete (arrows) with the result that there are holes therein. At foci the discrete organisation of the axonal cytoskeleton has been replaced by an amorphous ultrastructure (dotted circle). (Courtesy of Maxwell et al., 1995) *J. Neurocytol.* **24**: 925-942.

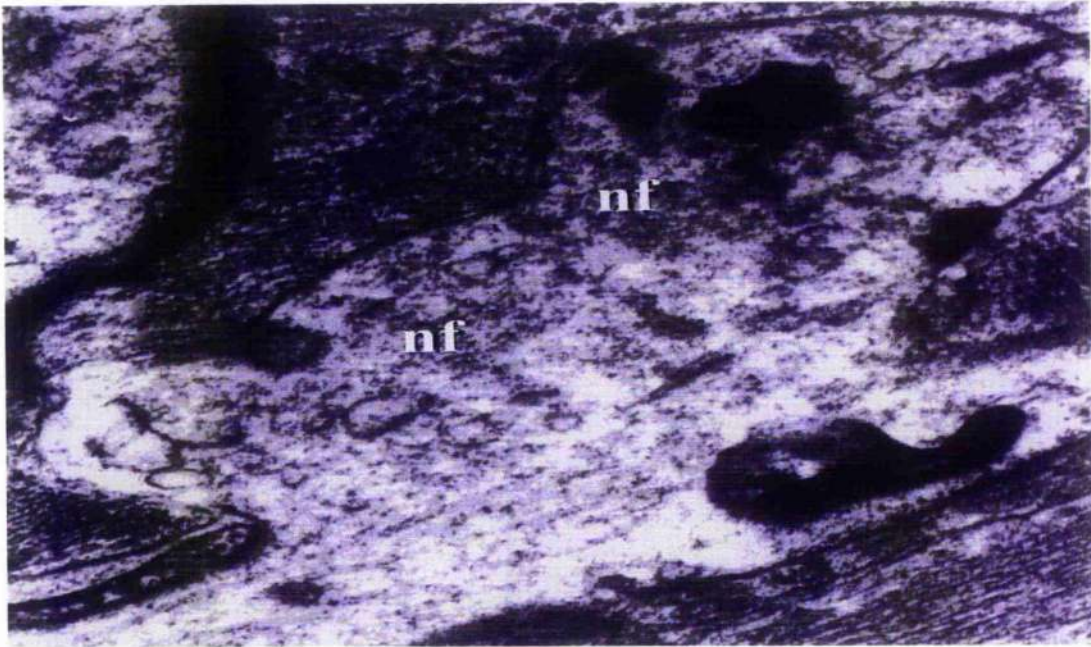


Fig. 5. Longitudinal (upper) and transverse (lower) sections of nodal blebs at 5 mins after stretch-injury to the right optic nerve of guinea pig. Axolemma limited protrusions extend into the periaxonal space. Within these there is a flocculent ultrastructure and some aggregates of membranous profiles, but MTs (mt/arrow) and NFs (nf/arrowheads) are lacking. The dense undercoating characteristic of the nodal axolemma (red arrow) is lacking from the limiting membrane of the bleb (right side of b and in a). (Courtesy of Maxwell, 1996 and Maxwell et al., 1991) *J. Neurocytol.* **20**: 157-164.

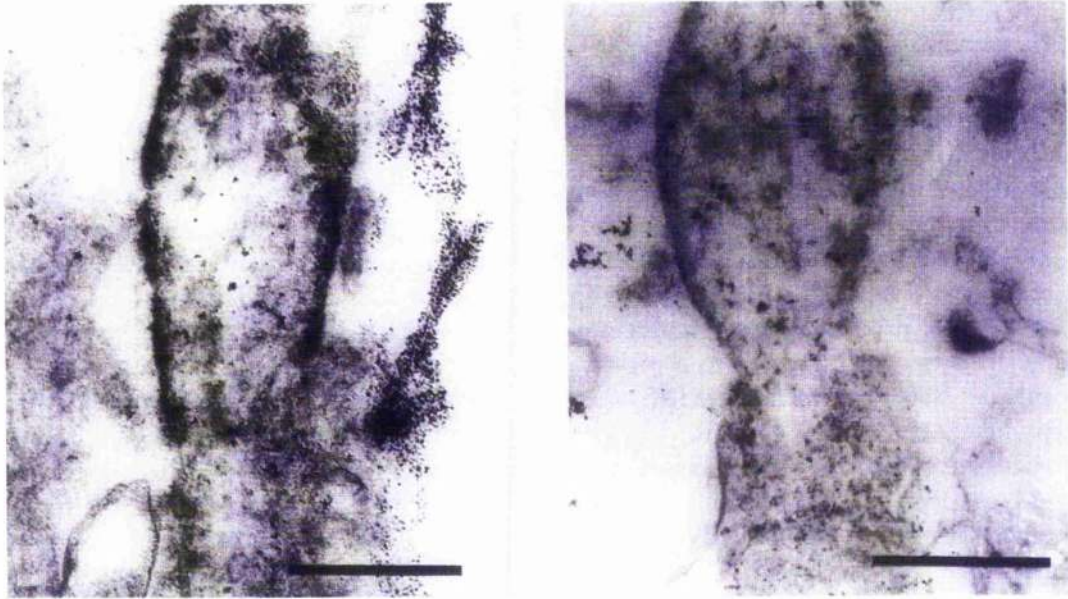


Fig. 6. Thin sections cytochemically treated to demonstrate activity of p-NPPase (Na/K-ATPase). In a control, uninjured node of Ranvier (left) reaction product (black deposit) occurs on the axoplasmic face of the axolemma. At 1 hour after injury (right) reaction product does not occur indicating a loss of activity by the pump. Bar = 1 μ m.

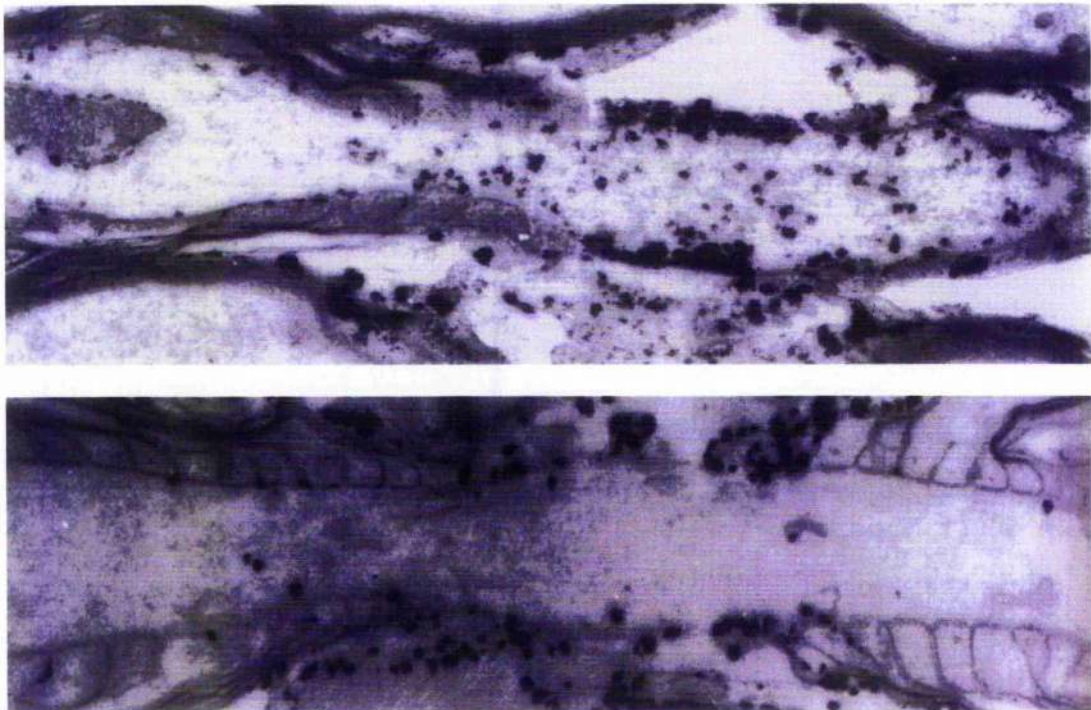


Fig. 7. Longitudinal thin sections of nodes of Ranvier from control (top) and 1 hour after injury (bottom) optic nerves processed for localisation of membrane pump Ca^{2+} -ATPase activity. There is marked loss of reaction product from the nodal axolemma in the injured axon demonstrating inactivation of the membrane pump. (Courtesy Maxwell et al., 1995) *J. Neurocytol.* 24: 925-942.

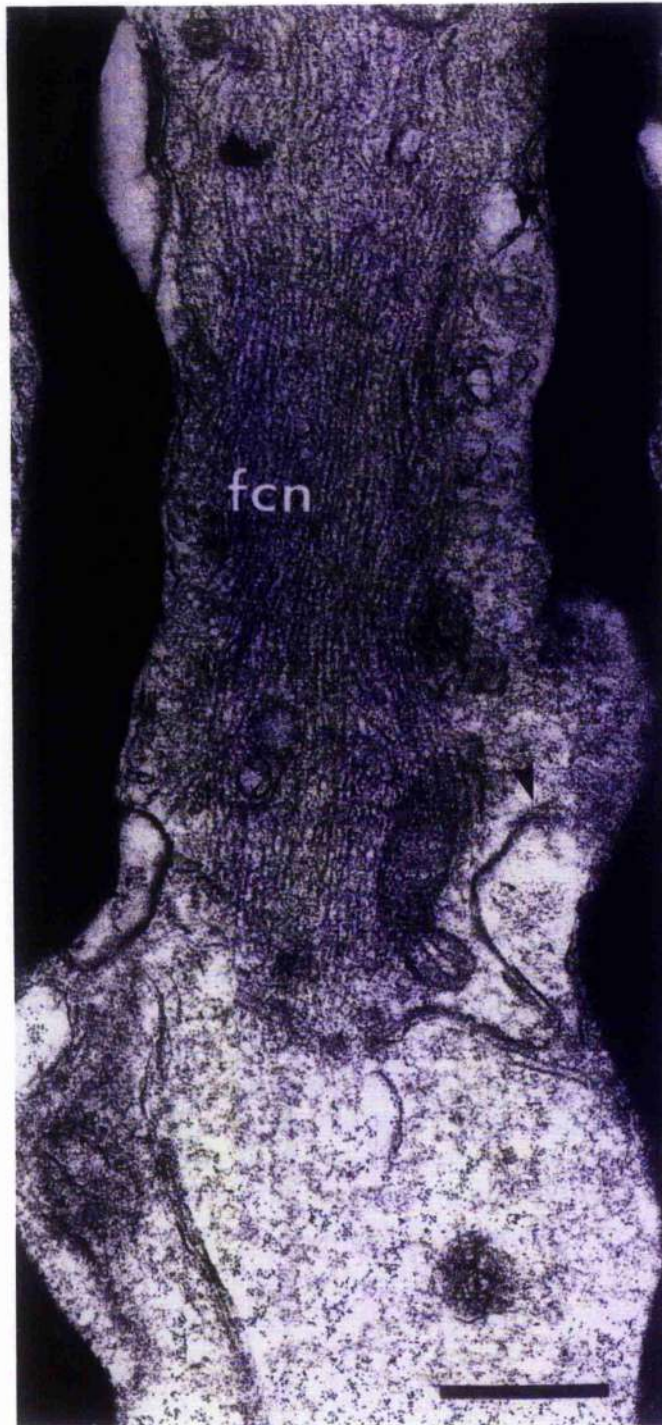


Fig. 8. A longitudinal thin section at the point of secondary axotomy obtained at 4 hours after stretch-injury to guinea pig optic nerve. NFs form a focus of neurofilament compaction (fcn) in the middle of the image. At the lower limit of this region the axolemma is fragmented (arrowheads) and below that point a flocculent precipitate replaces the linearly packed NFs. Here axonal continuity has been lost and the axon has undergone secondary axotomy. Bar = 1 μ m).

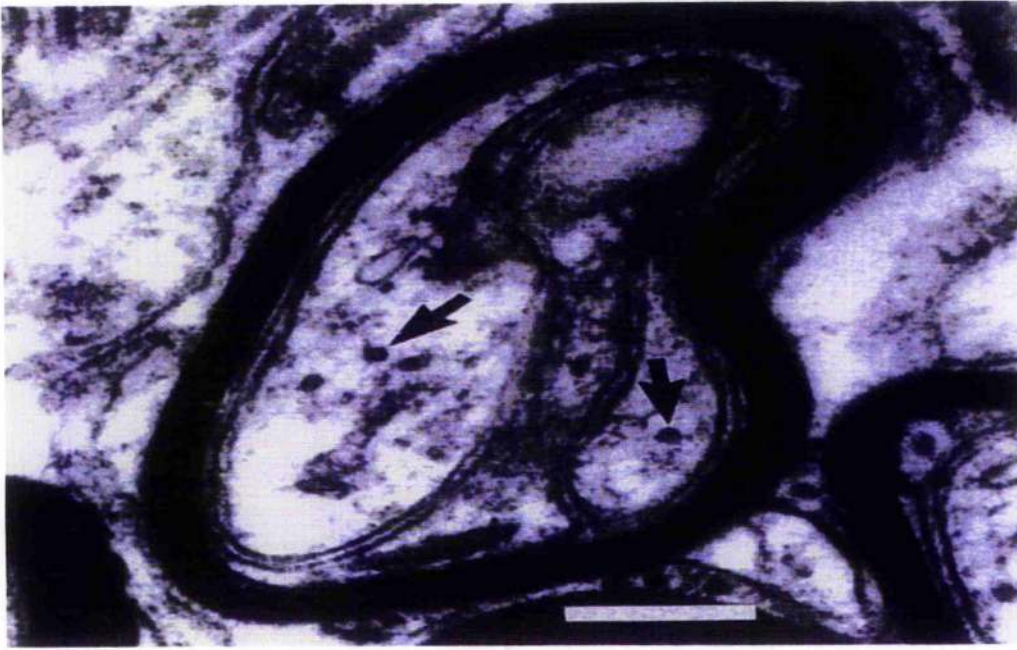


Fig. 9. A transverse thin section at 4 h after injury in which there is involution of the axolemma to provide an irregular axonal profile. There are very few cytoskeletal components present within the axoplasm (arrows = MTs). Bar = 1 μ m. (Courtesy of Maxwell and Graham *J. Neurotrauma* 14: 610).

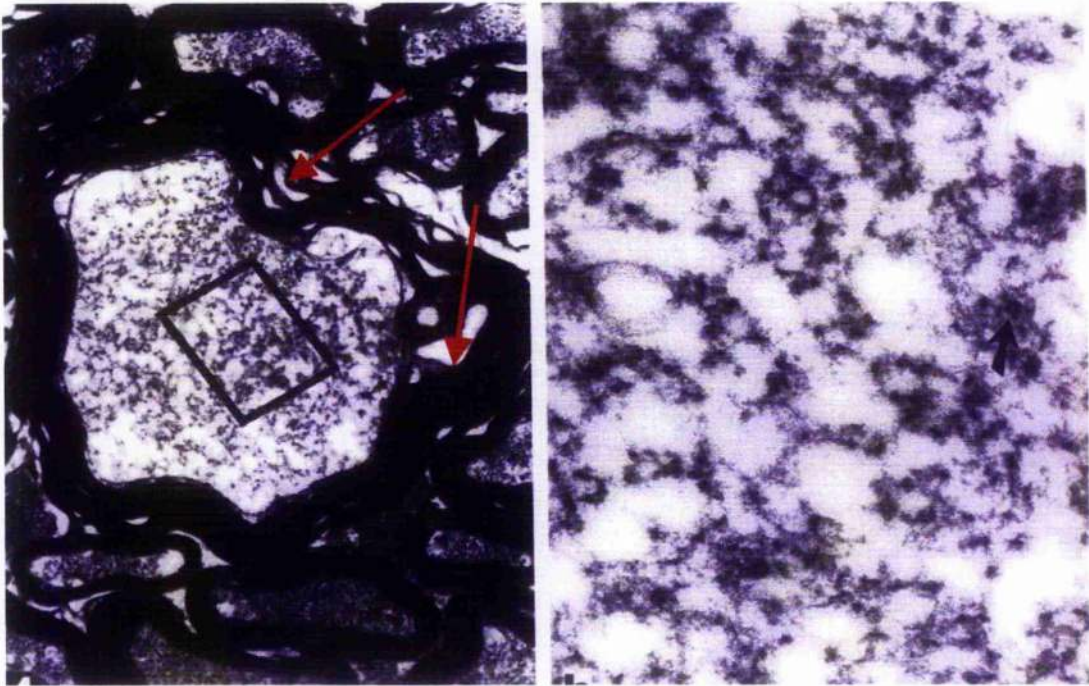


Fig. 10. A transverse thin section of a larger myelinated fibre at 4 hours after injury which has lost a high proportion of MTs (arrow on right) and myelin lamellae have separated to form "intramyelinic spaces" (red arrows). At higher magnification (right) from the demarcated area at low power, loss of MTs and an increased spacing between NFs is visible.

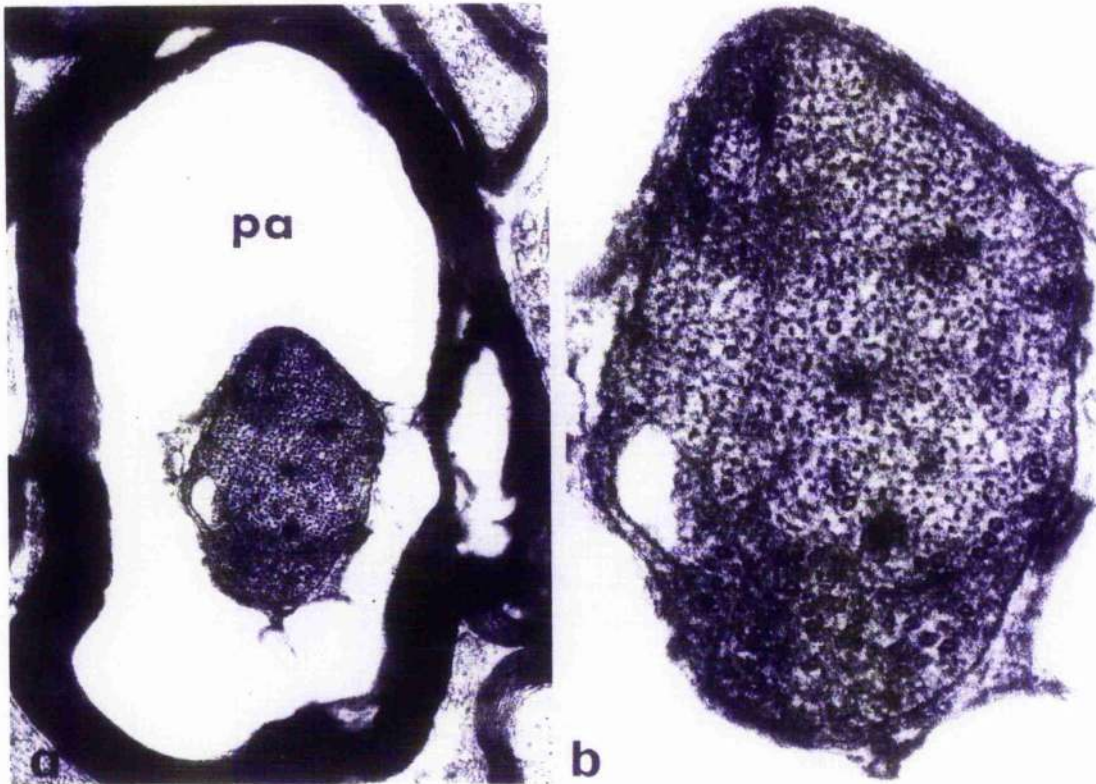
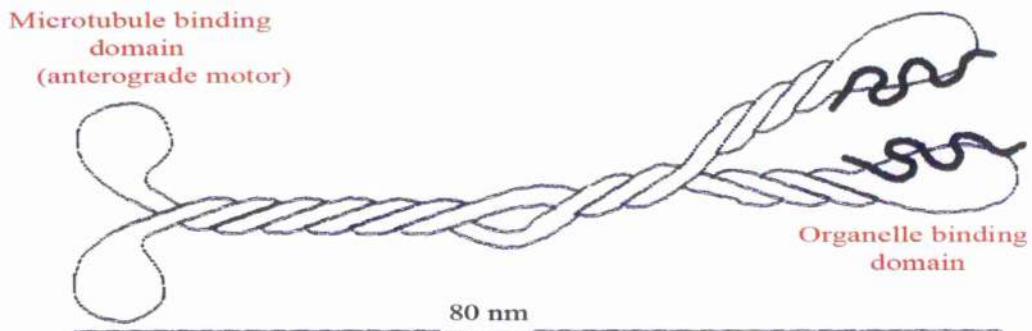


Fig. 11. A transverse thin section of a nerve fibre in which the periaxonal space (pa) is enlarged. The whole fibre with the limiting myelin sheath is shown in Fig a. Fig b is a detail of the axon to illustrate the low number of microtubules and the reduced spacing between or compaction of the neurofilaments. This specimen was obtained at 4 hours after TAI.

Fig. 12: Schema for kinesins



(modified after www.bms.ed.ac.uk)

Fig. 13. A schema, modified after www.bms.ed.ac.uk, for the organisation of dynein.

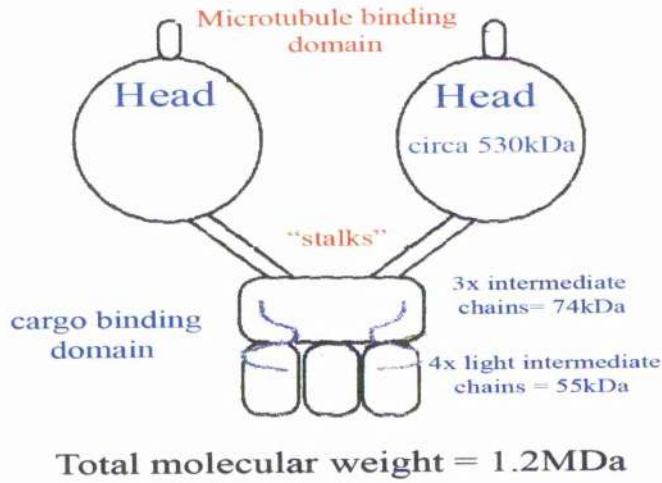


Fig.14. A schema illustrating the major components and cells active during Wallerian degeneration in the CNS. After injury, for example partial transection, to the spinal cord the astrocytes (orange) and oligodendrocytes (black) are rapidly activated. Macrophages (purple) enter the area of injury from the blood and begin to remove axonal and myelin debris. At the same time, reactive astrocytes enlarge and begin to proliferate. Astrocytes become interlinked by gap junctions and a glial scar is formed.

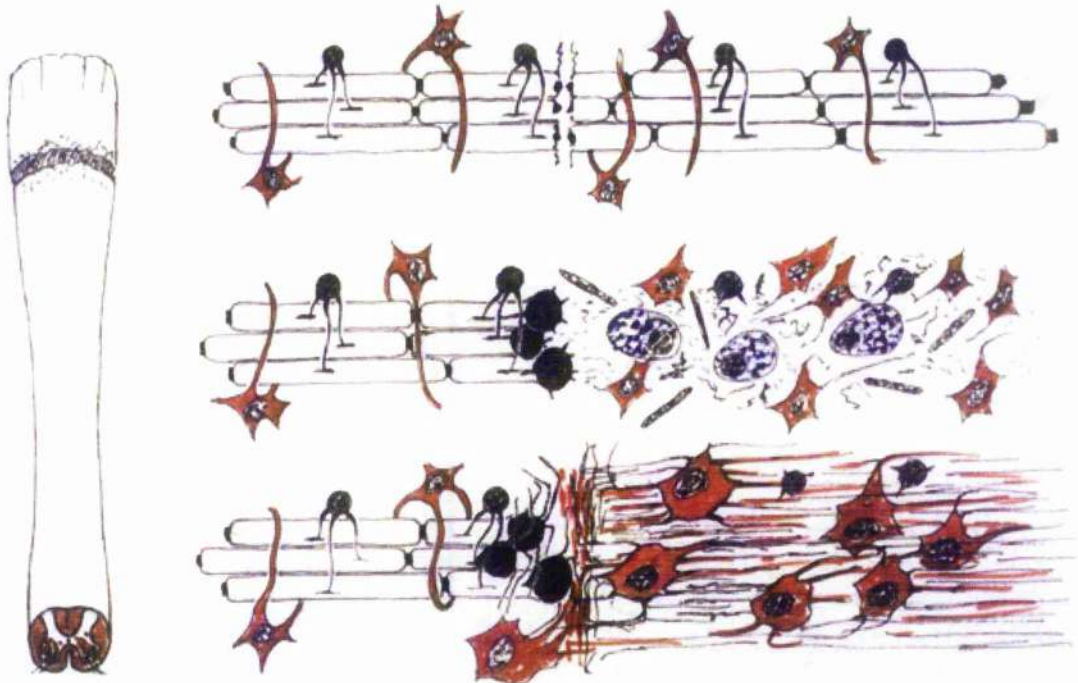
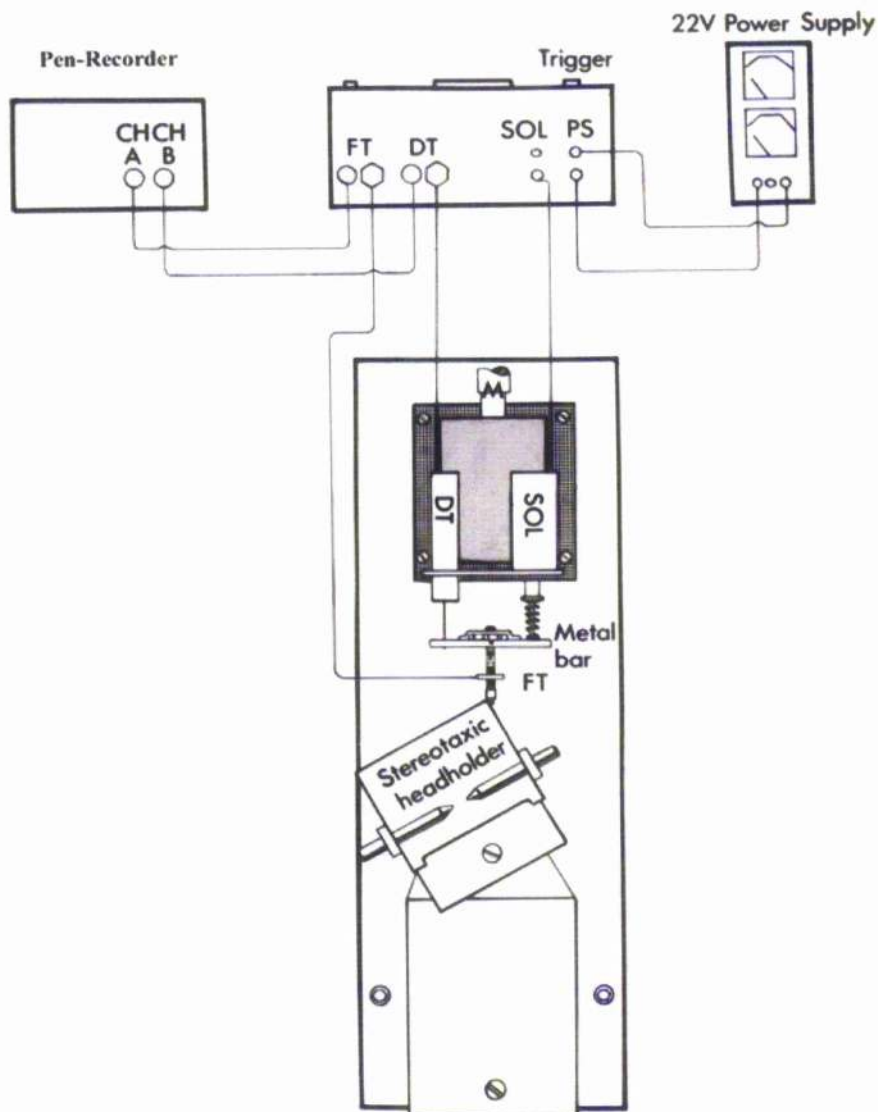




Fig. 15. A transverse thin section of two degenerating axons obtained 7 days after injury. The profile of the myelin sheath is irregular with a number of intramyelinic spaces. The axon has been lost and replaced by an amorphous, flocculent precipitate (fp). Bar = 1 μ m.

Fig. 16. Schema to illustrate the components of the custom stretch-injury apparatus designed to deliver a reproducible and measurable amount of elongation or tensile strain to the optic nerve.



(Meanings of Labels on the schema: FT = force transducer, DT = displacement transducer, SOL = solenoid, CHA and CHB recording channels on the pen recorder, PS = sockets for power supply input into the "trigger" control box)

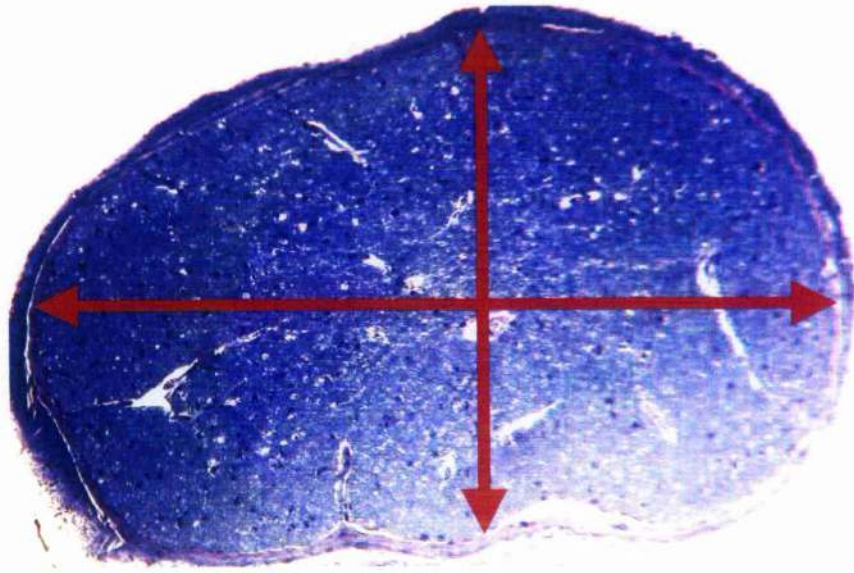


Fig. 17. A transverse, semi-thin section of a whole optic nerve stained with Toluidine blue to illustrate the orientation of the perpendicular axes used to calculate the cross-sectional area of the whole nerve.

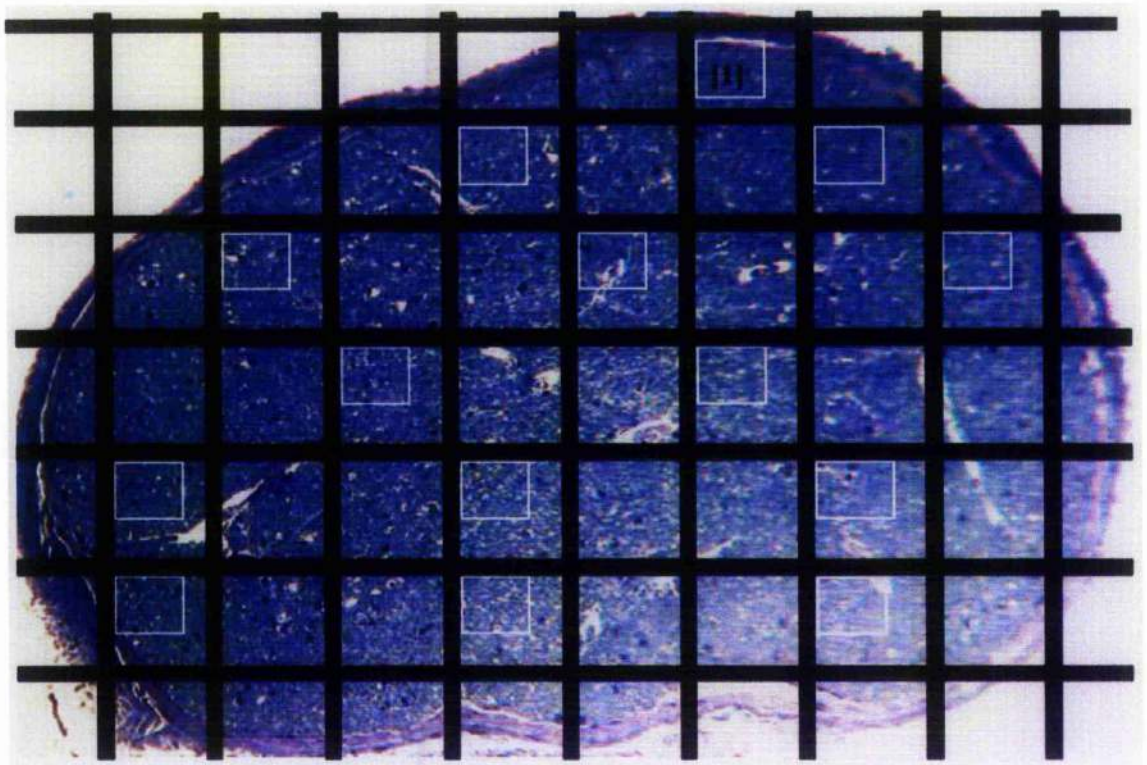


Fig. 18. A schema for the sampling method used in the TEM. The black lines represent the bars of a 300 fine mesh grid. Sampling starts at the first grid square [1] covered by the section from the top left hand corner. The white outlines indicate the area of the photographic plate taken in every third grid square across the whole transverse section of the optic nerve. Magnification circa x 90.

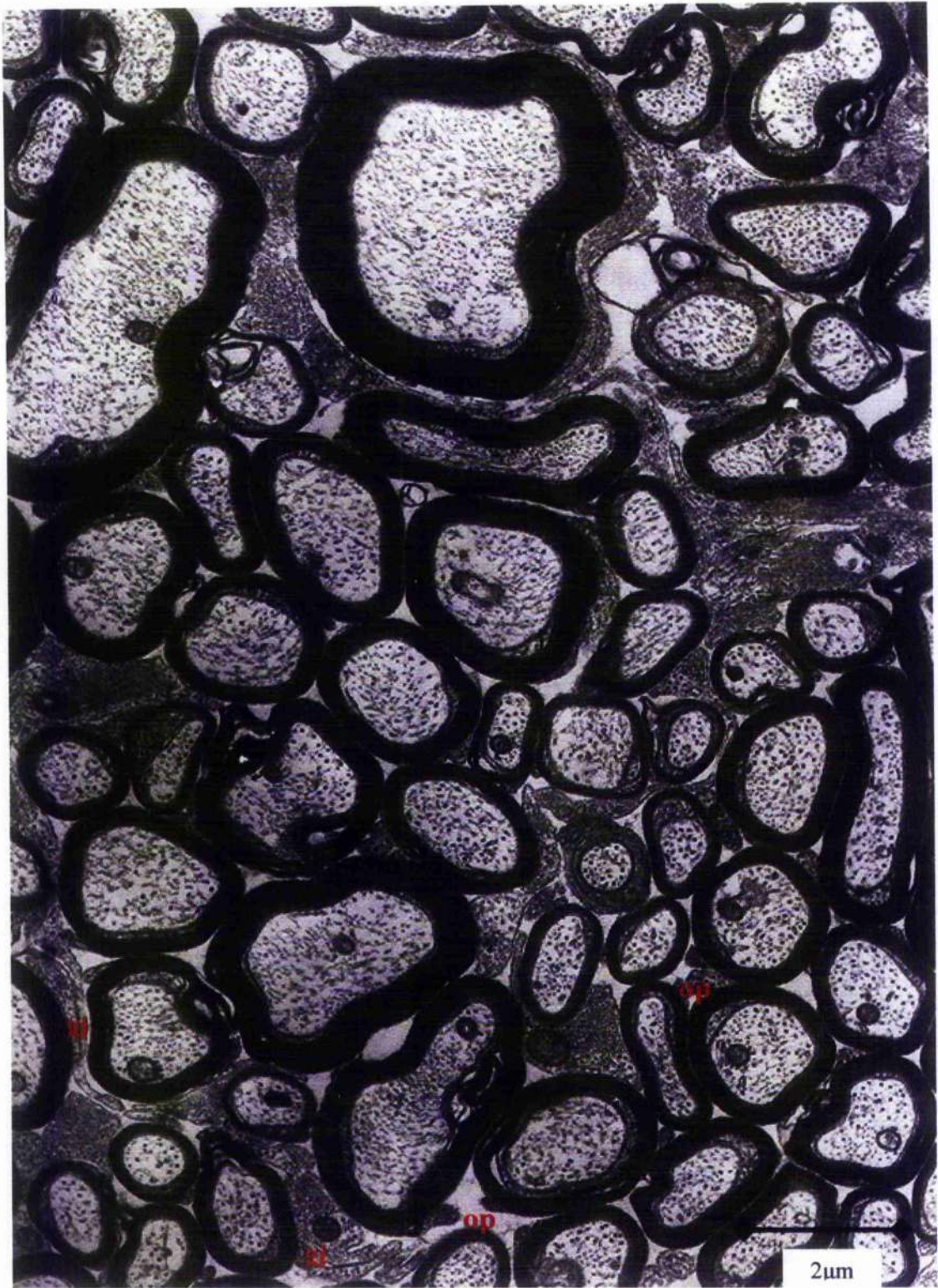


Fig. 19. A medium power field of axons from the right optic nerve of a sham/control animal. The axonal profiles are mostly smooth with a circularity greater than 0.8. The myelin sheaths are uniform and homogeneous with no evidence of intramyelinic spaces or myelin intrusions. The axoplasm is of a uniform density with clear spacing between individual components of the cytoskeleton. Occasional oligodendrocyte processes (op) occur on the outer edges of the myelin sheaths. The few astrocyte processes are joined by characteristic gap junctions (gj).

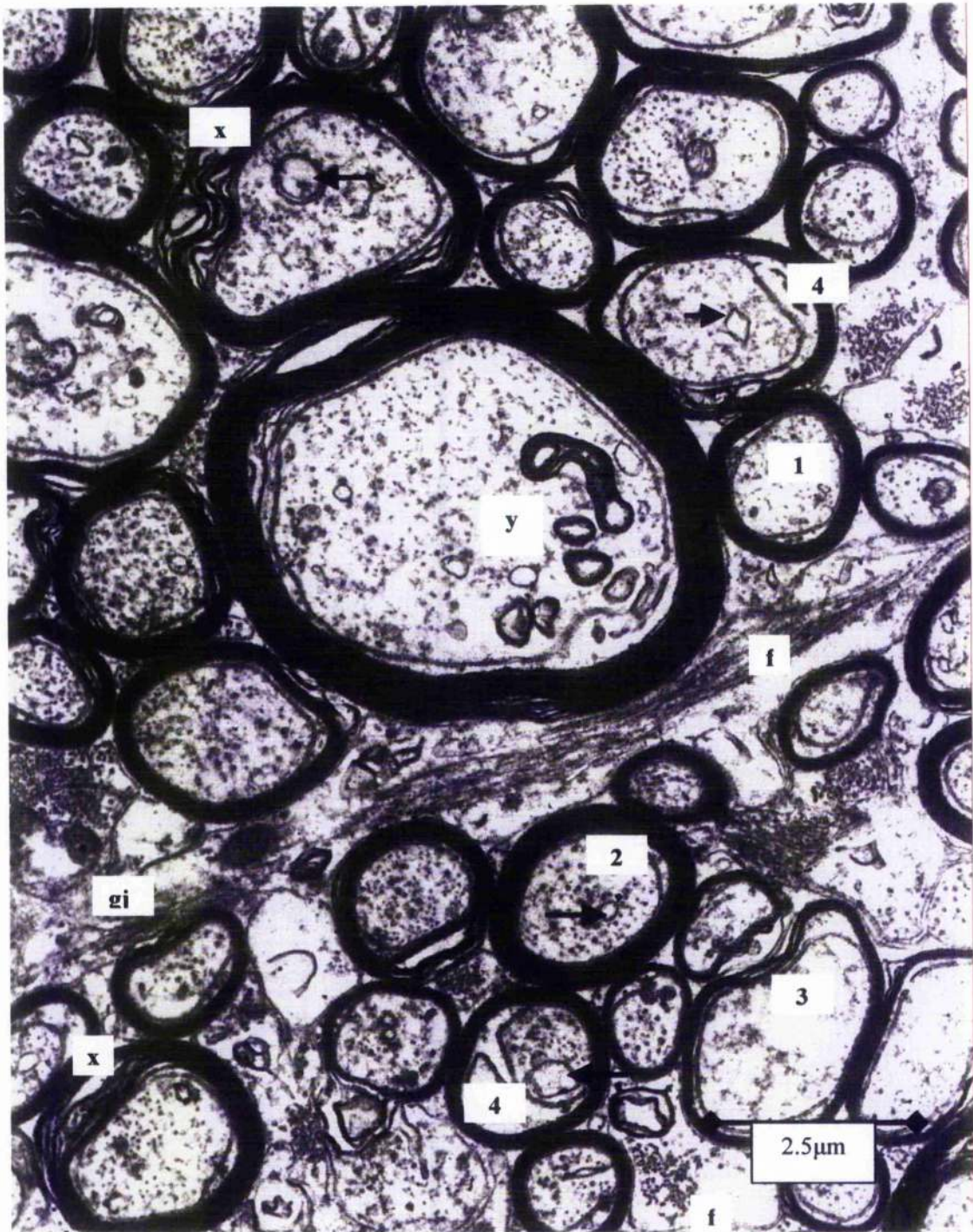


Fig. 20. A transverse, thin section of guinea pig right, optic nerve one week after stretch injury. The general organisation of the optic nerve is maintained and most fibres exhibiting a regular, circular profile in normal small (1), medium (2) and large axons. However, pathology is present either as (3) remnants of degenerated axoplasm, (x) separation of myelin lamellae, (y) myelin intrusions into the axoplasm, (arrows) swollen, lucent mitochondria and (4) an increase in the area of the tongue of oligodendrocyte cytoplasm. A gap junction (gi) is visible between adjacent, swollen astrocyte processes containing bundles of filaments (f).

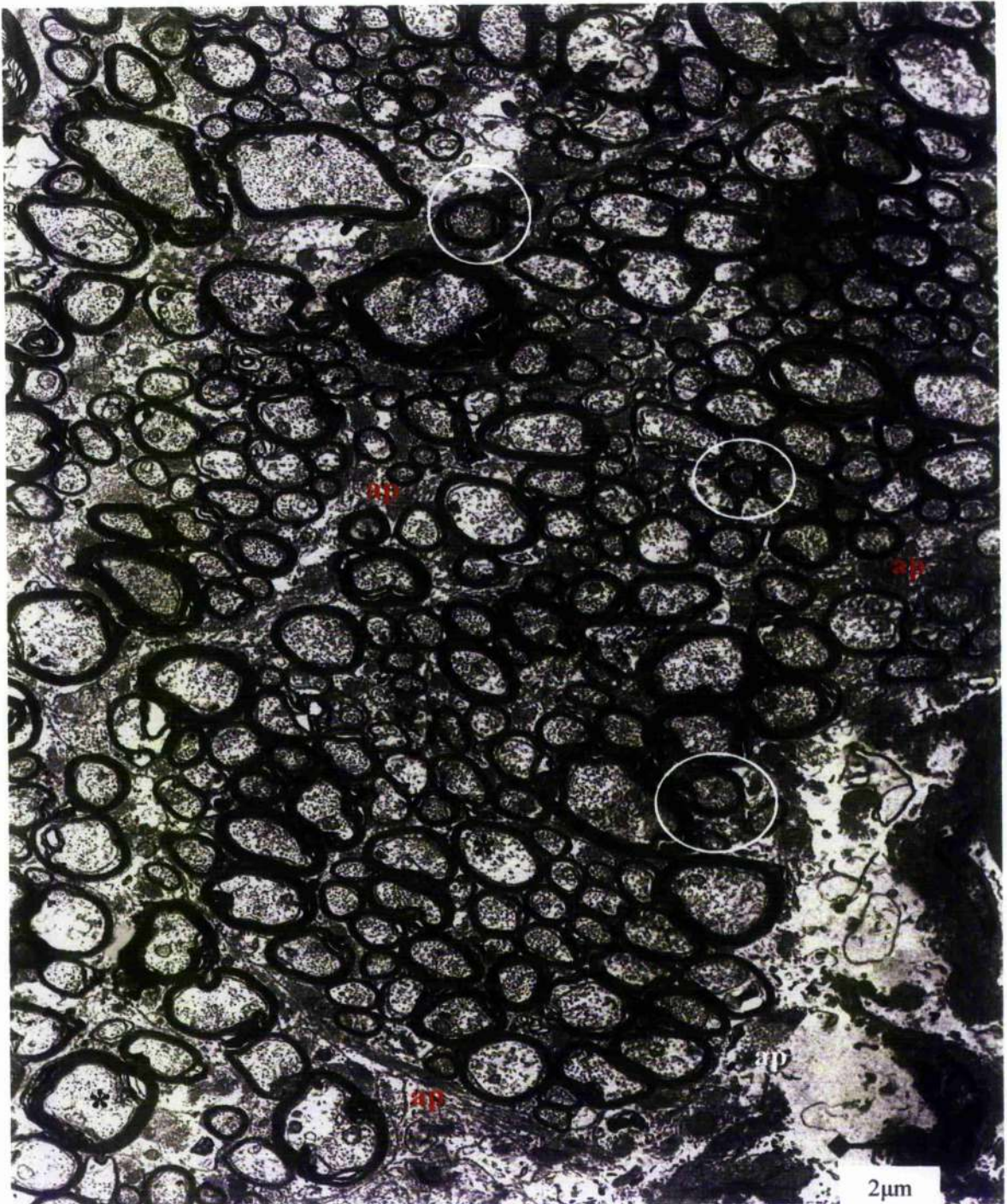


Fig. 21. Transmission electron micrograph of a transverse section of guinea pig optic nerve at two weeks after stretch-injury. Numerous axons have an irregular profile and the axons are more widely spaced. The intervening, enlarged periaxonal space is occupied by hypertrophic astrocyte processes (ap) parts of which contain aggregates of intermediate filaments. There is a notable loss of electron density in the axoplasm of some fibres (*) while in others the density is increased (white circle).

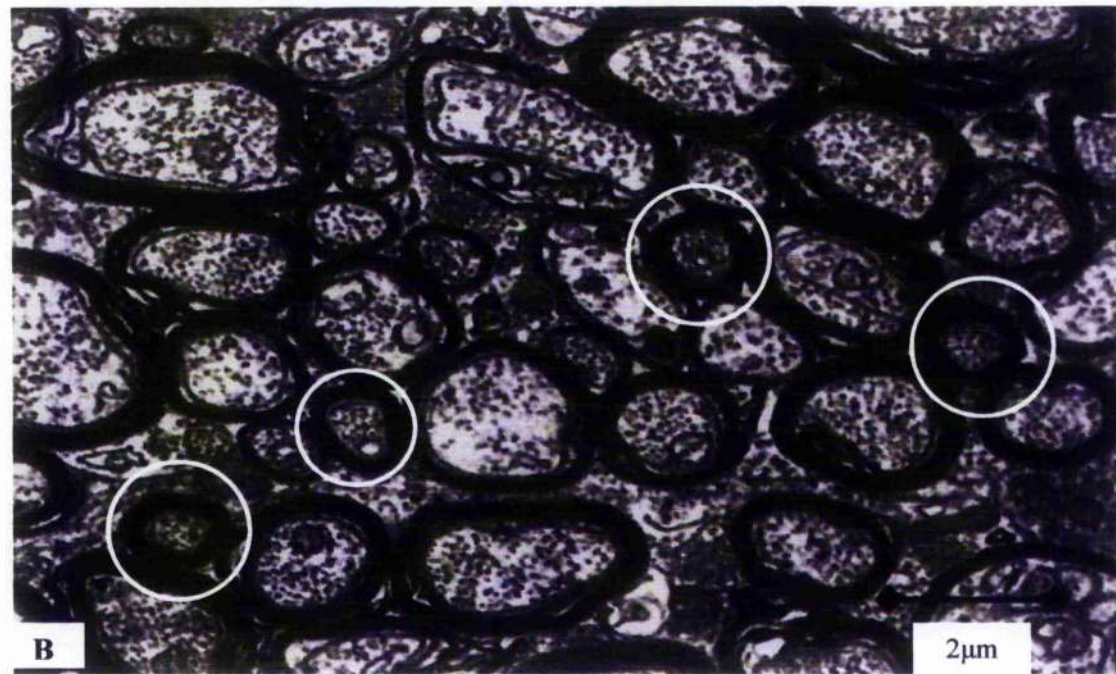
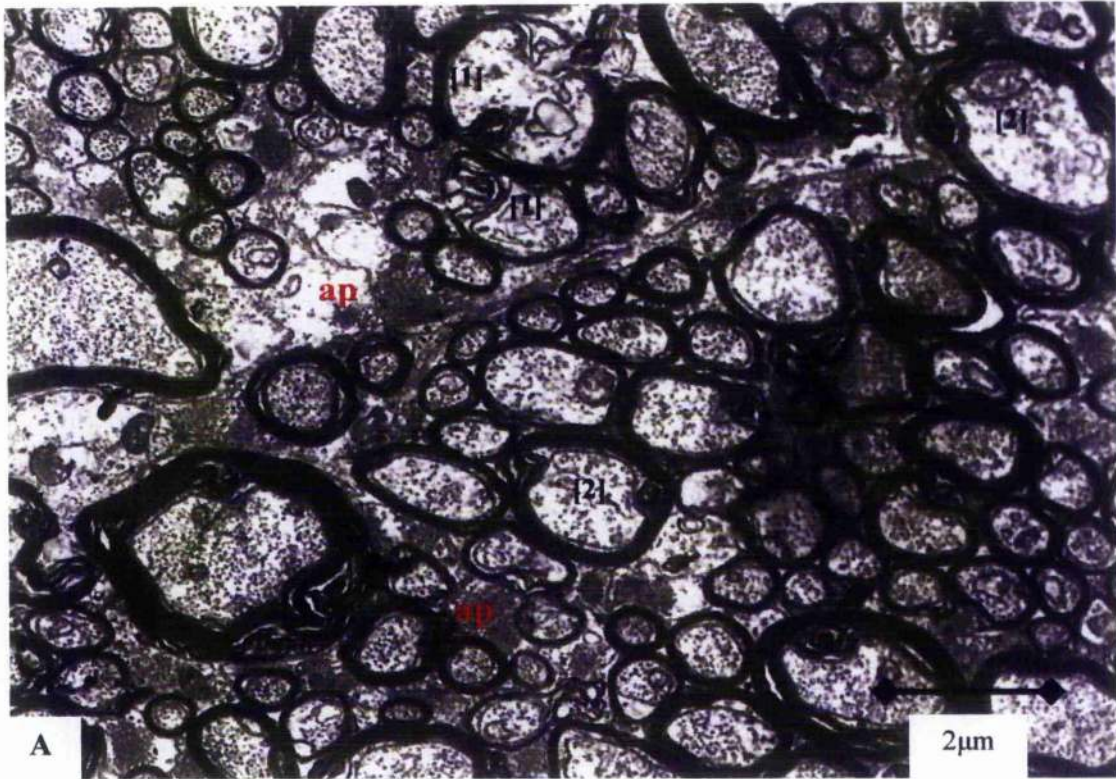


Fig. 22.

Details from Fig. 21.

- A. This illustrates loss of axoplasmic components to result in a pale axoplasm in fibres with myelin intrusions [1]. Other fibres [2] demonstrate foci of lucent axoplasm that contain low numbers of MTs and NFs.
- B. Small, electron dense axons with compacted NFs in their axoplasm are scattered through the plate (white circles).



Fig. 23. A medium power field of part of a right optic nerve at 3 weeks after injury. Several nuclei of astrocytes occur within the field and in two of these a discrete nucleolus is visible (*). Many fine processes of astrocytes (ap) extend between and among groups of nerve fibres. A variety of forms of axonal pathology occur in this field, irregular profiles with separated myelin lamellae (single arrow), larger axons surrounded by a highly convoluted myelin sheath (double arrow), myelin figures lacking any remnant of an axon (white circle) and electron dense axons with an intact myelin sheath (red circles). But many axons also have a normal structure.

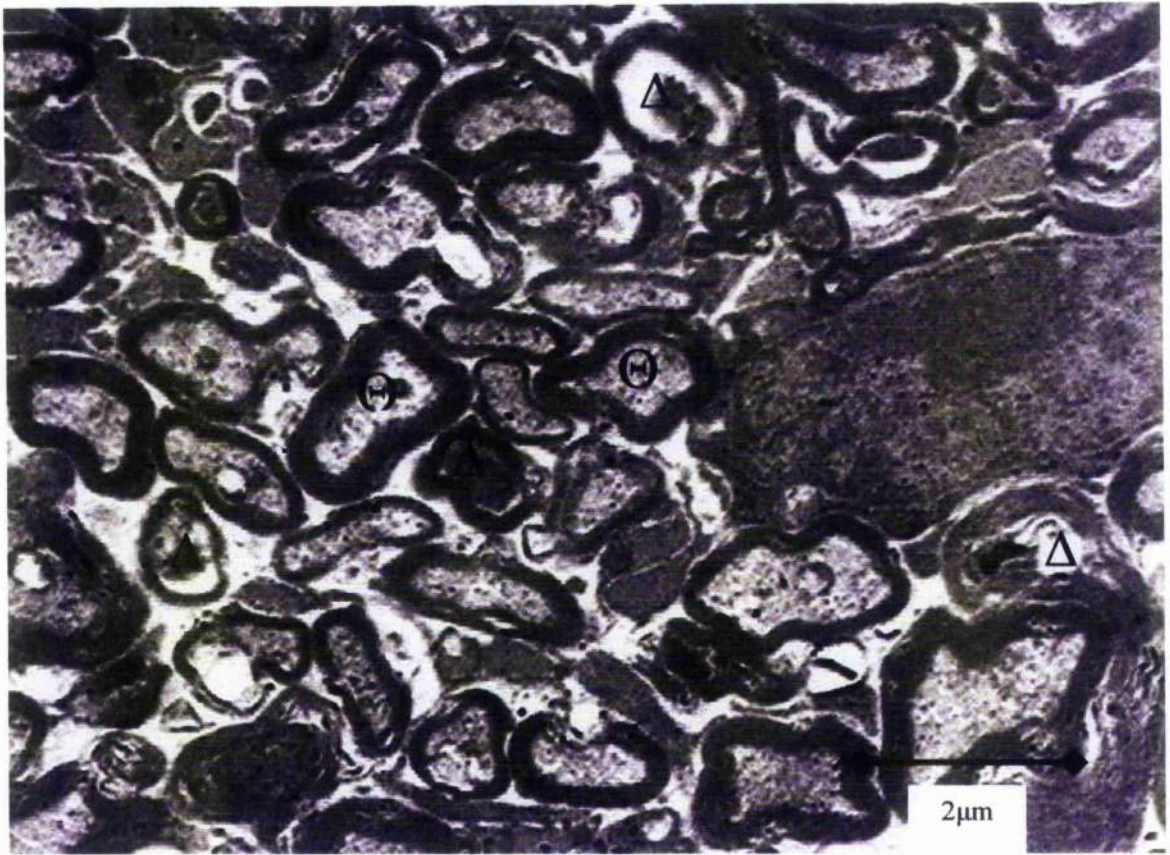


Fig. 24. A detail taken from Fig. 23 to illustrate a mixture of intact (Θ) and degenerating (Δ) nerve fibres at 3 weeks following stretch-injury. In the latter the lumen of the remnant of the myelin sheath frequently contains an amorphous, electron dense deposit. Between and among the nerve fibres extend many electron dense, astrocyte processes.

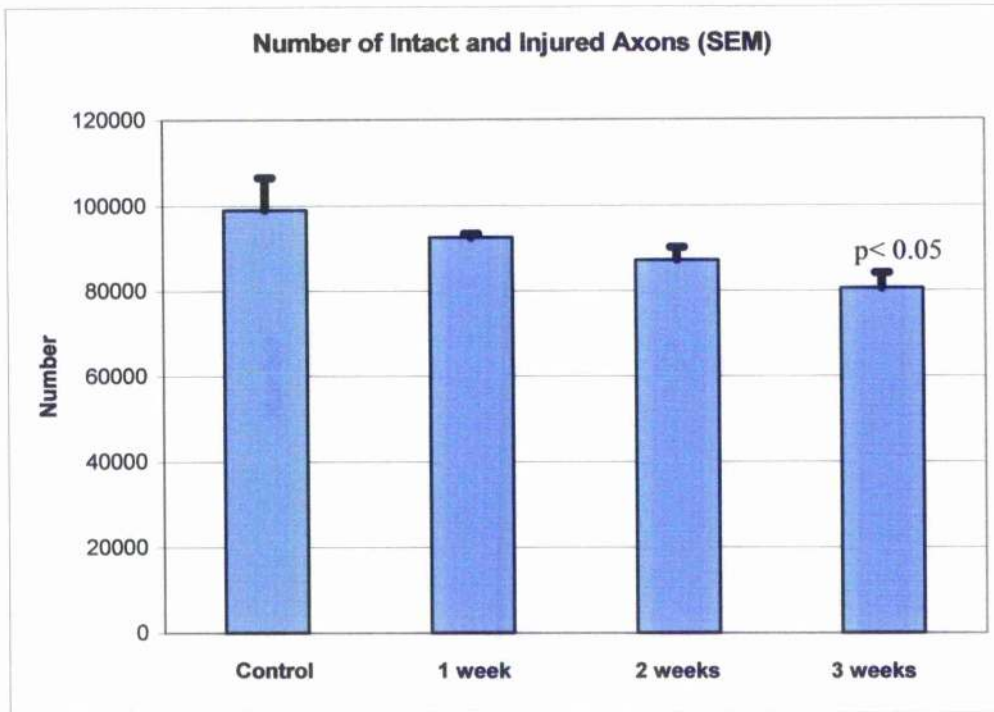


Fig. 25. A bar graph of the number of intact and injured axons in the right optic nerve at 1 week, 2 weeks and 3 weeks after injury. (n = 3 in each experimental group; or n = 12 overall). There is a difference only at 3 weeks ($p < 0.05$).

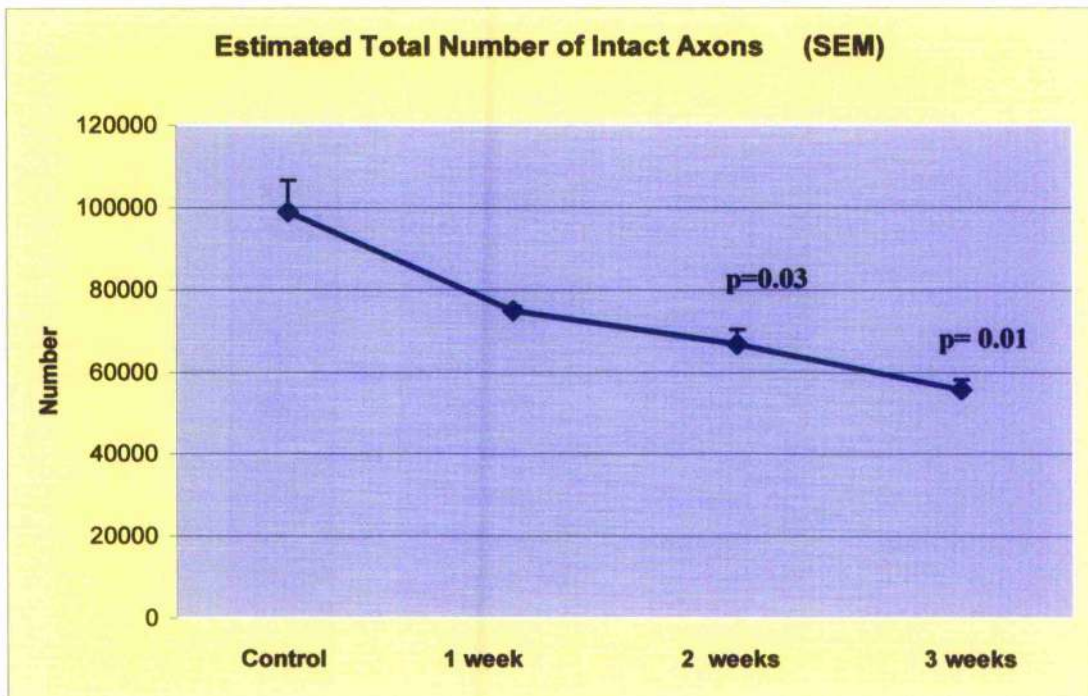


Fig. 26. A line graph of the estimate of the number of morphologically intact axons in optic nerves at 1 Week, 2 Weeks and 3 Weeks survivals after injury (\pm SEM, p = difference from control number). Note that there is loss of **intact** axons at 2 and 3 weeks after injury.

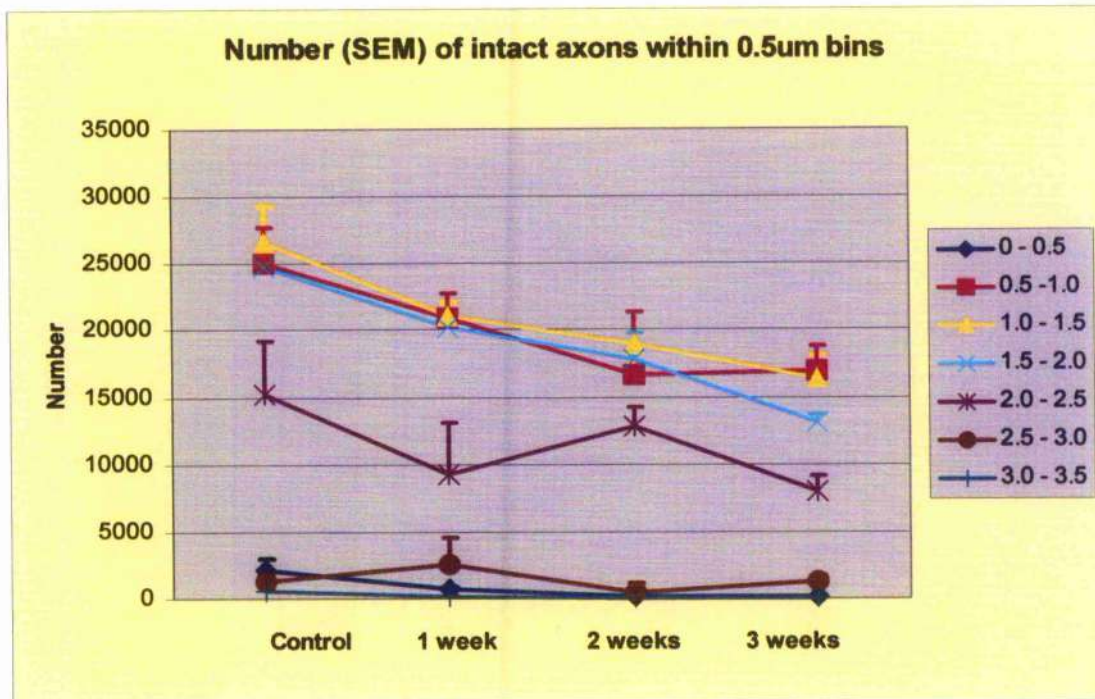


Fig. 27. A graphical representation of the changes in number of intact axons within 0.5µm bins within Control animals and 1 week, 2 weeks and 3 weeks survival animals (Total value for n = 12) after stretch-injury to the right optic nerve.

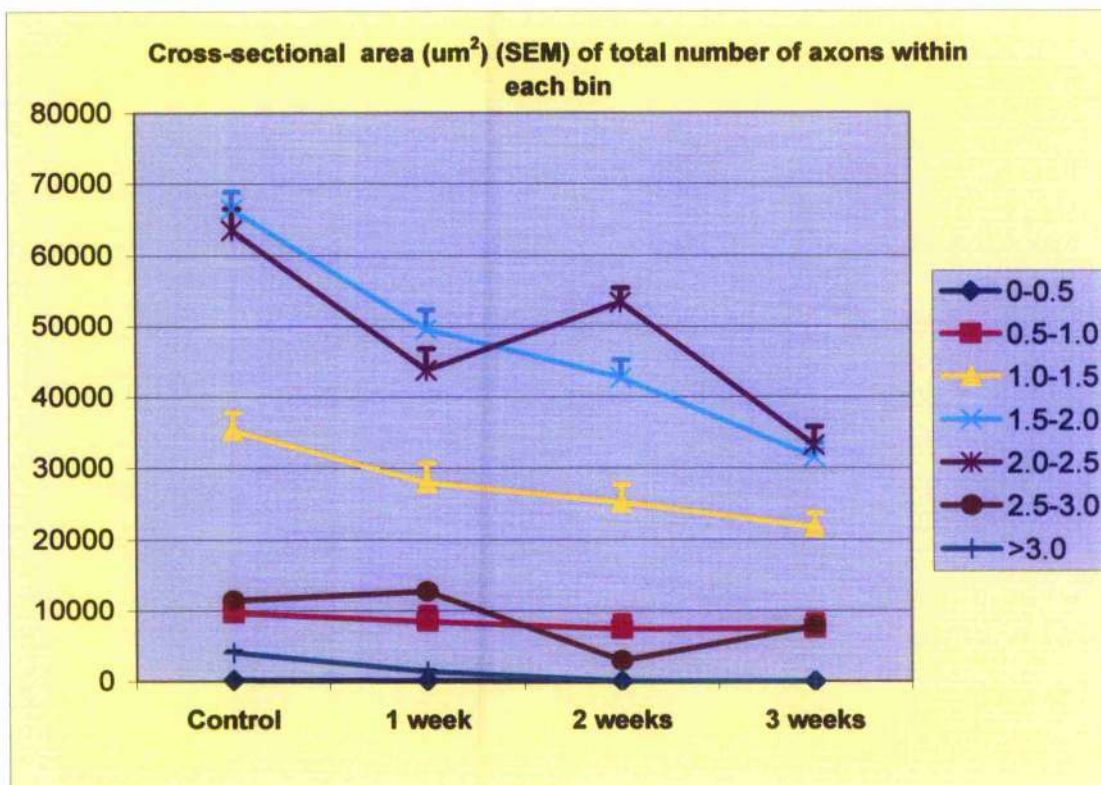


Fig. 28. A graphical representation of the changes in cross-sectional area of all of the intact axons within 0.5µm bins for Controls and 1,2 and 3 week survivals (Total value for n = 12) after stretch-injury to the right optic nerve.

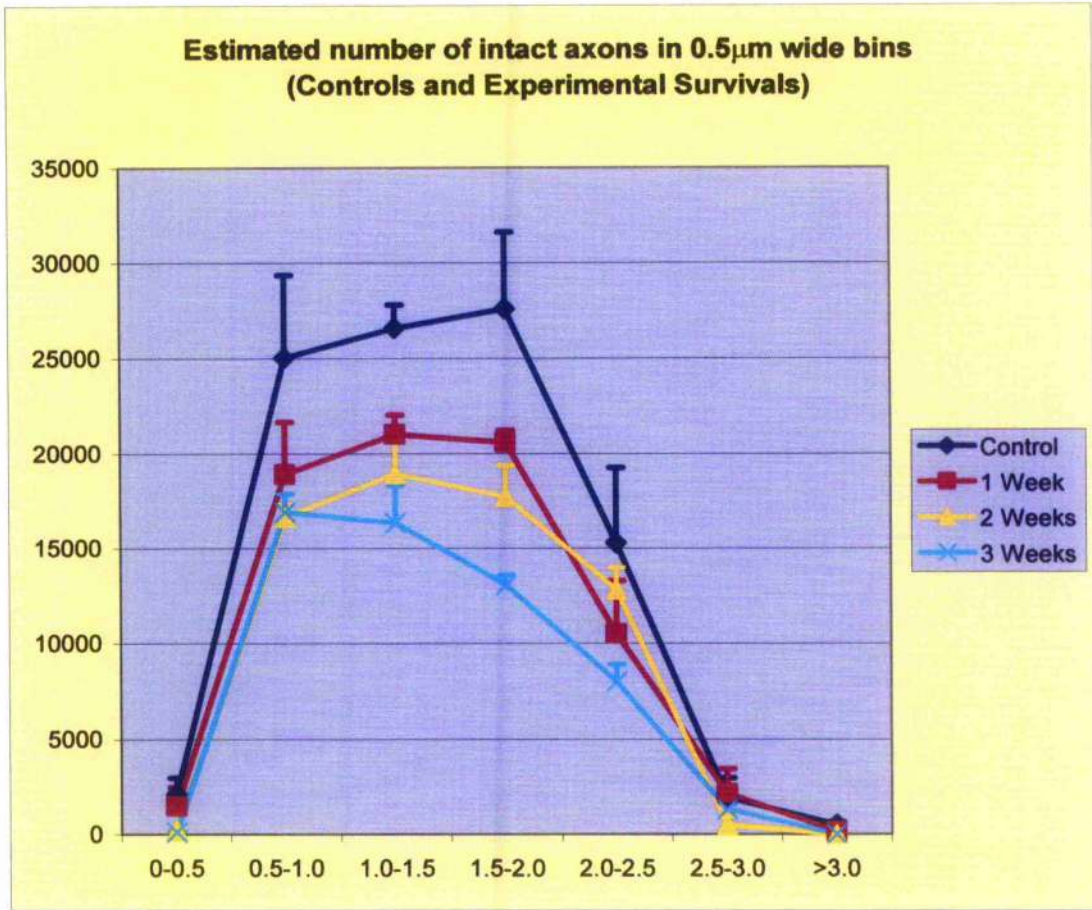


Fig. 29. Changes of the proportions of Intact axons within bins from Controls (n = 3) and animals that survived 1 Week (n = 3), 2 Weeks (n = 3) and 3 Weeks (n = 3) after stretch-injury to the right optic nerve of adult guinea pigs.

CHAPTER FIVE

DISCUSSION

1. Changes in cross-sectional area of the optic nerve after TAI:

There is no change in the cross-sectional area of the optic nerve between control animals and any of the experimental groups (Table 7, Appendix, page 195). This is unexpected in the light of results both for loss of the total number of axons and the reduction in the cross-sectional area of the intact axons in each survival group.

(a) Contribution by myelinated fibres to the cross-sectional area of control optic nerve.

In outline, the method of calculation was to take the median value of the diameter of axons in each bin, calculate the area of a circle with the same diameter and then multiply that value by the number of axons within that bin. The sum total of areas of axons within all of the bins provided an estimate of the contribution made by the total cross-sectional area of the axons to the value obtained for the cross-sectional area of the whole nerve (Table 26, page 213). The result was expressed as a percentage of the observed cross-section of the whole nerve. In control animals, the result demonstrated that the myelinated axons occupied 49.8% of the total cross-sectional area of the uninjured optic nerve.

As already stated in the Results, pages 89-90, in terms of numbers of axons, there is a loss of 24.40% at 1 week, 32.5% at 2 weeks and 43.74 % by 3 weeks. The loss in terms of the reduced cross-sectional area of myelinated, intact axons between controls and 1 week survivals was -24.5%, by 2 weeks was -30.9% and by 3 weeks survival was -46.6%. The reduction in cross-sectional area of all intact myelinated axons is highly significant where $p=0.0001$ (ANOVA). After injury myelinated axons formed 37.6% of the total cross-sectional area of the right optic nerve at one week, 34.3% at two weeks and 26.6% at three weeks.

Two factors influence or contribute to such a change. First, the cross-sectional area of the myelinated axons forms less than half of the cross-sectional area of the whole nerve. Thus, the loss of axons theoretically would contribute to a loss of cross-sectional area of only 4.3% at 3 weeks. However, the variance between control animals was relatively large at $\pm 7511.18\mu\text{m}^2$, or the equivalent of 2% of the cross-sectional area of the whole nerve. The variance across the three

animals in each experimental group was similar. It is therefore not surprising that a change of the total cross-sectional area of the right optic nerve was not detected. The better approach to address this problem would be to take a larger number of animals within each experimental subgroup, say an 'n' of six, in each of the control, 1, 2 and 3 week survival groups. However, if no significant difference is obtained using an 'n' of six then there can be confidence that the loss of axons does not result in any change in the cross-sectional area of the injured optic nerve. At present, it is clear that the experimental paradigms and the stereological techniques used in the current study were not sensitive enough to detect any change in cross-sectional area of the optic nerve as a whole. However, the fact that statistically significant differences for both the number of and the cross-sectional area of myelinated, intact axons is obtained with an 'n' of three strongly argues that loss of axons up to three weeks after injury does not result in a change in cross-sectional area of the whole nerve. However, the novel finding in the present study of a continued loss of intact axons with increasing post-traumatic survival allows generation of the hypothesis that if there is continued loss of axons in survivals for longer post-traumatic intervals than 3 weeks that a change in the cross-sectional area of the injured nerve may occur.

Second, there is differential loss of axons from within different bin sizes across the whole nerve, $p < 0.0001$ ANOVA. This finding extends and provides support for the hypothesis that different sizes of axon respond either with a different time course or as a result of differences in interactions, at the molecular level, between neurofilaments (NF) within the axonal cytoskeleton (Jafari et al., 1997, 1998; Maxwell et al., (2003). There is a loss of the summated axonal cross-sectional area in all but three bins at 1 week. There is no loss from the smallest ($0-0.5\mu\text{m}$) and largest axons ($>3\mu\text{m}$), and those with a diameter between 0.5 and $1.0\mu\text{m}$. The latter group of axons, however, is unique in the present study in that there is not a significant loss in their cross-sectional area throughout the experimental period. On the contrary, the summated cross-sectional area of axons in all but two sizes of bin is significantly reduced in parallel with the loss in number of axons. The two exceptions to that latter statement are, first, axons with a diameter between 2.5

and $3.0\mu\text{m}$ that increase in number between 1 and 2 weeks ($p < 0.01$, $q = 4.5$), followed by no change at 3 weeks ($p > 0.05$, $q = 1.9$). Second, axons with a diameter between 2.0 and $2.5\mu\text{m}$ that increase both in number and cross-sectional area between 1 and 2 weeks ($p < 0.01$, $q = 4.8$) (Figs 27 and 28, page 115). In only one bin, that with axons of a diameter greater than $3\mu\text{m}$, was there a complete or total loss of axons ($p < 0.01$, $q = 6.92$). However, the number of these axons is so small that their loss makes little contribution towards any overall loss of axons or the total cross-sectional area of myelinated axons.

Although the results above are intriguing, it is clear that application of a different analytical technique should be required to investigate changes in the cross-sectional area of the optic nerve. In any future analysis, however, the novel finding that although axons suffer irreversible damage and/or disappear, their remnants in the form of myelin figures may still occupy space within the nerve at 3 weeks survival. An example, where two large myelin figures occur and have a diameter greater than that of any of the axons within the same area is seen in Fig 23, page 112). Thus, unlike Wallerian degeneration in the PNS (Griffin et al., 1995) or experimental conditions in which the blood-brain barrier is disrupted in crush or transection injuries, the removal of myelin debris after TAI either does not occur or occurs with a time scale longer than 3 weeks. In the current study, little if any evidence for activation of intrinsic microglia as indicated by their adoption of an amoeboid form and formation of inclusion vesicles was obtained. Since the present study is the only one that has investigated axonal/cellular responses at more than 7 days after TAI there is no experimental data with which to compare the results. Investigations of responses by astrocytes, oligodendrocytes and immunocompetent cells in long-term survivals are limited to studies in patients (Maxwell et al., 2006). Immunocytochemical studies utilising markers for glia and/or activated monocytes/macrophages/microglia in models of white matter injury where axons are exposed to non-disruptive, transient tensile strain are entirely lacking. This lack of information needs to be rapidly addressed. The novel information obtained in the current study that the time course of any cellular responses may be of greater duration that has

previously been suggested in the literature concerning TAI also requires further investigation at least to determine whether axonal loss continues over weeks or months or a plateau is obtained at which no further loss of axons occurs.

b) Evidence for glial activation

A notable change in the same animals was an apparent hypertrophy of astrocytes and astrocyte processes between and amongst the remaining axons. There is a vast literature concerning glial cells. But almost all of the experimental literature relates to models in which axonal injury is severe enough to result in axotomy at the time of injury such as crush or transection;- see Introduction pages 43-45, 53-63.

Astrocytes normally occupy one third of the volume of the cerebral cortex and after trauma there is a great deal of published evidence for an increase in their number as demonstrated by an increase in astrocyte processes identified through immunocytochemical labelling with GFAP (reviewed by Norenberg 1994). However, Norenberg (1994) pointed out that use of GFAP antibodies will only identify astrocytes containing a high content of intermediate filaments. The expression of increased content of GFAP+ve intermediate filaments is a response manifested secondary to swelling of astrocytes which occurs within hours rather than days after injury. Literature published in the last five years has revealed that the interaction between astrocytes and other cells of the CNS is far more complex than had been appreciated (Hansson and Rönnbäck, 2003) with evidence for ionic and molecular interactions between astrocytes and all other cell types within the CNS. Nucleosides, nucleotides and glutamate are released in central grey matter after trauma and result in activation of both astrocytes and microglia. With an internal ATP concentration as high as 3-5 mM, astrocytes can release large amounts of ATP into the extracellular environment. This release of ATP is suggested to be a trigger for the initiation and maintenance of reactive astrogliosis that involves striking changes in the morphology and proliferation of astrocytes (Ncary et al., 1999). However, in models of TAI, responses by glia have been largely ignored, until at least very recently in some studies in patients (Wilson et al.,

2004; Maxwell et al., 2006). A contributing factor to this has been a lack of investigation of cellular responses beyond 7 days after axonal injury in any experimental models of TAI. There is reported thickening of astrocytic processes leading to disorganization of nerve fascicles after crush injury to opossum optic nerve (Narciso et al., 2001). But the timeframe over which these astrocyte responses occur is much shorter than that observed in the current study. For example astrocyte processes were more prominent with an increased content of intermediate filaments at 48 hours and resulted in a complete disarrangement of nerve fascicles, with astrocytes forming irregular septa among groups of nerve fibres, at 168 hours after crush injury (Narciso et al 2001). Thus, the response by astrocytes in opossum optic nerve after crush injury occurred within a week while they are only become discernable in guinea-pig optic nerve at 3 weeks after stretch-injury. There is ultrastructural evidence for mitosis by astrocytes after stretch-injury to the optic nerve (Graham and Maxwell, 1996) and the novel evidence for a slowly developing, 2-3 weeks after injury, hypertrophy of astrocytes in an animal model of TAI in the present study warrants further investigation of astrocytic responses within central white matter after TAI.

There are also major differences in time course of activation of macrophages and/or microglia between the PNS, white matter tracts in the CNS after transection of axons and after TAI. After crush injury, there is a four-fold increase in the number of macrophages/microglia in the distal segment of the mouse optic nerve at 7 days (Lawson et al 1994) while activation of microglia following human TBI has been reported in patients that survived more than 72 hours post injury (Engel et al., 2000; Guillemin and Brew, 2003). However, as indicated in the Introduction (page 52), an increase in the number of macrophages has been hypothesised to be dependent upon opening of the blood-brain barrier (Streit et al., 2004). In the stretch-injury model of TAI evidence for such opening has not been obtained (Maxwell et al., 1991). However, activation of microglia as indicated by labelling for macrophage-related proteins (MRP8 and MRP14) and CD4, has been reported from both contusion and non-contusion regions of brain only when patients survive at least 72 hours after injury (Engel et al., 2000).

Despite the fact that analysis of the response by glial cells was not the purpose of the experiments forming the content of the present study, nonetheless, it is posited that, at three weeks after trauma, the increase in volume by reactive astrocytes may compensate for any loss, in terms of volume, of axons and their related oligodendrocytes that degenerate. Clearly, however, testing of that hypothesis would involve a complex stereological analysis involving techniques for estimation of changes in cell volumes and/or number. Appropriate techniques are available (Mouton, 2000). The current study is valuable in that it has provided the first indication of a previously unsuspected astrocyte response in TAI that may occur more slowly within central white matter following TBI than has previously been documented after crush injury (Narciso et al., 2001).

2. Novel information about axonal pathology:

The major features of the development of axonal pathology in this animal model between one and three weeks after injury may be summarised as follows.

At one week after TAI the general organisation of the optic nerve is maintained although many fibres show evidence of pathology (Fig. 20; page 109). For example swelling of mitochondria, loss of MTs and NFs resulting in a lucent axoplasm, separation of myelin lamellae to form “intramyelinic spaces”, involution of parts of the myelin sheath into the axoplasm and an increase in the size of the inner tongue of oligodendrocyte cytoplasm. Such findings have previously been documented at 4 and 24 hours after TAI (Jafari et al., 1997,1998; Maxwell et al 2003) and 24 hours after crush injury (Narciso et al., 2001) in optic nerve. However, evidence of such pathology/damage at 1 week after injury is novel. Moreover, the time course of this pathology differs markedly from either transection or avulsion models of injury in PNS axons (Bunge et al., 1993; George and Griffin, 1994; Griffin et al., 1995; Avellino et al., 1995) or crush injury to the optic nerve (Narciso, 2001) where loss of the formed components of the axon occurs by 48-60 hours after injury. The current study provides novel evidence that the development of the early

stages of pathology after TAI in white matter of the CNS is slower and occurs over a much longer post-traumatic interval than previously reported.

At two weeks after injury the appearance of the cross-section of the optic nerve is irregular in that the nerve has become more oval than circular in profile. Within the nerve there is a widening of interaxonal spaces. These spaces are occupied by thickened or more numerous astrocyte processes which appear to subdivide groups of axons into fascicles. The astrocyte processes are particularly notable in the perivascular space around blood vessels.

Axon profiles are less regular and intramyelinic spaces occur in about 10% of fibres. Frequently the axoplasm of these latter nerve fibres is electron lucent with a reduced content of MTs and NFs (Figs. 21 and 22; page 110, 111). Mitochondria within these axons are frequently swollen and lucent. Scattered among the groups of nerve fibres occur a few, smaller axons which possess an electron dense cytoplasm and a thicker than normal myelin sheath (Fig. 22, page 111). However, MTs and NFs are discrete within the axoplasm. This ultrastructure is therefore not comparable to the dark degeneration described in axons at the point of the rapid autolysis described in distal segments of PNS axons undergoing Wallerian degeneration (George and Griffin, 1994; Griffin et al., 1995) where the ultrastructure has a granular or amorphous form. These latter images are suggestive of the axon having undergone shrinkage or a reduction in calibre. These smaller, dark axons constitute about 5% of the population of axons.

At three weeks after injury the cross sections of many nerve fibres are grossly distorted from a smooth circular form and there is loss of the normal organisation of optic nerve fibres (Fig. 23, page 112). A large proportion, some 85% of the axons, have an irregular, non-circular profile (Fig. 23). Nonetheless, their axoplasm retained discrete MTs and NFs that were regularly spaced throughout the axoplasm and these axons were regarded as intact despite their irregular profile. On the other hand, a wide range of pathological changes are seen, myelin figures, axons with

intramyelinic spaces in their myelin sheath (about 10%), axons with periaxonal spaces (about 5%), and involution of the axolemma (about 5%). However, a frequent pathology was replacement of recognisable cytoskeletal components by an amorphous, electron dense deposit that was not limited by an organised plasmamembrane (Figs. 23 and 24, pages 112,113). Nonetheless, the myelin sheath was intact with closely apposed lamellae. Such examples formed between 12 and 13% of the total number of axonal profiles within transverse sections of segment 2 of the injured optic nerve. The ultrastructure of these axons was comparable to the dark degeneration noted at the granular disintegration phase of Wallerian degeneration in PNS axons (George and Griffin, 1994; Griffin et al., 1995) and more recently described by Narciso et al. (2001) after crush injury to opossum optic nerve. The major difference, however, was the time scale over which such pathology occurred after TAI, at 2-3 weeks after injury rather than 48-72 hours.

3. Numerical distribution of axons in control/sham animals:

In the present study estimation of the total number of the axons in control or un-injured guinea pig optic nerves was $99,005 \pm 9,199.28$, and estimation of the number of axons within $0.5\mu\text{m}$ wide bins, demonstrated that the smallest ($<0.5\mu\text{m}$ diameter) and largest ($>3.0\mu\text{m}$) axons are relatively few in number. Axons of a greater diameter than $3\mu\text{m}$ represent only 0.5% of the total within the adult guinea pig optic nerve, and no axons greater than $3.5\mu\text{m}$ diameter occurred. Axons of $<0.5\mu\text{m}$ diameter form just over 2% of the total. This result is in close agreement with an earlier study (Guy et al., 1989) which reported a total number of $97,000 \pm 9,000$ axons.

Results obtained in the present study indicate that the majority of axons in the middle segment of the guinea pig optic nerve are between 0.51 and $2.5\mu\text{m}$ diameters and represent 95.4% of the total number of axons within the intact nerve. As already stated, the estimate of the total number of axons in the middle segment of the guinea pig optic nerve is $99,005 \pm 9,199.28$. In comparison,

this is only 10% of the number of axons in the optic nerve of humans and 33.6% of the number in rabbit (Robinson et al., 1987).

4. Changes in the number of intact axons within different sized bins after injury:

Clearly, maximum numbers of intact axons occur in control animals. Control right optic nerves contain $99,005 \pm 7511$ axons. A very large proportion of the nerve fibres occur within the three bins between 0.5 and 2.0 μm (Fig. 29, page 116 – dark blue line), and about 15,000 axons are between 2.0 and 2.5 μm in diameter.

At one week following injury, however, there is loss from all bins ($p < 0.001$, ANOVA) (Fig 29, page 116 - pink line) and expressed as the percentage of control numbers (Table 27, page 213).

However, different proportions of the control numbers are lost from different bins (Table 27). For example, 66% of axons with a diameter greater than 3.0 μm are lost ($p < 0.001$, ANOVA).

However, there is an 11% increase in the number of axons between 2.5 and 3.0 μm diameter ($p = 0.046$, ANOVA). There is loss of 32% of 2.0 and 2.5 μm diameter axons ($p = 0.038$, ANOVA); loss of 26% of 1.5 – 2.0 μm axons ($p = 0.003$, ANOVA); 21% of 1.0 – 1.5 μm axons ($p = 0.003$, ANOVA); 25% of 0.5 – 1.0 μm axons ($p = 0.014$, ANOVA) and 32% of the smallest axons with a diameter less than 0.5 μm at one week ($p = 0.015$, ANOVA).

At two weeks after TBI however, the relationships differ in that there is 100% loss of axons larger than 3 μm diameter ($p = 0.001$, ANOVA); and loss of 77.3% of the number of axons with a diameter of 2.5 – 3.0 μm at 1 week ($p = 0.03$, ANOVA) (Table 27, page 213). However, there is an increase in the number of axons 2.0 - 2.5 μm diameter from 68% to 84% of control values ($p = 0.38$, ANOVA). There is loss of 28% of axons 1.5-2.0 μm in diameter ($p = 0.003$, ANOVA); 29% of axons of 1.0-1.5 μm diameter ($p = 0.003$, ANOVA); 34% of 0.5-1.0 μm axons ($p = 0.014$, ANOVA) and 90% of the smallest axons ($p = 0.015$, ANOVA). That is to say, there is an increase in the number of axons with a diameter between 2.0-2.5 μm following on from a 32% loss at 1 week –*vide supra*. However, despite the data give above, ultrastructural evidence for a

widespread loss of axons as indicated by the occurrence of dark, degenerated axons and or numbers of empty myelin sheaths was lacking at 2 weeks – see Fig. 21, page 110. Therefore, the only other explanation for the change in relative proportion of different sizes of axon (Fig. 29, page 116) is that some axons have been reduced in calibre and fallen out of the 2.5-3.0 μ m wide bin into the 2.0-2.5 μ m bin.

Increased confidence for the latter argument is provided by further changes in relationships of numbers of axons in 0.5 μ m wide bins at three weeks (Table 27, page 213). No axons of diameter greater than 3 μ m occur at 3 weeks. The number of axons between 2.5 and 3.0 μ m diameter increase by 167.2% between 2 and 3 weeks such that there is no change from control values ($p = 0.18$). However, there is further or continued loss of 48% of 2.0-2.5 μ m; 47% of 1.5-2.0 μ m; 39% of 1.0-1.5 μ m axons; but a small increase of axons between 0.5 and 1.0 μ m in diameter ($p < 0.05$, $q = 3.79$, Dunnett). There is further loss of the smallest axons to less than 5% of control numbers. Thus the second largest size of axon (2.5-3.0 μ m diameter) increases in number at the same time that there is complete loss of their next largest neighbouring group of axons. There is also continuing loss of the smallest axons over the entire experimental period ($p = 0.015$, ANOVA). There is an increasing loss of axons with diameters between 1.0 and 2.5 μ m during the period one to three weeks after injury (Fig. 27, page 115). However, numbers of 0.5-1.0 μ m axons remain relatively stable ($p > 0.05$, $q = 0.77$).

In addition, when axons are grouped into 0.5 μ m wide bins, the bin with the largest number of axons changes over the experimental period of the present study. In controls, the largest number of axons, $27,594 \pm 4010$ or 27.9% of the total occurs in the bin between 1.5-2.0 μ m in diameter (Fig. 29, page 116 – dark blue line). At one week, the largest proportion of intact axons in any bin is 28.0% ($20,999 \pm 1,028$) but the size range of the bin has fallen to 1.0-1.5 μ m (Fig. 29, page 116 – pink line). That bin still contains the largest proportion of intact axons, $18,927 \pm 1,981$ (28.3%) at two weeks (Fig. 29, page 116 – yellow line). However, at three weeks the largest

proportion of intact axons, $16,872 \pm 964$ (30.3%) occurs in the bin containing axons only 0.5-1.0 μm in diameter (Fig. 29 – turquoise line).

This study has provided good quantitative evidence for changes of number in axons within different sizes of bin after TAI in central white matter. Logically, two arguments or explanations for such a response may be suggested. Either axons degenerate completely or there is an alteration in the size of an injured axon so that it becomes included within the next lower bin size. Support for the former hypothesis is lacking in that morphological evidence for loss of axons, for example the presence of myelin figures or apparently empty myelin sheaths, is obtained only at three weeks after TAI.

Table 6. Percentage of Control Numbers of Intact/Normal Axons within each Bin present at 1, 2 and 3 Weeks after traumatic axonal injury to guinea pig optic nerve. (the values for p indicate whether the loss in **number**, not the percentage change, was significant – see data in Table)

	Control	1 Week	2 Weeks	3 Weeks
0-0.5 μm	100	36	10 (p<0.05)	5 (p<0.05)
0.5-1.0 μm	100	83	66	67
1.01-1.5 μm	100	79	71	61 (p<0.05)
1.51-2.0 μm	100	81 (p<0.05)	72 (p<0.01)	53 (p<0.01)
2.01-2.5 μm	100	61	84	52
2.51-3.0 μm	100	163	38	102
> 3.01 μ	100	44	0 (p<0.05)	0 (p<0.05)

Support for the latter hypothesis is provided by several results obtained in the present study. The evidence that the number of axons within some bins increases, and within different bins at

different survivals is strong evidence that axons are not being lost but are changing their calibre. For example, at 1 week there is loss of axons with a diameter greater than 3 μ m but an increase in the number of axons within the adjacent bin with axons between 2.5 and 3.0 μ m diameter. This is followed at 2 weeks by an increase in the number of axons in the bin with diameter between 2.0 and 2.5 μ m. Further support is provided by evidence that the diameter of the largest number of axons within 0.5 μ m wide bins changes over the experimental period. The bin containing the largest proportion of axons in controls is 1.5-2.0 μ m in diameter, at 1 and 2 weeks is 1.0-1.5 μ m, and at 3 weeks is 0.5-1.0 μ m. This novel data provides the first evidence that a long term and continuing pathology occurs within a group of CNS axons exposed to transient tensile strain where the strain is not great enough to result in primary axotomy. However, the purpose of the present study was to provide an estimate of the number of intact axons at 1, 2 and 3 weeks after TAI. Further, in the micrographs used for estimation of the number of axons only those axons that did not exhibit overt pathology were counted. Nonetheless, there is a significant loss of axons at 2 and 3 weeks after TAI (Fig. 26, page 114). Alternatively, when the number of intact and damaged axons is considered there is only a significant difference from control numbers at 3 weeks (Fig. 25, page 114). The following questions arise from the above. What happened to the 3 μ m and greater diameter axons between 1 and 2 weeks? Why do the numbers within intermediated sized bins both rise and fall over the experimental period?

5. Consideration of mechanisms of axonal cytoskeletal responses

Maxwell et al., (2003) suggested that with post-traumatic alterations in the fine structure of the axonal cytoskeleton, notably a reduced spacing between or compaction of NFs, an axon's calibre might be reduced and the axon thereby fall into the adjacent smaller bin. In that study, evidence in support of the hypothesis was the increased content of NFs in small axons between 4 and 24 hours after injury where the number of neurofilaments was greater than in axons of the same diameter in control animals. However, in larger axons within the injured optic nerve, although the

number of NFs did not differ from controls, the spacing between adjacent NFs was reduced such that NFs formed groups within the central zone of the axoplasm rather than being uniformly distributed throughout. A notable point in that paper, however, was that the calibre of the larger axons did not appear to be reduced. However, because of the lack of application of suitable stereological techniques in that study changes in axonal calibre may have been missed.

The major purpose of the current study was to estimate the total number of intact axons within all sizes of bin. A novel technique was applied in order to obtain a representative sample at low magnification. As a result, resolution of detailed changes within the axoplasm of most axons was not possible. Nonetheless, good quantitative data in support of the hypothesis that the number of axons within all bins changes after TAI was obtained. In addition, however, within the Results (Chapter 3) some comments about the morphology of axons are included. These ranged from a reduced content of MTs and/or NFs in some pale or electron lucent axons to a number of small axons that were more electron dense and appeared to have an unusually thick myelin sheath. It is suggested that the latter images are new evidence for changes in the detailed organisation of the axonal cytoskeleton and that, when compaction of NFs occurs, the calibre of axons is decreased. It has long been accepted that the spacing between and the number of NFs in myelinated axons is a crucial influence in determining the diameter of an axon (Hoffman et al., 1984; Shaw et al., 1991; Hisanaga et al., 1991). Although the precise mechanism or mechanisms maintaining the regular spacing between NFs is still controversial (Kumar et al., 2003 a, b) the observation that spacing is reduced after TAI (Pettus et al., 1994; Pettus and Povlishock, 1996; Jafari et al., 1997, 1998; Povlishock et al., 1997; Maxwell et al., 2003) has gained wide acceptance. It is also now well recognised that NFs are interconnected with the plasmalemma through actin and the subaxolemma cytoskeleton (Trapp et al., 1989; Ichimura et al., 1991; Kumar et al., 2003a) and are strongly influenced by myelin associated glycoprotein (MAG) during myelination (Trapp et al., 1989; Lunn et al., 2002). So after TAI, when compaction of NFs occurs and their spacing is reduced, it is plausible that the axolemma will be retained in close relation to the outer region of

the core of compacted NFs unless the subaxolemma cytoskeleton is destroyed – *vide infra*. Thus, the calibre of the axon will fall. MAG is located primarily in lipid rafts that occur on the inner aspect of the internal lamina of the myelin sheath formed by myelinating oligodendrocytes (Trapp et al., 1989; Vinson et al., 2003). MAG interacts with a MAG receptor located in lipid rafts in the internodal axolemma to link the inner surface of the myelin sheath to the outer surface of the axon (Vinson et al., 2003). Hypothetically, the above linkage will maintain myelin-axolemma interaction in, at least some, examples of axons with a reduced calibre. However, further consideration will require a detailed analysis of axonal cytoskeletal relationships such has been completed in shorter-term survival experiments (Jafari et al., 1997, 1998; Maxwell et al., 2003).

Novel evidence obtained in the present study suggests a leftward migration toward the abscissa or reduction of axonal diameter between one and three weeks (Fig 29, page 116). The evidence supports the hypothesis that, over a period of weeks after TAI, there is an ongoing reduction in calibre of axons. This results in loss of larger axons over the period of three weeks after TAI. However, analysis of electron micrographs shows that large numbers of apparently normal axons are present even at three weeks after injury and the number of axons showing a documented pathology, for example pale and or dark axoplasm, or dissociation of myelin lamellae (Griffin et al., 1995; Narciso et al., 2001) is relatively small. It is presently unknown whether axons demonstrating post-traumatic compaction are still connected to their cell soma. However, the fact that the axon is intact and contains numerous cytoskeletal elements and membranous organelles strongly suggests that the compacted or shrunken axon is still connected to its cell soma and has therefore not undergone axotomy. Added weight is given to this argument by the observation that the myelin sheath is still intimately related to the axon surface in such fibres. This implies that intercellular signalling mechanisms between the axon and oligodendrocytes are intact. When compaction of NFs was first identified by Pettus et al., (1994) it was suggested that the change occurred soon after injury and did not change within a survival of up to six hours (Pettus and Povlishock, 1996; Stone et al., 1999, 2001, 2004). However, that research group has done no

quantitative analysis or any further ultrastructural analyses. Rather, that research group has relied upon immunocytochemical labelling of damaged axons using antibodies against β -amyloid precursor protein and an antibody named RM014 that labels sites at which NFs are compacted (Stone et al., 1999, 2001). The findings of the present study confirm and extend the initial suggestion that, having undergone compaction of NFs, such injured axons do not demonstrate any further pathology and remain as long as, at least, three weeks after injury. A major novel finding in the present study, however, is that numbers of axons demonstrating such pathology increase in number with increasing survival. Therefore, the question "What is the outcome of these axons?" remains unanswered and will necessitate examination of animals allowed to survive for a longer period than three weeks. Furthermore, it is probable that these axons have not undergone secondary axotomy. Together, these factors strongly support the hypothesis that axons in which post-traumatic compaction of NFs occurs are experiencing a completely different type of pathology from those axons that have undergone secondary axotomy. Moreover, such pathology may occur in only a proportion of patients and where such changes do occur, for reasons presently undefined, the patient may undergo a degree of improvement or recovery. There is anecdotal evidence of such improvement but no quantitative data.

6. Evidence of Wallerian degeneration

An aim of this study was to test the hypothesis that the number of intact or uninjured axons remains stable over time in an injured CNS white matter tract. The null hypothesis was that the number of intact axons was unchanged with increasing post-traumatic survival. The results show that neither the first nor the null hypothesis is supported. It is concluded that some axons are lost over the three-week post-traumatic survival period. This leads to generation of the hypothesis that Wallerian degeneration may be occurring during the experimental paradigm.

The occurrence of secondary axotomy as early as 4h after trauma has been documented in the optic nerve stretch-injury (Jafari et al., 1997, 1998) and fluid percussion models

(Povlishock et al., 1997). However, the latter is not a clean model in the sense that there is direct injury to both grey and white matter. In a recent report using the optic nerve model, injury occurs purely in white matter and evidence for the early stages of Wallerian degeneration, an increase of the length of nodes of Ranvier, was obtained in a very small proportion of injured fibres as early as 24 hours (Maxwell et al., 2003). In the same study, evidence for replacement of an axon by a dark, amorphous material comparable to that described at the end of granular degeneration (Griffin et al., 1995) in PNS Wallerian degeneration was obtained at 1 week.

Although the major aim of this study was not to investigate morphological changes, the present study has provided evidence that the cross sectional architecture of the optic nerve was normal at 1 week. Despite the appearance of a wide-range of axonal pathologies, such as intermyelinic spaces, or periaxonal spaces due to a reduction in axonal calibre, no direct evidence for Wallerian degeneration defined as complete loss of the axon was found until 3 weeks after TAI. In earlier work, the presence of the former two changes have been linked to the time course of secondary axotomy (Maxwell et al. 1991, 1997, 2003; Jafari et al., 1997, 1998). In the present study similar pathological changes, axonal swelling, separation of lamellae of the myelin sheath, involution of the axolemma, development of periaxonal spaces together with degradation of the axonal cytoskeleton was a consistent finding in a small proportion, about 15%, of axons at both one and two weeks after injury. The present study therefore provides novel evidence that axons may enter the pathophysiological cascade to secondary axotomy up to 2 weeks after injury. In addition, unequivocal evidence for completion of Wallerian degeneration as defined by the occurrence of an amorphous, dark structure within remnants of the myelin sheath was only obtained at 3 weeks after TAI. This novel finding allows generation of the hypothesis that the process of axonal loss or degeneration under conditions that result in TAI does not parallel the time course described for Wallerian degeneration after injury to PNS axons (Griffin et al., 1995) or after crush injury to axons in optic nerve (Narciso et al., 2001). Counts of the total number of intact and injured axons at one week post-injury did not differ from sham controls. A significant difference or evidence of

axonal loss was obtained, however, at three weeks survival. Importantly, it is also notable that in the three weeks survival animals a different range of pathologies was present. Swollen, pale axons were few in number. Rather myelin figures and myelin sheaths containing amorphous deposits occurred. The two latter are directly comparable to changes widely documented in analyses of Wallerian degeneration (Griffin et al., 1995; Kreutzberg, 1995). However, it is acknowledged, the time frame over which such changes occurred was much longer in the present study than has been documented in either peripheral nerves (Griffin et al., 1995) or following crush injury to optic nerve (Narciso et al., 2001). In the present study, it was found that greatest loss of axons occurred between two and three weeks. The question as to whether this trend is ongoing, that the rate of axonal loss has peaked or will continue and/or accelerate over time is still unresolved and requires study of long-term survival animals. However, it may be concluded, that Wallerian degeneration after TBI does occur within 3-4 days but has a time course extending to 2 to 3 weeks after injury.

In the present study, there is also evidence of a second, novel, slowly developing pathology. Using the technique of counting the number of intact (normal) axons, at different survivals, the current study has provided novel evidence that traumatic damage initiated at the time of injury, elicits a pathology that may act in a steady, slow manner over at least three weeks following injury. There is now a consensus that a lesser degree or severity of trauma probably will not directly interrupt the continuity of an axon at the time of injury but rather cause it to enter a pathological cascade which ends with secondary axotomy. The present study, however, indicates that other changes apart from secondary axotomy may also occur in that at 2 and more frequently at 3 weeks after TAI some axons become reduced in calibre and the axoplasm becomes darkened or more electron dense. However, the increase in electron density of these axons does not parallel the morphology of axons said to be undergoing granular degeneration that has been recognised for at least 10 years in the Wallerian degeneration literature (Griffin et al., 1995). The distinction is that axoplasmic organelles such as MI's and NF's, together with membranous organelles, are

present (Fig. 21, 22 pages 110, 111 and Fig. 23, page 112) and the axolemma is intact. Further, the myelin sheath appears abnormally wide although well organised since there is no evidence for intermyelinic spaces or other forms of pathology. The present study provides the first evidence of this type of pathology and, although it is noted, the detail of the relationships between components of the axonal cytoskeleton still needs to be investigated before it may be properly characterised or described.

7. Hypothetical mechanisms for compaction of neurofilaments

Despite numerous observations that NFs undergo a reduction in interneurofilament spacing after TAI (Pettus et al., 1994; Pettus and Povlishock, 1996; Jafari et al., 1997, 1998; Maxwell et al., 2003), the precise mechanisms leading to or resulting in compaction are still obscure. Several mechanisms have been suggested in the literature; breakage or collapse of the NF side-arms, dephosphorylation of those side-arms or removal of the side-arms through calpain mediated proteolysis (Maxwell et al., 1997; Buki et al., 1999; Stone et al., 2001; Marmarou et al., 2005). However, this lack of understanding is not helped by the fact that the mechanism whereby NFs spacing is controlled in uninjured nerve fibres remains controversial (Kumar et al., 2002a, b). The older literature suggests that if either NF-L, or NF-M or NF-H is expressed at high levels then NF spacing is altered. In transgenic mice with greater than normal expression of either NF-H or NF-M, then NF densities are low. But, despite the reduction in density of NFs within a field of axoplasm, NFs are clustered at foci within the axoplasm and the spacing between NFs is similar to that in axons of control or wild type animals (Xu et al., 1996). The above data does not account for the observed changes in NF spacing and or number after TAI, either when compaction of NFs has occurred (Pettus et al., 1994; Pettus and Povlishock, 1996; Jafari et al., 1997, 1998; Povlishock et al., 1997) or in the early stages of Wallerian degeneration (Maxwell et al., 2003). In the former the spacing between adjacent NFs is reduced, in the latter the density of NFs and MTs is reduced because the number of both is lowered within the pale axoplasm. The latter may

be compared with the degeneration termed “watery” following crush injury (Narciso et al., 2001). But, unfortunately, the magnification of the published micrographs in the latter report, are too low to allow detailed comparison.

In developing, un-injured animals, internurofilament spacing increases upon myelination in both the PNS (deWaegh et al., 1992; Hsieh et al., 1994; Martini et al., 2001) and the CNS (Nixon et al 1994; Sanchez et al., 1996). The myelin-associated glycoprotein (MAG), a sialic acid binding immunoglobulin-like lectin generated by Schwann cells (Sternberger et al., 1979; Martini, 2001; Lunn et al., 2002) has been linked to control of that spacing through phosphorylation of the side-arm structure of both NF-H and NF-M (Julien and Mushynski, 1983; Yin et al., 1998; Lunn et al., 2002). When MAG is not present or expressed, for example in a MAG-null mutant mouse (Yin et al 1998), axonal calibre is reduced and both internurofilament spacing and phosphorylation is reduced. There has also been the recent demonstration of a reduced internurofilament spacing in both demyelinated and widely spaced myelin axons in patients with paraproteinemic demyelinating peripheral neuropathy (Lunn et al., 2002) in which patients generate antibodies which bind to MAG and prevent its interaction with other proteins within the axon.

When MAG does interact, however, NFs are phosphorylated and acquire a negative charge (Wong et al., 1995). Current thinking has integrated the above to provide a mutual repulsive mechanism that may, in part, be related to the intrinsic charge within neurofilament side-arms that are unstructured polyelectrolyte chains (Kumar et al., 2002a). There is a NF-NF interaction electrical potential generated within each neurofilament and this electrical charge varies with the degree of phosphorylation of the NF side-arms. A current hypothesis is that the ratio of anionic to cationic residues, generate a fractional charge, of the value 0.067 units in normal axons. Here the fractional charge results from maximal phosphorylation of side-arms that occurs upon myelination through, at least in part, the direct influence of myelin associated glycoprotein (MAG) localized at the glial-axolemma interface (Trapp et al., 1989; Lunn et al., 2002; Kumar et

al., 2002). The neurofilament side-arms occupy a diffuse volume that extends a distance L from the filament core or backbone that has a radius R_c . The NF cores do not overlap as a result of the NF-NF interaction potential, $U(r)$ where elastostatic repulsion due to the fractional charge of each NF serves to repel one NF from its neighbour(s) and where $U(r) = \infty$ for $r < 2R_c$. When the NFs are far enough apart that there is no overlap between the side-arm layers, or $r > 2R_c + 2L$, then NFs do not interact electrostatically and $U(r) = 0$. Direct observation from electron micrographs (Kumar et al., 2002) has demonstrated that NFs are regularly spaced; have a Gaussian distribution, and are best described as a collection of single-pair NF-NF interactions. Thus a model in which either cross-bridges are (1) rigid and bind to the core and/or side-arms of an adjacent filament or (2) interact via soft or deformable cross-bridges, the “soft-strut” model, do not adequately allow mathematical description of the observed interneurofilament relationships because the predicted distribution of NFs is not Gaussian. Therefore, a third model in which long-range, repulsive interneurofilament potentials act through fractional charges to maintain the spacing between pairs of NFs has been tested (Kumar et al., 2002a, b). Since the fractional charge of each side-arm is dependent upon the extent of phosphorylation of that side-arm, the higher the degree of phosphorylation the larger the fractional charge, the greater the intermolecular repulsion (Pincus, 1991) and the greater the repulsive force between pairs of NFs. Hypothetically, the cross-linking proteins or the NF side-arms, are currently thought not to drive that organization but primarily serve to stabilize the relative positions of adjacent NFs (Herzfeld, 1996). Thus the side-arms and the degree of their phosphorylation stabilize the relative position of NFs within the axonal cytoskeleton rather than directly determining the spacing between those NFs. Rather, that spacing is primarily determined through intermolecular, electrical repulsion (Kumar et al. 2002a, b).

However, importantly, none of the consideration summarized above relates to conditions of observed, ultrastructural pathology after TAI. The scenario in which NF spacing is reduced or NFs are compacted, or when NF spacing is increased during Wallerian degeneration has not yet

been investigated at the biophysical level. However, if the hypothesis of intermolecular, electrical repulsion is true a number of predictions can be made which could be tested experimentally. First, compaction of NFs would require either dephosphorylation of NFs or a loss of their fractional charge. The former has been promulgated by several authors (Pettus and Povlishock, 1996; Jafari et al., 1997, 1998; Maxwell et al., 1997). However, direct evidence for NF dephosphorylation has only been provided in a model of TAI recently (Saatman et al., 2003). Importantly, Saatman et al. (2003) provided novel evidence that calpain-mediated proteolysis of spectrin has a biphasic time course. Use of the antibody Ab38 that recognizes a spectrin fragment generated specifically by activated calpain (Roberts-Lewis et al., 1994) indicated labelling of axons between 20min and 2 hours and loss of labelling by 4 hrs after stretch-injury to mouse optic nerve. Those findings extended earlier ultrastructural data (Buki et al., 1999) that calpain-mediated spectrin proteolysis occurred within minutes of TAI in a fluid-percussion model of TAI. Moreover, foci of calpain-mediated spectrin proteolysis (CMSP) progressed from the axolemma toward the central region of an injured/damaged axon over a short period, about 2 hours, after TAI (Buki et al., 1999). The latter study was important in that it provided the first evidence that the axolemma and subaxolemma cytoskeleton are the initial sites of activity of calpain-mediated proteolytic function and supports the hypothesis that loss of integrity of the axolemma and its subaxolemma cytoskeleton are key in the development of the subsequent pathology. However, Saatman et al., (2003) also provided evidence for a second phase of calpain activity in that SMI32 labelling of small axonal swellings, bulbs and the occasional thin axonal segment was obtained at 4 days after injury. Particularly pertinent to the present study, SMI32 labelling occurred at 4 days in axonal bulbs, swellings and axonal segments of fairly uniform calibre and there was widespread labelling with SMI32 at 14 days after TAI. In addition, the median percentage of damaged or labelled axons increased from 14% at 1 day to 65% at 4 days and to 86% at 14 days (Saatman et al., 2003). Significantly, however, no labelling for calpain-mediated spectrin proteolysis, Ab38, occurred at 14 days after injury. The identification of sites of calpain-

mediated spectin proteolysis did not therefore spatially or temporally match or co-localise at sites at which SMI32 labelling indicated that axonal NFs had been dephosphorylated.

The critical experiment in which co-localisation of SMI32 and RM014 labelling occurs has not yet been undertaken. Nonetheless, the present study provides independent evidence for an ongoing, slow and long term pathology in a large proportion of axons following TAI. Saatman et al. (2003) provided evidence for axonal pathology up to 14 days after TAI. The present study extends that data to three weeks after injury. Moreover, both experiments provide novel evidence for an increased number of damaged or injured axons with increasing survival. Clearly, longer post-traumatic survivals need to be examined to determine the time course of this recently recognised pathology. Although direct evidence for the action of calpains upon NF side-arms is presently lacking; it may be posited that calpain-mediated proteolysis is a component of the process during the early stages of axonal responses to TAI and may, hypothetically, lead to secondary axotomy. But the results of the current study, together with those of Saatman et al., (2003) allow generation of the hypothesis that a second, previously unsuspected, pathology is occurring which leads to a reduction in axonal calibre but does not result in loss of those axons up to three weeks after TAI.

CHAPTER SIX

BIBLIOGRAPHY

ADAMS J.H., MICHELL D.E., GRAHAM D.I., and DOYLE D. (1977) Diffuse brain damage of immediate impact type. *Brain* **100**: 489-502.

ADAMS J.H., GRAHAM D.I., and SCOTT G. (1980) Brain damage in non-missile injury. *J. Clin. Pathol.* **33**: 1132-1145.

ADAMS J.H., GRAHAM D.I., MURRAY L.S., SCOTT G. (1982) Diffuse axonal injury due to nonmissile head injury in human: analysis of 45 cases. *Ann. Neurol.* **12**: 557-563.

ADAMS J.H., DOYLE D., FORD I., GENNARELLI T.A., GRAHAM D.I., and McLELLAN D.R. (1989) Diffuse axonal injury in head injury: Definition, diagnosis and grading. *J. Histopathol.* **15**: 49-59.

ADAMS J.H., JENNET B., McLELLAN D.R., MURRY L.S., and GRAHAM D.I. (1999) The neuropathology of the vegetative state after head injury. *J. Clinical. Pathol.* **52**: 804-806.

ADAMS J.H., GRAHAM D.I., and JENNET B. (2000) The neuropathology of the vegetative state after an acute brain insult. *Brain* **123**: 1327-1338.

ADAMS J.H., GRAHAM D.I., and JENNET B. (2001) The structural basis of moderate disability after traumatic brain injury. *J. Neurol. Neurosurg. Psychiatry* **71**: 521-524.

ADAMS T. B., HOLMES M., SHAN Y., TEDESCO C.S., MASCARI C., KAUL A., WIGHT D.C., MORRIS R.E., SUSSMAN M., DIAMOND J., and PARYSEK I.M. (2003) An intact intermediate filament network is required for collateral sprouting of small diameter nerve fibers. *J. Neurosci.* **23**: 9312-9319.

ALLAN V.J., VALE R.D., and NAVONE F. (1991) Microtubule-based organelle transport in neurons. In *The Neuronal Cytoskeleton* Ed. Burgoyne RD. New York: Wiley-Liss pp. 257- 282.

AMADUCCI L., FORNO K.I., and ENG L.F. (1981) Glial fibrillary acidic protein in cryogenic lesions of the rat brain. *Neurosci. Lett.* **21**: 27-32.

- ANDERSON R.W.G., BROWN C.J., BLUMBERGS P.L., McLEAN A.J., and JONES N.R. (2003) Impact mechanics and axonal injury in a sheep model. *J. Neurotrauma* **20**: 961-974.
- ANDREW A., and GRAHAM T. (2001) Head injury in the United Kingdom. *World Journal of Surgery* **25**: 1210-1220.
- ANG B.T., YAP E., LIM J., TAN W.L., NG P-Y., IVAN N.G., and YFO T.T. (2003) Polymerase expression in human traumatic brain injury. *J. Neurosurg.* **99**: 125-130.
- ANGELIDES K.J., SMITH K.F., and TAKEDA M. (1989) Assembly and exchange of intermediate filament proteins of neurons: Neurofilaments are dynamic structures. *J. Cell Biol.* **108**: 1495-1506.
- ARBUTHNOTT E.R., BALLARD K.J., BOYD I.A., and KAL K.U. (1980) Quantitative study of the non-circularity of myelinated peripheral nerve fibres in cat. *J. Physiol. (Lond)* **308**: 99-123.
- ARMONDO B., IGNACIO P., DUARTE J.M., and FERRARI N. (2001) Advances in management of neurosurgical trauma in different continents. *World Journal of Surgery* **25**: 1174-1178.
- ASHEUER M., PFLUMIO F., BENHAMIDA S., DUBART-KUPPERSCHMITT A., FOUQUET F., IMAI Y., AUBOURG P and CARTIER N. (2004) Human CD34+ cells differentiate into microglia and express recombinant therapeutic protein. *Proc. Nat. Acad. Sci.* **101**: 3557-3562.
- AVELLINO A.M., HART D., DAILY A.T., MACKINNON M., ELLEGALA D., and KLIOT M. (1995) Differential macrophage responses in the peripheral and central nervous system during wallerian degeneration of axons. *Exp. Neurol.* **136**: 183-198.
- BAAS P.W., and HEIDMANN S.R. (1986) Microtubule reassembly from nucleating fragments during the regrowth of amputated neurites. *J. Cell Biol.* **103**: 917-927.

- BAAS P.W., SINCLAIR G.I., and HEIDEMANN S.R. (1987) Role of microtubules in the cytoplasmic compartmentation of neurons. *Brain Res.* **240**: 73-81.
- BAAS P.W., and BLACK M.M. (1990) Individual microtubules in the axon consist of domains that differ in both composition and stability. *J. Cell Biol.* **111**: 495-509.
- BAAS P.W., SLAUGHTER T., BROWN A., and BLACK M.M. (1991) Microtubule dynamics in axons and dendrites. *J. Neurosci. Res.* **30**: 134-153.
- BAAS P.W., AHMED F.J., PIENKOWSKI T.P., BROWN A., and BLACK M.M. (1993) Sites of microtubule stabilization for the axon. *J. Neurosci.* **13**: 2177-2185.
- BAAS P.W., PIENKOWSKI T.P., CIMBALNIK K.A., TOYAMA K., BAKALIS S., AHMED F.J., and KOSIK K.S. (1994) Tau confers drug stability but not cold stability to microtubules in living cells. *J. Cell Sci.* **107**: 135-143.
- BAITINGER C., LEVINE J., LORENZ T., SIMON C., SKENE P., and WILLARD M. (1982) Characteristics of axonally transported proteins. In *Axoplasmic Transport*. Ed. Weiss DG. Berlin: Springer Verlag, pp 110-120.
- BALLIN R.H.M., and THOMAS P.K. (1969) Changes at the nodes of Ranvier during Wallerian degeneration: an electron microscopic study. *Acta Neuropathol.* **14**: 237-249.
- BANATI R.B., GEHRMANN J., SCHUBERT P., and KREUTZBERG G.W. (1993) Cytotoxicity of microglia. *Glia* **7**: 111-118.
- BARRON K.D. (1983) Comparative observations on the cytologic reactions of central and peripheral nerve cells to axotomy. In *Spinal Cord Reconstruction* (Kao C.C., Bunge P.R., Reier P.J., ed.) pp 7-40. New York, Raven Press.
- BAUR P.S., and STACY T.R. (1977) The use of PIPES buffer in the fixation of mammalian and marine tissues for electron microscopy. *J. Microscopy* **109**: 315-327.

BEARER E.L., and REESE T.S. (1999) Association of actin filament with axonal microtubule tracts. *J. Neurocytol.* **28**: 85-98.

BEARER E.L., DeGIORGIS J.A., BODNER R.A., KOCO A.W., and REESE T.S. (1993) Evidence of myosin motors on organelles in squid axoplasm. *Proc. Acad. Natl. Sci.* **90**: 11252-11256.

BECHMANN I., KWIDZINSKI E., KOVAC A.D., SIMBURGER E., HORVATH T., GIMSA U., DIRNAG U., PRILLER J., and NITSCH R. (2001) Turnover of rat brain perivascular cells. *J. Exp. Neurol.* **168**: 242-249.

BEIROWSKI B., BEREK I., ADALBERT R., WAGNER D., GRUMME D.S., ADDIKS K., RIBCHESTER R.R., and COLEMAN M.P. (2004) Quantitative and qualitative analysis of Wallerian degeneration using restricted axonal labelling in YFP-H mice. *J. Neurosci. Methods* **15**: 23-35.

BEIROWESKI B., ADALBERT R., WAGNER D., GRUMME D.S., ADDICKS K., RIBCHESTER R.R., and COLEMAN M.P. (2005) The progressive nature of Wallerian degeneration in wild-type and slow Wallerian degeneration nerves. *B.M.C. Neurosci.* **6**: 1-27.

BENES F.M., and LANGE N. (2001) Two-dimensional versus three-dimensional cell counting: a practical perspective. *Trends in Neurosci.* **24**: 11-17.

BENTIVOGLIO M. (1999) The discovery of axonal transport. *Brain Res. Bull.* **50**: 383-384.

BERNHARDT R., and MATUS A. (1984) Light and electron microscopic studies of the distribution of microtubule-associated protein 2 in rat brain: a difference between dendritic and axonal cytoskeletons. *J. Comp. Neurol.* **226**: 203-221.

BIASCA N., WIRTH S., MAXWELL W., and SIMEN H-P. (2005) Minor traumatic brain injury (mTBI) in ice hockey and other contact sports. *Eur. J. Trauma* **31**: 105-116.

- BILLGER M., WALLIN M., and KARLSSON J.O. (1988) Proteolysis of tubulin and microtubule-associated 1 and 2 by calpain 1 and 2. Difference in sensitivity of assembled and disassembled microtubules. *J. Cell Calcium* **9**: 33-44.
- BISBY M.A., and BULGER V.T. (1981) Reversal of axonal transport similarity of proteins transported in anterograde and retrograde direction. *J. Neurochem.* **36**: 741-745
- BISBY M.A. (1987) Does recycling have a function other than disposal in axonal transport?. *J. Neurobiol.* **25**: 365-383.
- BLACK M.M., and LASEK R.J. (1980) Slow components of axonal transport: Two cytoskeletal networks. *J. Cell Biol.* **86**: 616-623.
- BLACK M.M., and LEE. V.Y.M. (1988) Phosphorylation of neurofilament proteins in intact neurons: demonstration of phosphorylation in cell bodies and axons. *J. Neurosci.* **9**: 3296-3305.
- BLIKSTAD I., SJUNDKVIST I., and ERIKSSON S. (1980) Isolation and characterization of profilactin and profiling from calf thymus and brain. *Eur. J. Biochem.* **105**: 425-434.
- BLOOM G.S. (1992) Motor proteins for cytoplasmic microtubules. *Curr. Opin. Cell Biol.* **4**: 66-73.
- BLUMBERGS P.C. (1995) Chapter 2: Pathology in *Head Injury* (Eds Bullock RM and Blumbergs PC) Academic Press.
- BLUMBERGS P.C., and SCOTT G. (1994) Staining of amyloid precursor protein to study axonal damage in mild head injury. *Lancet* **344**: 1055-1056.
- BLUMBERGS P.C., SCOTT G., MANAVIS J., WAINWRIGHT H., SIMPSON D.A., and MCLEAN A.J. (1995) Topography of axonal injury as defined by amyloid precursor protein and the sector scoring method in mild and severe closed head injury. *J. Neurotrauma* **12**: 565-572.

- BODIAN D. (1951) A note on nodes of Ranvier in the central nervous system. *J. Comp. Neurol.* **94**: 475-484.
- BRADY S.T., TYTELL M., HERIOT K., and LASEK R.J. (1981) Axonal transport of calmodulin: A physiological identification of long-term associations between proteins. *J. Cell Biol.* **89**: 607-614.
- BRADY S.T., and LASEK R.J. (1982) The slow components of axonal transport: Movements, compositions, and organization. In *Axoplasmic Transport*. Weiss D.G. (ed.) Berlin: Springer Verlag, pp 206-217.
- BRADY S.T. (1985) A novel brain ATPase with properties expected for the fast axonal transport motor. *Nature* **317**: 73-75.
- BRADY S.T. (1993) Axonal dynamics and regeneration. In *Neuroregeneration*, A. Gorio (Ed.) Raven Press, New York. Pp 7-36.
- BRADY S.T., LASEK R.J., and ALLEN R.D. (1997) Slow axonal transport: the polymer transport model. *Trends Cell Biol.* **7**: 380-384.
- BRAIN A.J. (1990) Ankyrin and the node of Ranvier. *Trends in Neurosci.* **13**: 119-121
- BRANDT R., LÉGER J., and LEE G. (1995) Interaction of tau with the neural plasma membrane mediated by tau's amino-terminal projection domain. *J. Cell Biol.* **131**: 1327-1340.
- BRANDT R. (1996) The tau proteins in neuronal growth and development. *Frontiers Biosci.* **1**: 18-130*
- BREATCHER A. (1991) Microfilament structure and function in the cortical cytoskeleton. *Ann. Rev. Cell Biol.* **7**: 337-374.

- BREUER A.C., LYNN M.P., ATKINSON S.M., CHOU S.M., WILBOURN A.J., MARKS K.E., CULVER J.E., and FLEEGLER E.J. (1987) Fast axonal transport in amyotrophic lateral sclerosis: an intra-axonal organelle traffic analysis. *Neurology* **37**: 738-748.
- BRIDGMAN P.C., and ELKIN L.E. (2000) Axonal myosins. *J. Neurocytol.* **29**: 831-841.
- BROWN A. (1997) Visualization of single neurofilaments by immunofluorescence microscopy of splayed axonal cytoskeletons. *Cell Motil. Cytoskelet.* **38**: 133-145
- BROWN A. (2000) Slow axonal transport: stop and go traffic in the axon. *J. Cell Biol.* **157**: 153-156.
- BROWN A. (2003) Axonal transport of membranous and non-membranous cargoes: a unified perspective. *J. Cell Biol.* **160**: 817-821.
- BROWN S.S. (1999) Cooperation between microtubule- and actin-based motor proteins. *Ann. Rev. Cell Devel. Biol.* **15**: 63-80.
- BRYAN J. (1976) Quantitative analysis of microtubule elongation. *J. Cell Biol.* **71**: 749-767.
- BUKI A., SIMAN R., TROJANOWSKI J.K., and POVLISHOCK J.T. (1999) The role of calpain-mediated spectrin proteolysis in traumatically induced axonal injury. *J. Neuropathol. Exp. Neurol.* **58**: 365-375.
- BUKI A., FARKAS O., KOVER F., and DOCZI T. (2000) Therapeutic possibilities in axonal injury caused by head trauma. *J. Orv. Hetil.* **143**: 499-503.
- BUKI A., OKONKWO D.O., WANG K.K., and POVLISHOCK J.T. (2000) Cytochrome c release and caspase activation in traumatically axonal injury. *J. Neurosci.* **20**: 2825-2834.

BUKI A., WALKER S.A., STONE J.R., and POVLISHOCK J.T. (2000) Novel application of tyramide signal amplification (ATS): ultrastructural visualization of double-labelled immunofluorescent axonal profiles. *J. Histochem. Cytochem.* **48**: 153-161.

BUNGE M.B., BUNGE R.P., PETERSON E.R., and MURRAY M.R. (1967) A light and electron microscopy study of long-term organized cultures of rat dorsal root ganglia. *J. Cell Biol.* **32**: 439-466.

BUNGE R.P., PUCKETT W.R., BECERRA J.L., MARCILLO A., and QUENCER R.M. (1993) Observations on the pathology of human spinal cord injury. A review and classification of 22 new cases with details from a case of chronic cord compression with extensive focal demyelination. *Adv. Neurol.* **59**: 75-89.

BUSS A., and SCHWAB M.E. (2003) Sequential loss of myelin proteins during Wallerian degeneration in the rat spinal cord. *Glia* **42**: 424-432.

BUSS A., BROOK G.A., KAKULAS B., MARTIN D., FRANZEN R., SCHOENEN J., NOTH J., and SCHMITT A.B. (2004) Gradual loss of myelin and formation of an astrocytic scar during Wallerian degeneration in the human spinal cord. *Brain* **127**: 34-44.

BUSS A., PECH K., MERKLER D., KAKULAS B. A., MARTIN D., SCHOENEN J., NOTH J., SCHWAB M.E., and BROOK G.A. (2005) Sequential loss of myelin proteins during Wallerian degeneration in the human spinal cord. *Brain* **128**: 356-364.

CAJAL S. R. y. (1928) "Degeneration and Regeneration of the Nervous System" translated and edited by R. M. May, London, Oxford University Press.

CAMPENOT R.B., and ENG H. (2000) Protein synthesis in axons and its possible functions. *J. Neurocytol.* **29**: 793-798.

CARBONELL A.L., BOYA J., CALVO J.L., and MARIN J.F. (1991) Ultrastructural study of the neuroglial and macrophage reaction in Wallerian degeneration of the adult rat optic nerve. *J. Histol. Histopathol.* **6**: 443-451.

CARBONELL W.S., and GRADY M.S. (1999) Regional and temporal characterization of neuronal, glial and axonal response after traumatic brain injury in the mouse. *Acta Neuropathol.* **98**: 396-406.

CARLIER M.F., SIMON C., CASSOLY R., and PRADEL L.A. (1984) Interaction between microtubule-associated protein tau and spectrin. *Biochem.* **66**: 305-311.

CAVALLI V., KUJULA P., KLUMPERMAN J., and GOLDSTEIN L.S.B. (2005) Sunday Driver Links axonal transport to damage signaling. *J. Cell Biol.* **168**: 775-787.

Centers for Disease Control and Prevention (2001) Traumatic brain injury(TBI): incidence and distribution. *Injury fact book 2001-2002.*

CEPURNA W.O., KAYTON R.J., JOHNSON E.C., and MORRISON J.C. (2004) Age related optic nerve axonal loss in adult brown Norway rats. *J. Exp. Eye Res.* **XX**: 1-8.

CERNAK I., VINK R., ZAPPLE D.N., CRUZ M.I., AHMED F., CHANG T., FRICKE S.T., and FADEN A.I. (2004) The pathobiology of moderate diffuse traumatic brain injury as identified using a new experimental model of injury in rats. *Neurobiol. Disease* **17**: 29-43.

CHIEN J., KANAI Y., COWAN N.J., and KIROKAWA N. (1992) Projection domains of MAP2 and tau determine spacings between microtubules in dendrites and axons. *Nature* **360**: 674-677.

CHEN X.H., MEANEY D.F., XU B.N., NONAKA M., MCINTOSH T.K., WOLFE J.A., SAATMAN K.E., and SMITH D.H. (1999) Evolution of neurofilament subtype accumulation in axons following diffuse brain injury in the pig. *J. Neuropathol. Exp. Neurol.* **58**: 588-596.

CHEN X.H., SIMAN R., IWATA A., MEANEY D.F., TROJANOWSKI J.Q., and SMITH D.H. (2004) Long- term accumulation of amyloid- β , β -secretase, presenilin-1, and caspase-3 in damaged axons following brain trauma. *Am. J. Pathol.* **165**: 357-371.

CHRISTMAN C.W., SALVAN J.B., WALKER S.A., and POVLISHOCK J.T. (1997) Characterization of a prolonged regenerative attempt by diffuse injured axons following traumatic brain injury in adult cat: a light and electron microscopic immunocytochemical study. *Acta Neuropathol.* **94**: 329-337.

CHRISTMAN C.W., GRADY M.S., WALKER S.A., HOLLOWAY K.L., and POVLISHOCK J.T. (1994) Ultrastructural Studies of Diffuse Axonal Injury in Humans. *J. Neurotrauma* **11**: 173-186.

CLEVELAND D.W., HWO S.V., and KIRSCHNER M.W. (1977) Physical and chemical properties of purified tau factor and the role of tau in microtubule assembly. *J. Mol. Biol.* **116**: 227-247.

COOK R.D., and WISNIEWSKI H.N. (1973) The role of oligodendroglia and astroglia in Wallerian degeneration of the optic nerve. *Brain Res.* **61**: 191-206.

COUCHIE D., MAVILIA C., GEORGIEFF I.S., LIEM R.K., SHELANSKI M.L., and NUNEZ J. (1992) Primary structure of high molecular weight tau present in the peripheral nervous system. *Proc. Natl. Acad. Sci. USA* **89**: 4378-4381.

CREVEL H.V., and VERHAART W.J.C. (1963) The rate of secondary degeneration in the central nervous system. The optic nerve of the cat. *J. Anat.* **97**: 451-464.

CROWE M.J., BRESNAHAN J.C., SHUMAN S.L., MASTER J.N., and BEATTIE M.S. (1997) Apoptosis and delayed degeneration after spinal cord injury in rats and monkeys. *Nat. Med.* **3**: 73-76

CULL G., CIOFFIN G.A., DONG J., HOMER I., and WANG L. (2003) Estimating normal optic nerve axon number in non-human primate eyes. *J. Glaucoma* **12**: 301-306.

DE S., TRIGUEROS M.A., KALYVAS A., and DAVID S. (2003) Phospholipase A2 plays an important role in myelin breakdown and phagocytosis during Wallerian degeneration. *J. Mol. Cell Neurosci.* **24**:753-765.

DEACON S.W., SERPINSKAYA A.S., VAUGHAN P.S., FANARRAGA K.T., and GELFAND V.I. (2003) Dynactin is required for bidirectional organelle transport. *J. Cell Biol.* **160**: 297-301.

DEKKER-OHNO K., ILAYASAKA S., TAKAGISHI Y., ODA S., WAKASUGI N., MIKOSHIBA K., INOUE M., and YAMAMURA H. (1996) Endoplasmic reticulum is missing in dendritic spines of Purkinje cells of the ataxic mutant rat. *Brain Res.* **714**: 226-230

DENNY-BROWN J.P., and RUSSEL W.R. (1941) Experimental cerebral concussion. *Brain* **64**: 93-164.

DEWAEGH S.M., LEE V.M.Y., and BRADY S.T. (1992) Local modulation of neurofilament phosphorylation, axonal caliber, and slow axonal transport by myelinating Schwann cells. *Cell* **68**: 451-463.

DIETRICH D.W., ALONSO O., and HALLEY M. (1994) Early microvascular and neuronal consequences of traumatic brain injury: A light and electron microscopic study in rats. *J. Neurotrauma* **11**: 289-301.

DIKA S., STEART P.V., ZHANG E.T., and WELLER R.O. (1993) Perivascular cells act as scavengers in the cerebral perivascular spaces and remain distinct from pericytes, microglia and macrophages. *Acta Neuropathol.* **85**: 646-652.

DOLINAK D., SMITH C., and GRAHAM D.I. (2000) Global hypoxia per se is an unusual cause of axonal injury. *Acta Neuropathol.* **100**: 553-560.

- DONAGHY M., KING R.H.M., THOMAS P.K., and WORKMAN S.J.M. (1988) Abnormalities of the axonal cytoskeleton in giant axonal neuropathy. *J. Neurocytol.* **17**: 197-208.
- DONNET C.W. (1964) New tables for multiple comparisons with a control. *Biometrics* **20**: 482-491.
- DYER C.A. (2002) The structure and function of myelin: from inert membrane to perfusion pump. *J. Neurochem. Res.* **27**: 1279-1292.
- EBNETH A., GODEMANN R., STAMER K., ILLENBERGER S., TRINCZEK B., and MANDELKOW E. (1998) Overexpression of *tau* protein inhibits kinesin-dependent trafficking of vesicles, mitochondria, and endoplasmic reticulum: implications for Alzheimer's disease. *J. Cell Biol.* **143**: 777-794.
- ELDADAH B.A., and FADEN A.I. (2000) Caspase pathways, neuronal apoptosis, and CNS injury. *J. Neurotrauma* **7**: 811-829.
- ELDER G.A., FRIEDRICH V.L., PEREIRA D., TU P-H., ZHANG B., LEE V.M.Y., and LAZZARINIA R.A. (1999) Mice with disrupted mid-sized and heavy neurofilament genes lack axonal neurofilaments but unaltered numbers of axonal microtubules. *J. Neurosci.* **57**: 23-32.
- EMERY D.L., RAGUPATHI R., SAATMAN K.E., FISCHER I., GRADY M.S., and McINTOSH T.K. (2000) Bilateral growth-related protein expression suggests a transient increase in regenerative potential following brain trauma. *J. Comp. Neurol.* **424**: 521-531.
- ENGEL S., SCHLUESENER H., MITTELBRONN M., SEID K., ADJODAH D., WEHNER H.D., and MEYERMANN R. (2000) Dynamics of microglial activation after human traumatic brain injury are revealed by delayed expression of macrophage-related proteins MRP8 and MRP14. *Acta Neuropathol (Berl)*. **100**, 313-322.

- ESPREAFIGO C.M., CHENEY R.E., MATTEOLI M., NASCIMENTO A.A., De CAMILLI P.V., LARSON R.E., and MOOSEKER M.S. (1992) Primary structure and cellular localization of chicken brain myosin-V(p190), an unconventional myosin with calmodulin light chains. *J. Cell Biol.* **119**: 1541-1557.
- EUGENIN E.A., ECKARDT D., THEIS M., WILLECKE K., BENNETT M.V.L. and SÁEZ J.C. (2001) Microglia at brain stab wounds express connexin 43 and *in vitro* form functional gap junctions after treatment with interferon- γ and tumor necrosis factor- α . *Proc. Natl. Acad. Sci. USA* **98**: 4190-4195.
- EVANS L.L., HAMMER J. and BRIDGMAN P.C. (1997) Subcellular localization of myosin V in nerve growth cones and outgrowth from dilute-lethal neurons. *J. Cell Sci.* **110**: 439-449.
- EVANS L.L., LEE A.J., BRIDGMAN P.C., and MOOSEKER M.S. (1998) Vesicle-associated brain myosin-V can be activated to catalyze actin-based transport. *J. Cell Sci.* **111**: 2055-2066.
- FADEN A.L. (1992) Comment on the need for standardization of animal models of spinal cord injury. *J. Neurotrauma* **9**: 169-172.
- FATH K.R., TRIMBUR G.M., and BURGESS D.R. (1994) Molecular motors are differentially distributed on Golgi membranes from polarized epithelial cells. *J. Cell Biol.* **126**: 661-675.
- FERNANDEZ-VALLE C., BUNGE R.P., and BUNGE M.B. (1995) Schwann cells degrade myelin and proliferate in the absence of macrophages: evidence from *in vitro* studies of Wallerian degeneration. *J. Neurocytol.* **24**: 667-679.
- FIALA M., LIU Q.N., SAYRE J., POP V., BRAHMANDAM V., GRAVES M.C. and VINTERS H.V. (2002) Cyclooxygenase-2-positive macrophages infiltrate the Alzheimer's disease brain and damage the blood-brain barrier. *Eur. J. Clin. Invest.* **32**: 360-371.

FISCHER D., HEIDUSCHKA P., and THANOS S. (2001) Lens- injury- stimulated axonal regeneration throughout the optic pathway of adult rats. *J.Exp. Neurol.* **172**: 257-272.

FIZPATRICK M.O., MAXWELL W.L., and GRAHAM D.I. (1998) The role of the axolemma in the initiation of traumatically induced axonal injury. *J. Neurol. Neurosurg. Psychiatry* **64**: 285-287.

FLIEGNER K.II., CHING G.Y., and LIEM P.K. (1990) The predicted amino acid sequence of alpha-internexin is that of a novel neuronal intermediate filament protein. *EMBO J.* **9**: 749-755.

FRANCON J., LENNON A.M., FELLOUS A., MARECK A., PIERRE M., and NUNEZ J. (1982) Heterogeneity of microtubule-associated proteins and brain development. *Eur. J. Biochem.* **129**: 465-471.

FRANZEN R., TANNER S.L., DASHIELL S.M., ROTTKAMP C.A., HAMMER J.A., and QUARLES R.H. (2001) Microtubule-associated protein 1B: a neuronal binding partner for myelin-associated glycoprotein. *J. Cell Biol.* **155**: 893-898.

FRAPPIER T., DERANCOURT J., and FRADEL L.A. (1992) Actin and neurofilament binding domain of brain spectrin β subunit. *Eur. J.Biochem.* **205**: 85-91.

FREIDRICH V.L., and MUGNAINI E. (1983) Myelin sheath thickness in the CNS is regulated near the axon. *Brain Res.* **274**: 329-331.

GALBRATH J.A., and GALLANT P.E. (2000) Axonal transport of tubulin and actin. *J. Neurocytol.* **29**: 889-911.

GALLANT P. E., and GALBRAITH J.A. (1997) Axonal structure and function after axolemmal leakage in the squid giant axon. *J. Neurotrauma* **14**: 811-822.

GALLANT P.E. (2000) Axonal protein synthesis and transport. *J. Neurocytol.* **29**: 779-782.

- GASKIN F., CANTON C.R., and SHELANSKI M.L. (1975) Biochemical studies in *in vitro* assembly and disassembly of microtubules. *Ann. N. Y. Acad. Sci.* **253**: 133-146.
- GEDDES J.F., WHITWELL H.L., and GRAHAM D.I. (2000) Traumatic axonal injury: practical issues for diagnosis in medicolegal cases. *J. Neuropathol. Appl. Neurobiol.* **26**: 105-116.
- GEE M.A., HEUSER J.E., and VALLEE R.B. (1997) An extended microtubule-binding structure within the dynein motor domain. *Nature* **390**: 636-639.
- GEHRMANN J. and KREUTZBERG G.W. (1991) Characterisation of two new monoclonal antibodies directed against rat microglia. *J Comp Neurol.* **313**: 409-430.
- GEHRMANN J., MONACO S., and KREUTZBERG G.W. (1991) Spinal cord microglial cells and DRG satellite cells rapidly respond to transection of the rat sciatic nerve. *Restor. Neurol. Neurosc.* **2**: 181-198.
- GEHRMANN J., BANATI R.B., WIESSNER C., HOSMANN K.A., and KREUTZBERG G.W. (1995) Reactive microglia in cerebral ischaemia: an early mediator of tissue damage?. *Neuropathol. Appl. Neurobiol.* **21**: 277-289.
- GENNARELLI T.A., THIBAUT L.E., ADAMS J.H., GRAHAM D.I., THOMPSON C.J., MARCINCIN R.P. (1982) Diffuse axonal injury and traumatic coma in the primate. *Ann. Neurol.* **12**: 564-574.
- GENNARELLI T.A., THIBAUT L.E., TIPPERMAN R., TOMEI G., BROWN M., MAXWELL W.L., GRAHAM D.I., ADAMS J.H., IRVINE A., GENNARELLI L.M., DUHAIME A.C., BOOCK R. and GREENBERG J. (1989) Axonal injury in the optic nerve: a model simulating diffuse axonal injury in the brain. *J. Neurosurg.* **71**: 244-253.
- GENNARELLI T.A. (1993) Mechanisms of brain injury. *J. Emerg. Med.* **11** supp. **1**: 5-11.
- GENNARELLI T.A. (1994) Animate models of human head injury. *J. Neurotrauma* **11**: 357-368.

GENTLEMAN S., NASH M., and SWEETING C. (1993) Amyloid precursor protein as a marker for axonal injury after head injury. *Neurosci. Lett.* **160**: 1132-1145.

GENTLEMAN S.M., ROBERTS G.W., GENNARELLI T.A., MAXWELL W.L., ADAMS J.H., KERR S., and GRAHAM D.I. (1995) Head injury: a universal consequence of fatal closed head injury?. *Acta Neuropathol.* **89**: 537-543.

GEORGE R., and GRIFFIN J.W. (1994a) The proximodistal spread of axonal degeneration in the dorsal columns of the rat. *J. Neurocytol.* **23**: 657-667.

GEORGE R., and GRIFFIN J.W. (1994b) Delayed macrophage responses and myelin clearance during Wallerian degeneration in the central nervous system: The dorsal radicotomy model. *Exp. Neurol.* **129**: 225-236.

GLASS D., SCHIRYER B.L., and GRIFFIN J.W. (1994) Calcium-mediated degeneration of axonal cytoskeletal in the Ola mouse. *J. Neurochem.* **62**: 2472-2475.

GLASS J.D., and GRIFFIN J.W. (1991) Neurofilament redistribution in transected nerves: evidence for bidirectional transport of neurofilaments. *J. Neurosci.* **11**: 3146-3154.

GOEDERT M., SPILLANTINI M.G., and CROWTHER R.A. (1992) Cloning of a big tau microtubule-associated protein characteristic of the peripheral nervous system. *Proc. Natl. Acad. Sci. USA* **89**: 1983-1987.

GOLDMAN S.S. (1982) The role of calcium on the cellular response following injury to the nervous system. In *Head Injury: Basic and Clinical Aspects* (ed. Grossmann GR and Gildenberg PL). New York, Raven Press, pp 85-92.

GOODSON H.V., and HAWSE W.F. (2002) Molecular evolution of the actin family. *J. Cell Sci.* **115**: 2619-2622.

- GORRIE C., OAKES S., DUFLOU J., BLUMBERGS P., and WAITE M.E. (2002) Axonal injury in children after motor vehicle crashes: extent, distribution, and size of axonal swellings using β -APP immunohistochemistry. *J. Neurotrauma* **19**: 1171-1182.
- GOTOW T., and TANAKA T. (1994) Phosphorylation of neurofilament H subunit as related to arrangement of neurofilaments. *J. Neurosci. Res.* **37**: 673-684.
- GOTOW T., TANAKA J., NAKAMURA Y., and TAKEDA. M. (1994) Dephosphorylation of largest neurofilament H subunit protein influences the structure of crossbridges in reassembled neurofilaments. *J. Cell Sci.* **107**: 1949-1957.
- GRADY S.M., McLAUGHLIN M.R., CHRISTMAN C.W., VALADKA A.B., FLIGNER C.L., and POVLISHOCK J.T. (1993) The use of antibodies targeted against the neurofilament subunits for the detection of diffuse axonal injury in humans. *J. Neuropathol. Exp. Neurol.* **52**: 143-152.
- GRAEBER M.B., and STREIT W.J. (1990) Perivascular microglia defined. *Trends in Neurosci.* **13**: 174-178.
- GRAEBER M.B., BISE K., and MEHRAEIN P. (1994) CR3/43, a marker for activated human microglia: application to diagnostic neuropathology. *Neuropathol. Appl. Neurobiol.* **20**: 406-408.
- GRAEBER M.B., STREIT W.J., and KREUTZBERG G.W. (1988) Axotomy of the rat facial nerve leads to increased CR3 complement. *J. Neurosci. Res.* **21**: 18-24.
- GRAFSTEIN B., and FORMAN D.S. (1980) Intracellular transport in neurons. *Physiol. Rev.* **60**: 1167-1183.
- GRAHAM D.I., ADAMS J.H., and GENNARELLI T.A. (1993) Pathology of brain damage in head injury. In *Head injury* 3rd ed. PR Cooper, ed. Baltimore; London: Williams S and Wilrins.Pps. 91-113.

GRAHAM D.I., ADAMS J.H., NICOLI J.A.R., MAXWELL W.L. and GENNARELLI T.A. (1995) The nature, distribution and causes of traumatic brain injury. *Brain Pathol.* **5**: 397-406.

GRAHAM D.I., RAGHUPATHI R., SAATMAN K.E., MEANEY D., and McINTOSH T.K. (2000) Tissue tears in the white matter after lateral fluid percussion brain injury in the rat: relevance to human brain injury. *Acta Neuropathol.* **99**: 117-124.

GRAHAM D.I., GENNARELLI T.A., McINTOSH T.K. (2002) Trauma. In: *Greenfield's Neuropathology* (7th edition) D.I. Graham, PL Lantos, ed. London: Arnold 2002. pp 823-898.

GRANT P., and PANT H.C. (2000) Neurofilament protein synthesis and phosphorylation. *J. Neurocytol.* **29**: 843-872.

GRAY'S ANATOMY: The Anatomical Basis of Medicine and Surgery, 39th Edition, 2004. (Ed. Susan Standring.) Elsevier, London and Rotterdam.

GREENBERG S.G., and LASEK R.J. (1988) Neurofilament protein synthesis in DRG neurons decreases more after peripheral axotomy than after central axotomy. *J. Neurosci.* **8**: 1739-1746.

GRIFFIN J.W., GEORGE R., and HO T. (1993) Macrophage systems in peripheral nerves. A review. *J. Neuropathol. Exp. Neurol.* **52**: 553-560.

GRIFFIN J.W., GEORGE E.B., HSIEH S-T., and GLASS J.D. (1995) Axonal degeneration and disorders of the axonal cytoskeleton. In *The Axon* (Waxman SG, Kocsis JD, Stys PK ed.) pp375-390, New York, Oxford University Press.

GRIFFITH L.M., POLLARD T.D. (1982) The interaction of actin filaments with microtubules and microtubule-associated proteins. *J. Biol. Chem.* **257**: 9143-9151.

GUILLEMIN G.J., and BREW B.J. (2003). Microglia, macrophages, perivascular macrophages, and pericytes: a review of function and identification. *J. Leukocyte Biol.* **75**: 1-10.

- GULLERY R.W., and TAYLOR J.H. (1993) Different rates of axonal degeneration in the crossed and uncrossed retinofugal pathways of *Monodelphis domestica*. *J. Neurocytol.* **22**: 707-716.
- GULLERY R.W. (2002) Commentary on counting and counting errors. *J. Comp. Neurol.* **447**: 1-7.
- GULTEKIN S.H., and SMITH T.W. (1994) Diffuse axonal injury in craniocerebral trauma: a comparative histologic and immunohistochemical study. *Arch. Pathol. Lab. Med.* **118**: 168-171.
- GUO X., OYAMA M., and SUGITA S. (2001) Quantitative analysis of the optic nerve of the horse. *J. Vet. Med. Sci.* **63**: 971-975.
- GURURAJ G. (2002) Epidemiology of traumatic brain injuries: Indian scenario. *Neurological Res.* **24**: 24-28.
- GUTIERREZ E., HUANG Y., HAGLID K., BAO F., HANSSON II-A., HAMBERGER A., and VIANO D. (2001) A new model for diffuse brain injury by rotational acceleration: I. Model, gross appearance, and astrocytosis. *J. Neurotrauma* **18**: 247-257.
- GUY J., ELLIS F.A., KELLEY K., and HOPE G.M. (1989) Spectra of G ratio, myelin sheath thickness, and axon and fiber diameter in the Guinea pig optic nerve. *J. Comp. Neurol.* **287**: 446-454.
- HABURA A., TIKHONENKO I., CHISHOLM R.L., and KOONCE M.P. (1999) Interaction mapping of a dynein heavy chain. Identification of dimerization and intermediate-chain binding domains. *J. Biol. Chem.* **274**: 15447-15453.
- HALL G.F., and LEE V.M.Y. (1995) Neurofilament sidearm proteolysis is a prominent early effect of axotomy in lamprey giant central neurons. *J. Comp. Neurol.* **353**: 38-49.

HAMBERGER A., HUANG Y.L., ZHU H., BAO F., DING M., BLENNOW K., OLSSON A., HANSSON H.A., VIANO D., and HAGLID K.G. (2003) Redistribution of neurofilaments and accumulation of β -Amyloid protein after brain injury by rotational acceleration of the head. *J. Neurotrauma* **20**: 169-178.

HANSSON E. and RÖNNBÄCK L. (2003) Glial neuronal signaling in the central nervous system. *FASEB J.* **17**: 341-348.

HASAKA T.P., MYERS K.A., and BAAS P.W. (2004) Role of actin filaments in the axonal transport of microtubules. *J. Neurosci.* **24**: 11291-11301.

HAWLEY C.A., WARD A.B., MAGNAY A.R., and LONG J. (2002) Children's brain injury: a postal follow-up of 525 children from one health region in the UK. *Brain Injury* **11**: 969-985.

HAWLEY C.A., WARD A.B., MAGNAY A.R., and LONG J. (2003) Outcomes following childhood head injury: a population study. *J. Neurol. Neurosurg. Psychiatry* **75**: 737-742.

HAWLEY C.A. (2003) Reported problems and their resolution following mild, moderate and severe traumatic brain injury amongst children and adolescents in the UK. *J. Brain Injury* **17**: 105-129.

HCHEN Z.J., NEGRA X., LEVINE A., UGHRIN Y., and LEVINE J.M. (2002) Oligodendrocyte precursor cells: Reactive cells that inhibit axon growth and regeneration. *J. Neurocytol.* **31**: 481-495.

HEDREEN J.C., and KOLIATSOS. V.E. (1994) Phosphorylated neurofilaments in neuronal perikarya and dendrites in human brain following axonal damage. *J. Neuropathol. Exp. Neurol.* **53**: 663-671.

HEIDEMANN S.R., HAMBORG M.R., THOMAS S.J., SONG B., LINDLEY S., and CHU D. (1984) Spatial organization of axonal microtubules. *J. Cell Biol.* **99**: 1289-1295.

HELLAWELL D.J., TAYLOR R., and PENTLAND B. (1999) Cognitive and psychosocial outcome following moderate or severe traumatic brain injury. *Brain Injury* **13**: 489-504.

HEN X.H., MEANEY D. F., XU B.N., NONAKA M., MCINTOSH T.K., WOLF J.A., SAATMAN K.E., and SMITH D.H. (1999) Evolution of neurofilament subtype accumulation in axons following diffuse brain injury in the pig. *J. Neuropathol. Exp. Neurol.* **58**: 588-596.

HERZFELD J. (1996) Entropically-driven order in crowded solutions from liquid crystals to cell biology. *Acc. Chem. Res.* **29**: 31-37.

HICKEY WF and KIMURA H. (1988) Perivascular microglial cells are bone marrow derived and present antigen *in vivo*. *Science* **239**: 290-292.

HIROKAWA N., SHIOMURA Y., and OKABE S. (1988) Tau proteins: The molecular structure and mode of binding on microtubules. *J. Cell Biol.* **107**: 1449-1459.

HIROKAWA N. (1991) Molecular architecture and dynamics of the neuronal cytoskeleton. In *The Neuronal Cytoskeleton*. Ed. Burgoyne RD: New York, Wiley-Liss: pp 5-74.

HIROKAWA N. (1998) Kinesins and dynein superfamily proteins and the mechanism of organelle transport. *Science* **279**: 519-526.

HIROKAWA N., and REIKO T. (2004) Kinesin superfamily proteins and their various functions and dynamics. *J. Exp. Cell Res.* **301**: 50-59.

HIROKAWA N., and REIKO T. (2004) Molecular motors in neuronal development, intracellular transport and disease. *Curr. Opin. Neurobiol.* **14**: 564-573.

HIROKAWA N., and TAKEMURA R. (2005) Molecular motors and mechanisms of directional transport in neurons. *Nature Rev. Neurosci.* **6**: 201-214.

HISANAGA S., GONDA Y., INAGAKI M., IKAI A., and HIROKAWA N. (1990) Effects of phosphorylation of the neurofilament L protein on neurofilamentous structures. *Cell Regul.* **1**:237-248.

HISANAGA S., KUSUBATA M., GKUMURA E.M., and KISHIMOTO T. (1991) Phosphorylation of neurofilament H subunit at the tail domain by CDC2 kinase dissociates the association to microtubules. *J. Biol. Chem.* **226**: 21798-21803.

HOFFMAN P.N., and LASEK R.J. (1975) The slow component of axonal transport: identification of major structural polypeptides of the axon and their generality among mammalian neurons. *J. Cell Biol.* **66**: 351-366

HOFFMAN P. N., GRIFFIN J.W., and PRICE D.L. (1984) Control of axonal caliber by neurofilaments transport. *J. Cell Biol.* **99**: 705-714.

HOFFMAN P.N, LOPATA M.A., WALSON D.F., and LUDUENA R.F. (1992) Axonal transport of class 2 and class 3 beta-tubulin: evidence that the slow component wave represents the movement of only a small fraction of the tubulin in the mature motor axons. *J. Cell Biol.* **119**: 595-604.

HOFFMAN P.N., STEPHEN C., POLLOCK S.C., and STRIPH G.G. (1993) Altered gene expression after optic nerve transection: reduced neurofilament expression as a general response to axonal injury. *J. Exp. Neurol.* **119**: 32-36.

HOLLENBECK P.J. (1989) The transport and assembly of the axonal cytoskeleton. *J. Cell Biol.* **108**: 223-227.

HOLLENBECK P.J. (1993) Phosphorylation of neuronal kinesin heavy and light chains *in vivo*. *J. Neurochem.* **60**: 2265-2275.

- HONJIN R., SAKATO S., and YAMASHITA T. (1977) Electron microscopy of mouse optic nerve: a quantitative study of the total optic nerve fibres. *Arch. Histol. Jpn.* **40**: 321-332.
- HSICH S.T., CRAWFORD T.O., and GRIFFIN J.W. (1994) Neurofilament distribution and organization in the myelinated axons of peripheral nervous system. *Brain Res.* **642**: 316-326.
- HUBER G., ALAIMO-BEURET D., and MATUS A. (1985) MAP3 : characterization of a novel microtubule-associated proteins. *J. Cell Biol.* **100**: 496-507.
- HUBER G., PEHLING G., and MATUS A. (1986) The novel microtubule-associated protein MAP3 contribute to the in vitro assembly of brain microtubules. *J. Biol. Chem.* **261**: 2270-2273.
- HUH J.W., RAGHUPATHI R., LAURER H.M., HIELFAER M.A., and SAATMAN E. (2003) Transient loss of microtubules associated protein 2 immunoreactivity after moderate brain injury in mice. *J. Neurotrauma* **21**: 119-124.
- HUNT D., HOSSAIN-IBRAHIM K., MASON M.R., COFFIN R.S., LIEBERMAN A.R., WINTERBOTTOM J., and ANDERSON P.N. (2004) A TF3 upregulation in glia during Wallerian degeneration: differential expression in peripheral nerves and CNS white matter. *J. Neurosci.* **5**: 5-9.
- HURLEY R.A., MCGOWAN J.C., ARFANAKIS K., and TABBER K.H. (2004) Traumatic axonal injury: Novel insights into evolution and identification. *J. Neuropsych. Clin. Neurosci.* **16**: 1-17.
- ICHIMURA T., and ELLISMAN M.H. (1991) Three-dimensional fine structure of cytoskeletal membrane interactions at nodes of Ranvier. *J. Neurocytol.* **20**: 667-681.
- IEDE R.L., and SAMORAJSKI T. (1970) Axon caliber related to neurofilaments and microtubules in sciatic nerve fibres of rats and mice. *Anat. Rec.* **167**: 379-388.

IWATA A., STYS P.K., WOLF J.A., CHEN X-H., TAYLOR A.G., MBANEY D.F., and SMITH D.H. (2004) Traumatic axonal injury induces proteolytic cleavage of the voltage-gated sodium channels modulated by tetrodotoxin and protease inhibitors. *J. Neurosci.* **24**: 4605-4613.

JAFARI, S.S., MAXWELL W.L., NIELSON M., and GRAHAM D.I. (1997) Axonal cytoskeletal changes after non-disruptive axonal injury. *J. Neurocytol.* **26**: 207-221.

JAFARI S.S., NIELSON M., GRAHAM D.I., and MAXWELL W.L. (1998) Axonal cytoskeletal changes after non-disruptive axonal injury. II. Intermediate sized axons. *J. Neurotrauma* **15**: 955-966.

JANDER S., LAUSBERG. F., and STOOL G. (2001) Differential recruitment of CD8+ M macrophages during Wallerian degeneration in the peripheral and central nervous system. *Brain Pathol.* **11**: 27-38.

JENKINS R., TETZLAFF W., and HUNT S.P. (1993) Differential expression of immediate early genes in rubrospinal neurons following axotomy in rat. *Eur. J. Neurosci.* **5**: 203-209.

JENNETT B., ADAMS J.H., MURRAY L.S., and GRAHAM D.I. (2001) Neuropathology in vegetative and severely disabled patients after head injury. *Neurol.* **56**: 486-490.

JOB D., FISCHER E.H., and MARGOLIS R.L. (1981) Rapid disassembly of cold -stable microtubules by calmodulin. *Proc. Natl. Acad. Sci. U.S.A.* **78**: 4679-4682.

JUAN D.V. (1958) The early changes in the axoplasm during Wallerian degeneration. *J. Biophys. Biochem. Cytol.* **4**: 551-555.

JULIEN J.P., and MUSHYNSKI W.E. (1982) Multiple phosphorylation sites in mammalian neurofilament polypeptides. *J. Biol. Chem.* **257**: 10467-10470.

JUNG C., and SHEA T.B. (1999) Regulation of neurofilament axonal transport by phosphorylation in optic axons *in situ*. *J. Cell Motil. Cytoskel.* **42**: 230-240.

- KAETHER C., SKEHEL P., and DOTTI C.G. (2000) Axonal membrane proteins are transported in distinct carriers: a two-color video microscopy study in cultured hippocampal neurons. *Mol. Biol. Cell* **11**:1213-1224.
- KAMAL A., ALMENAR-QUERALT A., LeBLANCE J.F., ROBERTS E.A., and GOLDSTEIN I.S. (2001) Kinesin-mediated axonal transport of a membrane compartment containing beta-secretase and pencilin-1 requires APP. *Nature* **414**: 643-648.
- KANG J., LEMAIRE H.G., UNTERBECK A., SALBAVM J.M, MASTER C.L, GEZESCHIK K.H., MULTHAUP G., BEYREUTHER K., and MULLER-HILL B. (1987) The precursor of Alzheimer's disease amyloid A4 protein resembles a cell-surface receptor. *Nature* **325**: 733-736.
- KASSAB A., AOYAMA M, and SUGITA S. (2002) Quantitative study of the optic nerve in buffaloes. *J. Animal Sci.* **73**: 59-65.
- KATO H., KOGURE K., ARAKI T., and ITOYAMA Y. (1995) Graded expression of immunomolecules on activated microglia in the hippocampus following ischemia in a rat model of ischemic tolerance. *Brain Res.* **694**: 85-93.
- KEKKER-OHNO K., HAYASKA S., TAKAGISHI Y., ODA S., WAKASUGI N., MIKOSHIBA K., INOUE M., and YAMAMURA H. (1996) Endoplasmic reticulum is missing in dendritic spines of Purkinje cells of the ataxic mutant rat. *Brain Res.* **714**: 226-330.
- KENNEY A.M., and KOCSIS J.D. (1998) Peripheral axotomy induces long term c-jun amino-terminal kinase-1 activation and activator protein-1 binding activity by c-jun and junD in adult rat dorsal root ganglia *in vivo*. *J. Neurosci.* **18**:1318-1328.
- KETTENMAN H., ORKAND R.K., and SCHACHNER M. (1983) Coupling among identified cells in mammalian nervous system cultures. *J. Neurosci.* **3**: 506-516.

- KIDA S., STEART P.V., ZHANG E.T., and WELLER R.O. (1993) Perivascular cells act as scavengers in the cerebral perivascular spaces and remain distinct from pericytes, microglia and macrophages. *Act Neuropathol.* **85**: 646-652.
- KIMELBERG H.K., and NOREMBERG M.D. (1994) Astroglial responses in CNS trauma. In: *The neurobiology of central nervous system trauma*. Salzman KS, Faden AI, eds. New York: Oxford University Press, pp 193-208.
- KING S.J., BROWN C.L., MAIER K.C., QUINTYNE N.J., and SCHROER T.A. (2003) Analysis of the dynein-dynactin interaction in *vitro* and *vivo*. *Mol. Biol. Cell* **14**: 5089-5097.
- KING S.M. (2000) The dynein microtubule motor. *Biochem. Biophys. Acta* **1496**: 60-75.
- KINNEY H.C., and SAMUELS M.A. (1994) Neuropathology of the persistent vegetative state. A review. *J. Neuropathol. Exp. Neurol.* **53**: 548-558.
- KOBAYASHI T., TSUKITA S., and YAMAMOTO Y. (1986) Subaxolemmal cytoskeleton in squid giant axon. Biochemical analysis of microtubules, microfilaments, and their associated high-molecular weight proteins. *J. Cell Biol.* **102**:1699-1709.
- KOENIG E., KINSMAN S., REPASKY E., and SULTZ L. (1985) Rapid mobility of motile varicosities and inclusions containing α -spectrin, actin, and calmodulin in regenerating axons *in vitro*. *J. Neurosci.* **5**: 715-729.
- KOO E.H., SISODIA S.S., ARCHER D.R., MARTIN L.J. WEIDEMANN A., BEYREUTHER K., FISCHER P., MASTERS C.L., and PRICE D. (1990) Precursor of amyloid protein in Alzheimer disease undergoes fast anterograde axonal transport. *Proc. Natl. Acad. Sci. USA.* **87**: 1561-1565.

- KOSIINAGA M., and WHITTEMORE S.R. (1995) The temporal and spatial activation of microglia in fiber tracts undergoing anterograde and retrograde degeneration following spinal cord lesion. *J. Neurotrauma* **12**: 209-222.
- KREUTZBERG G.W. (1995) Reaction of the neuronal cell body to axonal damage. In: *The Axon* (Waxman SG, Kocsis DJ, Stys PK, eds) pp 355-374. New York: Oxford University Press.
- KUMAR S.M., PORTERFIELD D.M., MULLER K.J., SMITH P.J.S. and SAHLEY C.L. (2001) Nerve injury induces a rapid efflux of nitric oxide (NO), detected with a novel NO microsensor. *J. Neurosci.* **21**: 215-220.
- KUMAR S., YIN X., TRAPP B.D., PAULAITIS M.F., and HOH J.H. (2002) Role of long-range repulsive force in organizing axonal neurofilament distribution: evidence from mice deficient in myelin-associated glycoprotein. *J. Neurosci. Res.* **68**: 681-690.
- KUMAR S., YIN X., TRAPP B.D., HOH J.H., and PAULAITIS M.E. (2002) Relating interaction between neurofilament distributions through polymer brush models. *Biophys J.* **82**: 2360-2372.
- KURSULA P. (2001) The current status of structural studies on proteins of the myelin sheath (review). *Int. J. Mol. Med.* **8**: 474-479.
- LAMBERT S., DAVIS J.Q., and BENNETT V. (1997) Morphogenesis of the node of Ranvier: co-clusters of ankyrin and ankyrin-binding integral proteins define early developmental intermediates. *J. Neurosci.* **17**: 7025-7036.
- LAMPERT P.W. (1967) A comparative electron microscopic study of reactive, degenerating, and dystrophic axons. *J. Neuropathol. Exp. Neurol.* **26**: 345-368.
- LANGFORD C., and SEFTON A.J. (1992) The relative time course of axonal loss from the optic nerve of developing guinea pig is consistent with that of other mammals. *J. Vis. Neurosci.* **9**: 555-564.

- LARSEN J.O. (1998) Stereology of nerve cross sections. *J. Neurosci. Meth.* **85**: 107- 118.
- LASEK R.J., GARNER J.A., and BRADY S.T. (1984) Axonal transport of the cytoplasmic matrix. *J. Cell Biol.* **99**: 212-221.
- LAURER H.L., and MCINTOSH T.K. (1999) Experimental models of brain trauma. *Curr. Opin. Neurol.* **12**:715-721.
- LAURER H.L., LENZLINGER P.M., and McINTOSH. T.K. (2000) Models of traumatic brain injury. *Eur. J.Trauma* **26**: 95-100.
- LAURER H.L., MEANEY D.F., MARGULIES S.S., and MCINTOSH T.K. (2002) Modeling brain injury/trauma. In: *Encyclopedia of human brain.* (Ramachandran VS, cd). Academic Press/ Elsevier Science. San Diego, CA, USA.
- LAWRENCE C.J., DAWE R.K., CHRISTIE K.R., CLEVELAND D.W., DAWSON S.C., ENDOW S.A., GOLDSTEIN L.S.B., GOODSON H.V., HIROKAWA N., HOWARD J., MALMBERG R.J., McINTOSH J.R., MIKI H., MITCHISON T.J., OKADA Y., REDDY A.S.N., SAXTON W.M., SCHLIWA M., SCHOLEY J.M., VALE R.D., WALCZAK C.E., and WORDEMAN L. (2004) A standardized kinesin nomenclature. *J. Cell Biol.* **167**: 19-22.
- LAWSON J.J., PERRY V.H., and GORDON S. (1992) Turnover of the resident microglia in the normal adult mouse brain. *Neurosci.* **48**: 405-415.
- LAWSON L.J., FROST L., RISBRIDGER J., FEARN S., and PERRY V.H. (1994) Quantification of the mononuclear phagocyte response to Wallerian degeneration of the optic nerve. *J. Neurocytol.* **23**: 729-744.
- LAZAROV O., MORFINI G.A., LEE E.B., FARAH M.H., SZODORAI A., DEBOER S.R., KOLIATSOS V.E., KINS S., LEE V.M-Y., WONG P.C., PRICE D.L., BRADY S.T., and

SISODIA S. (2005) Axonal transport, amyloid precursor protein, kinesin-1, and the processing apparatus: revisited. *J. Neurosci.* **25**: 2386-2395.

LEAH J.D., HERBEGEN T., MURASHOV A., DRAGUNOW M., and BRAVO R. (1993) Expression of immediate early gene protein following axotomy and inhibition of axonal transport in the rat central nervous system. *J. Neurosci.* **57**: 53-66.

LECLERCQ P.D., STEPHENSON M.S., MURRAY L.M., McINTOSH T.K., GRAHAM D.I., and GENTLEMAN S.M. (2002) Simple morphometry of axonal swellings can not be used in isolation for dating lesions after traumatic brain injury. *J. Neurotrauma* **19**: 1183-1192.

LEVINE J., and WILLARD M. (1980) Composition and organization of axonally transported proteins in the retinal ganglion cells of the guinea pig. *Brain Res.* **194**: 137-154.

LEWIS S.A., IVANOV I.E., LEE G.H., and COWAN N.J. (1989) Organization of microtubules in dendrites and axons is determined by a short hydrophobic zipper in microtubules-associated proteins MAP2 and tau. *Nature* **342**: 498-505.

LEWIS S.B., FINNIE J.W., BLUMBERGS P.C., SCOTT G., MANAVIS J., BROWN C., REILLY P.L., JONES N.J., and McLEAN A.J. (1996) A head impact model of early axonal injury in the sheep. *J. Neurotrauma* **13**: 505-514.

LIEBERMAN A.R. (1971) The axon reaction: a review of the principal features of perikaryal responses to axonal injury. *Int. Rev. Neurobiol.* **14**: 49-124.

LIGHTHALL J.W. (1988) Controlled cortical impact: A new experimental brain injury model. *J. Neurotrauma* **5**: 1-15.

LIGHTHALL J.W., DIXON C.E., and ANDERSON T.E. (1989) Experimental models of brain injury. *J. Neurotrauma* **6**: 83-97.

- LIGHTHALL J.W., GOSHGARIAN H.G., and PINDERSKI C.R. (1990) Characterization of axonal injury produced by controlled cortical impact. *J. Neurotrauma* **7**: 65-76.
- LIGON I.A., and STEWARD O. (2000) Movement of mitochondria in the axons and dendrites of cultured hippocampal neurons. *J. Comp. Neurol.* **427**: 340-343.
- LIU Y., JACOBOWITZ D.M., barone f., MCCARRON R., SPATZ M., FEUERSTEIN G., HALLENBECK J.M., and SIREN A.L. (1994) Quantitation of perivascular monocytes and macrophages around cerebral blood vessels of hypertensive and aged rats. *J. Cereb. Blood Flow Metab.* **14**(2): 348-352.
- LORENZ T., and WILLARD M. (1978) Subcellular fractionation of intra-axonally transported polypeptides in the rabbit visual system. *Proc. Natl. Acad. Sci. USA* **75**: 505-509.
- LU J., MOOCHHALA S., KAUR C., and LING E.A. (2001) Cellular inflammatory response associated with break down of the blood-brain barrier after closed head injury in rats. *J. Neurotrauma* **18**: 399-407.
- LUBINSKA L. (1977) Early course of Wallerian degeneration in the myelinated fibers of the rat phrenic nerve. *Brain Res.* **130**: 47-63.
- LUDWIN S.K. (1990) Oligodendrocytes survival in Wallerian degeneration. *Acta Neuropathol.* **80**: 184-191.
- LUNN M.P., CRAWFORD T.O., HUGHES R.A., GRIFFIN J.W., and SHIEKH K.A., (2002) Anti-myelin-associated glycoprotein antibodies alter neurofilament spacing. *Brain* **125**: 904-911
- LYE R.J., PORTER M.E., SCHOLEY J.M., and McINTOSH J.R. (1987) Identification of a microtubule-based cytoplasmic motor in the nematode *C. elegans*. *Cell* **51**: 309-318.

- MA D., HIMES B.T., SHEA T.B., and FISCHER I. (2000) Axonal transport of microtubule-associated protein 1B (MAP1B) in the sciatic nerve of adult rat: distinct transport rates of different isoforms. *J. Neurosci.* **20**: 2112-2120.
- MACK T.G.A., REINER M., BEIROWSKI B., MI W., EMMANUELLI M., THOMAS D., GILLINGWATER T., COURT P., CONFORTI L., FERNANDO F.S., TARLTON A., ANDERSSON C., ADDICKS K., MAGNI G., RIBCHESTER R.R., PERRY V.H., and COLEMAN M.P. (2001) Wallerian degeneration of injured axons and synapses is delayed by a *Ube4b/Nmnat* chimeric gene. *Nature Neurosci.* **4**: 1199-1206.
- MANDELKOW E., and MANDELKOW E.M. (2002) Kinesin motors and disease. *Trends in Cell Biol.* **12**: 585-591.
- MANDELKOW E.M., STAMER K., VOGEL R., THIES E., and MANDELKOW E. (2003) Clogging of axons by tau, inhibition of axonal traffic and starvation of synapses. *Neurobiol. Aging* **24**: 1079-1085.
- MARK R.E. (2002) The big eye in the 21st century: The role of electron microscopy in modern diagnostic neuropathology. *J. Neuropathol. Exp. Neurol.* **61**: 1027-1039.
- MARKIN V.S., TANELIAN D.T., JERSILD R.A., and OCHS S. (1999) Biomechanics of stretch-induced beading. *Biophys. J.* **76**: 2852-2860.
- MARMAROU C.R., WALKER S.A., DAVIS C.L., POVLISHOCK J.T. (2005) Quantitative analysis of the relationship between intra-axonal microfilament compaction and impaired axonal transport following diffuse traumatic brain injury. *J. Neurotrauma* **22**: 1066-1080.
- MARQUES S.A., TAFFAREL M., and MARTINEZ M.B. (2003) Participation of neurofilament proteins in axonal dark degeneration of rat's optic nerves. *Brain Res.* **969**: 1-13.

- MARTIN S., LEVINE A.K., CHEN Z.J., UGHRIN Y., and LEVINE J.M. (2001) Deposition of the NG2 proteoglycan at nodes of Ranvier in the peripheral nervous system. *J. Neurosci.* **21**: 8119-8128.
- MARTINEZ A.J., and R. L. FRIEDE. (1970) Accumulation of axoplasmic organelles in swollen nerve fibres. *Brain Res.* **19**: 183-198.
- MATA M., KUPINA N., and FINK D.J. (1992) Phosphorylation-dependent neurofilament epitopes are reduced at node of Ranvier. *J. Neurocytol.* **21**: 199-210.
- MATTHIES H.J., MILLER R.J., and PALFREY H.C. (1993) Calmodulin binding to c-AMP-dependent phosphorylation of kinesin light chains modulate kinesin ATPase activity. *J. Biol. Chem.* **268**: 11176-11187.
- MAXWELL W.L. (1996) Histopathological changes at central nodes of Ranvier after stretch injury. *J. Micros. Res. Tech.* **34**: 522-535.
- MAXWELL W.L., and GRAHAM D.I. (1997) Loss of axonal microtubules and neurofilaments after stretch-injury to guinea pig optic nerve fibers. *J. Neurotrauma* **14**: 603-614.
- MAXWELL W.L., POVLISHOCK J.T., and GRAHAM D.I. (1997) A mechanistic analysis of nondisruptive axonal injury: A review. *J. Neurotrauma* **14**: 419-440.
- MAXWELL W.L., KANSAGRA A.M., GRAHAM D.I., ADAMS J.H., and GENNARELLI T.A. (1988) Freeze-fracture studies of reactive myelinated nerve fibres after diffuse axonal injury. *Acta Neuropathol.* **76**: 395-406.
- MAXWELL W.L., IRVINE A., STRANG R.H.C., GRAHAM D.I., ADAMS J.H., and GENNARELLI T.A. (1990) Glycogen accumulation in axons after stretch injury. *J. Neurocytol.* **19**: 235-241.

- MAXWELL W.L., IRVINE A., GRAHAM D.I., ADAMS J.H., GENNARELLI T.A., TIPPERMAN R., and STURATIS M. (1991a) Focal axonal injury: the early axonal response to stretch. *J. Neurocytol.* **20**: 157-164.
- MAXWELL W.L., IRVINE A., WATT C., GRAHAM D.I., ADAMS J.H., and GENNARELLI T.A. (1991b) The microvascular response to stretch injury in the adult guinea pig visual system. *J. Neurotrauma* **8**: 271-279.
- MAXWELL W.L., WATT C., PEDIANI J.D., GRAHAM D.I., ADAMS J.H., and GENNARELLI T.A. (1991) Localisation of calcium ions and calcium-ATPase activity within myelinated nerve fibres of the adult guinea pig optic nerve. *J. Anat.* **176**: 71-79.
- MAXWELL W.L., WATT C., GRAHAM D.I., and GENNARELLI T.A. (1993) Ultrastructural evidence of axonal shearing as a result of acceleration of the head in non-human primates. *Acta Neuropathol.* **86**: 136-144.
- MAXWELL W.L., ISLAM M.N., GRAHAM D.I., and GENNARELLI T.A. (1994) A qualitative and quantitative analysis of the response of the retinal ganglion cell soma after stretch injury to the adult guinea-pig optic nerve. *J. Neurocytol.* **23**: 379-392.
- MAXWELL W.L., McCREATH B.J., GRAHAM D.I., and GENNARELLI T.A. (1995) Cytochemical evidence for redistribution of membrane pump calcium-ATPase and ccto-Ca-ATPase activity, and calcium influx in myelinated nerve fibres of the optic nerve after stretch injury. *J. Neurocytol.* **24**: 925-942.
- MAXWELL W.L., DONNELLY S., SUN X., FENTON T., PURI N., and GRAHAM D.I. (1999) Axonal cytoskeletal response to non-disruptive axonal injury and the short-term effect of posttraumatic hypothermia. *J. Neurotrauma* **16**: 1225-1234.

- MAXWELL W.L., KOSANLAVIT R., McCREATH B.J., REID O., and GRAHAM D.I. (1999) Freeze-fracture and cytochemical evidence for structural and functional alteration in the axolemma and myelin sheath of adult guinea pig optic nerve fibers after stretch injury. *J. Neurotrauma* **16**: 237-284.
- MAXWELL W.L., DOMLEO A., McCOLL G., JAFARI S.S., and GRAHAM D.I. (2003) Post-acute alterations in the axonal cytoskeleton after traumatic axonal injury. *J. Neurotrauma* **20**: 151-168.
- MAXWELL W.L., WATSON A., QUEEN R., CONWAY B., RUSSELL D., NEILSON M., and GRAHAM D.I. (2005) Slow, medium or fast re-warming following post-traumatic hypothermia therapy. An ultrastructural perspective. *J. Neurotrauma* **24**: 873-884.
- MAXWELL W.L., MACKINNON M-A., SMITH D.H., MCINTOSH T.K., and GRAHAM D.I. (2006) Thalamic Nuclei in Blunt Head Injury Patients. *Neuropathol. Exp. Neurol.* (in press)
- McINTOSH T.K., VINK R., NOBLE L., YAMAKAMI I., SOARES H., and FADEN A.L. (1989) Traumatic brain injury in the rat: characterization of lateral fluid-percussion model. *Neurosci.* **28**: 233-244.
- McKENZIE K.J., McLELLAN D.R., GENTLEMAN S.M., MAXWELL W.L., GENNARELLI T.A., and GRAHAM D.I. (1996) Is β -APP a marker of axonal damage in short-surviving head injury?. *Acta Neuropathol.* **92**: 608-613.
- McKERRACHER L., HIRSCHMEIER A. (1992) Slow transport of the cytoskeleton after axonal injury. *J. Neurobiol.* **23**: 568-578.
- McQUARRIE I.G., BRADY S.T., and LASEK R.J. (1986) Diversity in the axonal transport of structure proteins: major differences between optic and spinal axons in the rat. *J. Neurosci.* **6**: 1593-1605.

- MEDANA I. M., and ESIRI M.M. (2003) Axonal damage: a key predictor of outcome in human CNS diseases. *Brain* **126**: 515-530.
- MEYTHALER J.M., PEDUZZI-NELSON J.D., ELEFThERIOU E., and NOVACK T.A. (2001) Current concepts: diffuse axonal injury-associated traumatic brain injury. *Arch Phys Med Rehabil.* **82**:1461-1471.
- MIKELBERG F.S., DRANCE S.M., SCHULZER M., YIDEGILIGNE H.M., and WEIS M. (1989) The normal human optic nerve axon count and axon diameter distribution. *J. Ophthalmol.* **96**: 1325-1328.
- MIKI H., SETOU M., RIKEN GER Group, GSL Members, and HIROKAWA N. (2003) Kinesin superfamily proteins (KIFs) in the mouse transcriptome. *Genome Res.* **13**: 1455-1465.
- MILLER C.C.J., ACKERLEY S., BROWNLESS J., GRIESON A.J., JACOBSEN N.J.O., and THORNHILL P. (2002) Axonal transport of neurofilaments in normal and disease states. *J. Cell Mol. Life Sci.* **59**: 323-330.
- MILLS J., and REINER P.B. (1999) Regulation of amyloid precursor protein cleavage. *J. Neurochem.* **72**: 443-460.
- MIZUNO N., TOBA S., EDAMATSU M., NISHII J.W., HIROKAWA N., TOYOSHIMA Y.Y., and KIKKAWA M. (2004) Dynein and kinesin share an overlapping microtubule-binding site. *E.M.B.O Journal* **23**: 2459-2467.
- MONACO S., GEHRMANN J., RAIVICH G., and KREUTZBERG G.W. (1992) MHC-positive, ramified macrophages in the normal and injured rat peripheral nervous system. *J. Neurocytol.* **21**: 623-634.
- MORRIS R.L., and HOLLENBECH P.J. (1993) The regulation of bidirectional mitochondrial transport is coordinated with axonal outgrowth. *J. Cell Sci.* **104**: 917-927.

- MORRIS R.L., and HOLLENBECK P.J. (1995) Axonal transport of mitochondria along microtubules and F-actin in living vertebrate neurons. *J. Cell Biol.* **131**: 1316-1326.
- MOSKOWITZ P.F., SMITH R., PICKETT J., FRANKFURTER A., and OBLINGER M.M. (1993) Expression of the class 111 beta-tubulin gene during axonal regeneration of the rat dorsal root ganglion neurons. *J. Neurosci. Res.* **34**: 129-134.
- MOUTON P.R. (2002) Principles and practices of unbiased stereology. John Hopkins University Press: Baltimore and London.
- MURESAN V. (2000) One axon, many kinesins: What's the logic? *J. Neurocytol.* **29**: 799-818.
- NAKATA T., TERADA S., and HIROKAWA N. (1998) Visualization of the dynamics of synaptic vesicle and plasma membrane proteins in living axons. *J. Cell Biol.* **140**: 659-674.
- NAKAYAMA Y., AOKI Y., and NITSU H. (2001) Studies on the mechanisms responsible for the formation of focal swelling on neuronal processes using a novel in vitro model of axonal injury. *J. Neurotrauma* **18**: 545-554.
- NAKAZAWA E., and ISHIKAWA H. (1995) Occurrence of fasciculated microtubules at nodes of Ranvier in rat spinal roots. *J. Neurocytol.* **24**: 399-407.
- NARCISO M.S., HOKOC J.N., and MARTINEZ A.M. (2001) Watery and dark axons in Wallerian degeneration of the opossum's optic nerve: different patterns of cytoskeletal breakdown. *J. Acad. Bras Cienc.* **73**: 569-575.
- NEARY J.T., KANG Y., BU Y., YU E., AKONG K., and PETERS C.M. (1999) Mitogenic signaling by ATP/PY2 purinergic receptors in astrocytes: involvement of a calcium-independent protein kinase C, extracellular signal-regulated protein kinase pathway distinct from the phosphatidylinositol-specific phospholipase C/calcium pathway. *J. Neurosci.* **19**: 4211-4220.

- NESS J.K., VALENTINO M., McIVER S.R., and GOLDBERG M.P. (2005) Identification of oligodendrocytes in experimental disease models. *Glia* **50**: 321-328.
- NEWMAN E. A. (1986) High potassium conductance in astrocyte endfeet. *Science* **233**, 453-454.
- NISS C., GRAUEL U., TOENNES S.W., and BRATZKE H. (2002) Incidence of axonal injury in human brain tissue. *Acta Neuropathol.* **104**: 79-84.
- NISHIDA E., and SAKAI H. (1977) Calcium sensitivity of the microtubule reassembly system: Difference between crude brain extracts and purified microtubule proteins. *J. Biochem. (Tokyo)* **82**: 303-306.
- NISHIDA E., MAEKAWA S., and SAKAI H. (1984) Characterization of the action of procine brain profiling on actin polymerization. *J. Biochem.* **94**: 399-404.
- NIXON R.A. (1991) Axonal transport of cytoskeletal proteins. In *The Neuronal Cytoskeleton*. Ed. Burgoyne RD New York, Wiley-Liss, pp 257-282.
- NIXON R.A., PASKEVICH P.A., SIHAG P.K., and THAYER C.Y. (1994) Phosphorylation on a carboxy-terminus domains of neurofilament proteins in retinal ganglion cell neurons *in vivo* influences on regional neurofilament accumulation, interneurofilament spacing, and axon caliber. *J. Cell Biol.* **126**: 1031-1046.
- NORENBERG M.D. (1994) Astrocyte responses to CNS injury. *J. Neuropathol. Exp. Neurol.* **53**: 213-220.
- OKONKWO D.O., and POVLISHOCK J.T. (1999) An intrathecal bolus of cyclosporine A before injury preserves mitochondrial integrity and attenuates axonal disruption in traumatic brain injury. *J. Cereb. Blood Flow Metab.* **19**: 443-451.

- OKONKWO D.O., MELON D.E., PELLICANE A.J., RUBIN L.K., STONE J.R., and GREGORY A. (2003) Dose-response of cyclosporine A in attenuating traumatic axonal injury in rat. *Neuro. Report* **14**: 463-466.
- OLMSTED J.B., and BORISY G.G. (1975) Ionic and nucleotide requirements for microtubule polymerization *in vitro*. *Biochem.* **14**: 2996-3005.
- ORKAND R. K., NICHOLLS J. G. and KUFFLER S. W. (1966) Effect of nerve impulses on the membrane potential of glial cells in the central nervous system of amphibian. *J. Neurophysiol.* **29**: 788-806.
- OTSUKA N., TOMONAGA M., and IKEDA K. (1991) Rapid appearance of β -amyloid precursor protein immunoreactivity in damaged axons and reactive glial cells in rat brain following needle stab injury. *J. Brain Res.* **568**: 335-338.
- PAPASOZOMENOS S.C., and BINDER L.I. (1987) Phosphorylation determines two distinct species of tau in the central nervous system. *Cell Motil. Cytoskel.* **8**: 210-226.
- PARYSEK L.M., DEL CERRO M., and OLMSTED J.B. (1985) Microtubule-associated protein 4 antibody; A new marker for astroglia and oligodendroglia. *Neuroscience* **15**: 869-875.
- PASCHAL B.M., SHPETNER H.S., and VALLEE R.B. (1987) MAP1C is a microtubule-activated ATPase which translocates microtubules *in vitro* and has dynein-like properties. *J. Cell Biol.* **105**: 1273-1282.
- PEERLESS S.J., and REWCASTLE N.B. (1967) Shear injuries of the brain. *J. Can. Med. Assoc.* **96**: 577-582.
- PERKFRIS R., and TERRIAN D.M. (1997) Brain myosin V is a synaptic vesicle-associated motor protein: evidence for a Ca^{2+} -dependent interaction with the synaptobresin synaptophysin complex. *J. Cell Biol.* **137**: 1589-1601.

- PERRIN F.E., LACROIX S., AVILES T., and DAVID S. (2005) Involvement of monocyte chemo-attractant protein-1, macrophage inflammatory protein-1 α and interleukin β in Wallerian degeneration. *Brain* **128**: 854-866.
- PETTUS E.H., CHRISTMAN C.W., GIEBEL M.L., and POVLISHOCK J.T. (1994) Traumatically induced altered membrane permeability: Its relationship to traumatically induced reactive axonal change. *J. Neurotrauma* **11**: 507-522.
- PETTUS E.H., and POVLISHOCK J.T. (1996) Characterization of a distinct set of intra-axonal ultrastructural changes associated with traumatically induced alteration in axolemma permeability. *Brain Res.* **722**: 1-11.
- PIERCE J.E.S., TROJANOWSKI J.Q., GRAHAM D.I., SMITH D.H., and McINTOSH T.K. (1996) Immunohistochemical characterization of alteration of amyloid precursor proteins and β -amyloid peptide after experimental brain injury in the rat. *J. Neurosci.* **16**: 1083-1090.
- PINCUS P. (1991) Colloid stabilization with grafted polyelectrolytes. *Macromolecules* **24**: 2912-2919.
- POSMANTUR R., HAYES R.L., DIXON C.E., and TAFT W.C. (1994) Neurofilament 68 and Neurofilament 200 protein levels decrease after traumatic brain injury. *J. Neurotrauma* **11**: 533-545.
- POVLISHOCK J.T. (1986) Traumatically induced axonal damage without concomitant change in focally related neuronal somata and dendrites. *Acta Neuropathol.* **70**: 53-59.
- POVLISHOCK J.T. (2000) Pathophysiology of neural injury: therapeutic opportunities and challenges. *Clin. Neurosurg.* **46**: 113-126.
- POVLISHOCK J.T. (1992) Traumatically induced axonal injury: pathogenesis and pathobiological implications. *Brain Pathol.* **2**: 1-12.

- POVLISHOCK J. T., And CHRISTMAN C.W. (1995) The pathobiology of traumatically induced axonal injury in animals and humans: A review of current thoughts. *J. Neurotrauma* **12**: 555-564.
- POVLISHOCK J.T., and PETTUS E.H. (1996) Traumatically induced axonal damage: evidence for enduring changes in axolemmal permeability with associated cytoskeletal change. *Acta Neurochir Suppl.* **66**: 81-86.
- POVLISHOCK J.T., BECKER D.P., and CHENG C.L.Y. (1983) Axonal change in minor head injury. *J. Neuropathol. Exp. Neurol.* **42** : 225-242.
- POVLISHOCK J. T., HAYES R.L., MICHEL M.F., and McINTOSH T.K. (1994) Workshop on animal models of traumatic brain injury. *J. Neurotrauma* **11**: 723-732.
- POVLISHOCK J.T., MARMAROU A., McINTOSH T., TROJANOWSKI J.Q., and MOROI J. (1997) Impact acceleration injury in the rat: Evidence for focal axolemmal and related neurofilament sidearm alteration. *J. Neuropathol. Exp. Neurol.* **56**: 347-359.
- POVLISHOCK J.T., BUKI A., KOIZIUMI H., STONE J., and OKONKWO D.O. (1999) Initiating mechanisms involved in the pathobiology of traumatically induced axonal injury and interventions targeted at blunting their progression. *Acta Neurochir. Suppl.* **73**: 15-20.
- PRAHLAD V., HELFAND B.T., LANGFORD G.M., VALE R.D., and GOLDMAN R.D. (2000) Fast transport of neurofilaments protein along microtubules in squid axoplasm. *J. Cell Sci.* **113**: 3939-3946.
- PRICE P.L., PAGGI P., LASEK R.J., and KATZ. M.J. (1988) Neurofilaments are spaced randomly in the radial dimension of axons. *J.Neurocytol.* **17**: 55-62.

- RABCHEVSKY A.G., WEINIT J.M., COULPIER M., FAGES C., TINEL M., and JUNIER M.P. (1998) A role for transforming growth factor alpha as an inducer of astrogliosis. *J. Neurosci.* **18**: 10541-10552.
- RAGHUPATHI R., GRAHAM D.I., and McINTOSH T.K. (2000) Apoptosis after traumatic brain injury. *J. Neurotrauma* **17**: 927-938.
- RANSOM B., BEHAR T., and NEDERGAARD M. (2003) New roles for astrocytes. *Trends in Neurosci.* **26**: 520-530.
- RAPP B.D., ANDREWS S.B., WONG A., O'CONNELL M., and GRIFFIN J.W. (1989) Co-localization of the myelin-associated glycoprotein and the microfilament components, F-actin and spectrin, in Schwann cells of myelinated nerve fibres. *J. Neurocytol.* **18**: 47-60.
- RASH J.E., YASUMURA T., SUE HUDSON C., AGRE P., AND NIELSEN S. (1998) Direct immunogold labeling of aquaporin-4 in square arrays of astrocyte and ependymocyte plasma membranes in rat brain and spinal cord. *Proc. Natl. Acad. Sci. USA.* **95**, 11981-11986
- REICHARD R.R., WHITE III C.L., HLADIK C.L., and DOOLINAK D. (2003) Beta- amyloid precursor protein staining of non-accidental central nervous system injury in pediatric autopsies. *J. Neurotrauma* **20**: 347-355.
- REICHARD R.R., SMITH C., and GRAHAM D.I. (2005) The significance of β -APP immunoreactivity in forensic practice. *J. Neuropathol. Applied Neurobiol.* **31**: 304-331.
- RIEDE R.L. (1972) Control of myelin formation by axon caliber (with a model of the control mechanism). *J. Comp. Neurol.* **144**: 233-252.
- RELES A., and FRIEDE R.L. (1991) Axonal cytoskeleton at the nodes of Ranvier. *J. Neurocytol.* **20**: 450-458.

ROBERTS-LEWIS J.M., SAVAGE M.J., MARCH V.R., PINSKER L.R., and SIMAN R. (1994) Immunolocalization of calpain 1-mediated spectrin degradation to vulnerable neurons in the ischemic gerbil brain. *J. Neurosci.* **14**: 3934-3944.

ROBINSON S.R., HORSBURGH G.M., DREHER B., and McCALL M.J. (1987) Changes in the numbers of retinal ganglion cells and optic nerve axons in the developing albino rabbit. *Brain Res.* **432**: 161-174.

RODRIGUEZ-PAEZ A.C., BRUNSCHWIG J.P., and BRAMLETT H.M. (2005) Light and electron microscopic assessment of progressive atrophy following moderate traumatic brain injury in the rat. *Acta Neuropathol.* **109**: 603-616.

ROY S., COFFE P., SMITH G., LIEM R.K., BRADY S.T., and BLACK M.M. (2000) NF is transported rapidly but intermittently in axons: implications for slow axonal transport. *J. Neurosci.* **20**: 6849-6861.

SAATMAN K.E., BOZYCZKO-COYNE D., MARCY V., SIMAN R., and McINTOSH T.K. (1996) Prolonged calpain-mediated spectrin break down occurs regionally following experimental brain injury in the rat. *J. Neuropath. Exp. Neurol.* **55**: 850-860.

SAATMAN K.E., GRAHAM D.I., and McINTOSH T.K. (1998) The neuronal cytoskeleton is at risk after mild and moderate brain injury. *J. Neurotrauma* **15**: 1047-1058.

SAATMAN K.E., ABAI B., GROSVENOR A., VORWERK C.K., SMITH D.II., and MEANY D.F. (2003) Traumatic axonal injury results in biphasic calpain activation and retrograde transport impairment in mice. *J. Cereb. Blood Flow Metab.* **23**: 34-42.

SATO-YOSHITAKE R., SHIOMURA Y., MIYASAKA H., and HIROKAWA N. (1989) Microtubule-associated protein 1 β : molecular structure, localization, and phosphorylation dependent expression in developing neurons. *Neuron* **3**: 229-238.

- SANCHEZ L., HASSINGER L., PASKEVICH P.A., SHINE H.D., and NIXON R.A. (1996) Oligodendroglia regulate the regional expression of axon caliber and local accumulation of neurofilaments during development independently of myelin formation. *J. Neurosci.* **16**: 5095-6005.
- SANCHEZ R.M., DUNKELBERGER G.R., and QUIGLEY H.A. (1986) The number and diameter distribution of axons in the monkey optic nerve. *J. Invest. Ophthalmic. Vis. Sci.* **27**: 1342-1350.
- SANTAMBROGIO L., BELYANSKAYA S.L., FISCHER F.R., CIPRIANI B., BROSNAN C.F. RICCIARDI-CASTAGNOLI P, STERN L.J., STROMINGER J.L. and RIESE R. (2001) Developmental plasticity of CNS microglia. *Proc. Natl. Acad. Sci. USA* **98**: 6295-6300.
- SELLERS J.R. (2000) Myosin : a diverse superfamily. *Biochem. Biophys. Acta.* **1496**: 3-22.
- SERVADEI F., TEASDALE G.M., and MERRY G. (2001) Defining acute mild head injury in adults: A Proposal based on prognostic factors, diagnosis, and management. *J. Neurotrauma* **18**: 657-664.
- SHAH J.V., FLANAGAN L.A., JANMEY P.A., and LETERRIER J.F. (2000) Bidirectional translocation of neurofilaments along microtubules mediated in part by dynein/dynactin. *Mol. Biol. Cell* **11**: 3495-3508.
- SHARPE R., MAXWELL W., and GRAHAM D. (1996) Glial responses to optic nerve stretch injury: initial results. *Neuropathol. Appl. Neurol.* **22**, 451.
- SHAW G. (1991) Neurofilament proteins. In *The Neuronal Cytoskeleton*. Ed. Burgoyne RD, New York, Wiley-Liss, pp 185-214.
- SHEA T.B. (2000) Microtubule motors, phosphorylation and axonal transport of neurofilaments. *J. Neurocytol.* **29**: 873-887.

SHEN Z.L., LASSNER F., BADER A., BECKER M., WALTER G.F., and BERGER A. (2000) Cellular activity of resident macrophages during Wallerian degeneration. *J. Microsurg.* **20**: 255-261.

SHERRIFF F.E., BRIDGES L.R., GENTLEMAN S.M., SIVALOGANATHAN S., and WILSON S. (1994) Marker of axonal injury in post mortem human brain. *Acta Neuropathol.* **88**: 433-439.

SHI S.R., COTE R.J., and TAYLOR C.R. (1997) Antigen retrieval immunohistochemistry: past, present, and future. *J. Histochem. Cytochem.* **45**: 327-343.

SHIOMURA Y., and HIROKAWA N. (1987) The molecular structure of microtubule-associated protein 1A (MAP1A) *in vivo* and *in vitro*. An immunoelectron microscopy and quick-freeze, deep-etch study. *J. Neurosci.* **7**: 1461-1469.

SIMON J. R., GRAFF R.D., and MANESS P.F. (1998) Microtubule dynamics in a cytosolic extract of fetal rat brain. *J. Neurocytol.* **28**: 671-683.

SIMS T.J., WAXMAN S.G., and GILMORE S.A (1984) Specificity in central myelin: evidence for local regulation of myelin thickness. *Brain Res.* **292**: 179-185.

SINGLETON R.H., and POVLISHOCK J.T. (2004) Identification and characterization of heterogeneous neuron injury and death in regions of diffuse brain injury: evidence for multiple independent injury phenotype. *J. Neurosci.* **24**: 3543-3553.

SINGLETON R.H., ZHU J., STONE J.R., and POVLISHOCK J.T. (2002) Traumatically induced axotomy adjacent to the soma does not result in acute neuronal death. *J. Neurosci.* **22**: 791-802.

SMITH C. (2005). The neuropathology of head injury. *ACNR* **5**: 22-24.

SMITH C.B., CRANE A.M., KADEKARO M., AGRNOFF B.W., and SOLOKOFF L. (1984) Stimulation of protein synthesis and glucose utilization in the hypoglossal nucleus induced by axotomy. *J. Neurosci.* **4**: 2489-2496.

SMITH D.H. and MEANEY D.F. (2000) Axonal damage in traumatic brain injury. *Neuroscientist* **6**: 483-495.

SMITH D.H., CHEN X-H., MONAKA M., TROJANOWSKI J.Q., LEE V.M-Y., SATMANN K.E., LEONI M.J., XU B.N., WOLF J.A., and MEANEY D.F. (1999) Accumulation of amyloid β and tau and the formation of neurofilament inclusions following diffuse brain injury in the pig. *J. Neuropathol. Exp. Neurol.* **58**: 982-992.

SMITH D.H., NONAKA M., MILLER R., LEONI M., CHEN X-H., ALSOP D., and MEANEY D.F. (2000) Immediate coma following inertial brain injury dependent on axonal damage in the brainstem. *J. Neurosurg.* **93**: 315-322.

SMITH D.H., CHEN X-H., IWATA A., and GRAHAM D.I. (2003) Amyloid β accumulation in axons after traumatic brain injury in humans. *J. Neurosurg.* **98**: 1072-1077.

SMITH D.H., MEANEY D.F., and SHULL W.H. (2003) Diffuse axonal injury in head trauma. *J. Head Trauma Rehabil.* **18**: 307-316.

STALHAMMAR D. (1986) Experimental model of head injury. *Acta Neurochir Supp (Wien)*. **36**: 33-46.

STENCE N., WAITE M., and DAILY M.E. (2001) Dynamics of microglial activation: a confocal analysis in hippocampal slices. *Glia* **33**: 256-266.

STERNBERG J.A., and STERNBERG N.H. (1983) Monoclonal antibodies distinguish phosphorylated and nonphosphorylated forms of neurofilaments *in situ*. *Proc. Acad. Sci. USA.* **80**: 6126-6130.

STERNBERGER N.H., QUARLES R.H., ITOYAMA Y., and WEBSTER H.F. (1979) Myelin-associated glycoprotein demonstrated immunocytochemically in myelin and myelin-forming cells of developing rats. *Proc. Natl. Acad. USA* **76**: 1510-1514.

STOLL G., TRAPP B.D., and GRIFFIN G.W. (1989) Macrophage function during wallerian degeneration of rat optic nerve; clearance of degenerating myelin and Ia expression. *J. Neurosci.* **9**: 2327-2335.

STOLL G., SCHROETER M., JANDER S., SIEBERT H., WOLLRATH A., KLEINSCHNITZ C., and BRÜCK W. (2004) Lesion-associated expression of transforming growth factor-beta-2 in the rat nervous system: Evidence for down-regulating the phagocytic activity of microglia and macrophages. *Brain Pathol.* **14**: 51-58.

STONE J.R., and CAMPION J.E. (1978) Estimate of the number of myelinated axons in the cat's optic nerve. *J. Comp. Neurol.* **15**: 799-806.

STONE J.R., WALKER S.M., and POVLISHOCK J.T. (1999) The visualization of a new class of traumatically injured axons through the use of a modified method of microwave antigen retrieval. *Acta Neuropathol.* **97**: 335-345.

STONE J.R., SINGLETON R.H., and POVLISHOCK J.T. (2000) Antibodies to the C-terminus of the β -amyloid precursor protein (APP): a site-specific marker for the detection of traumatic axonal injury. *Brain Res.* **871**: 288-302.

STONE J.R., SINGLETON R.H., and POVLISHOCK J.T. (2001) Intra-axonal neurofilament compaction does not evoke local axonal swelling in all traumatically injured axons. *J. Exp. Neurol.* **172**: 320-331.

STONE J.R., OKONKWO D.O., SINGLETON R.H., MUTLU L.K., HELM G.A., and POVLISHOCK J.T. (2002) Caspase-3- mediated cleavage of amyloid precursor protein and formation of amyloid β peptide in traumatic axonal injury. *J. Neurotrauma* **19**: 601-614.

STONE J.R., OKONKWO D.O., DIALO A.O., RUBIN D.G., MUTLU L.K., POVLISHOCK J.T., and HELM G.A. (2004) Impaired axonal transport and altered axolemmal permeability occur in distinct population of damaged axons following traumatic brain injury. *J. Exp. Neurol.* **190**: 59-69.

STRICH S.J. (1956) Diffuse degeneration of cerebral white matter and severe dementia following head injury. *J. Neurol. Neurosurg. Psychiatry.* **19**:163-185.

STRICH S.J. (1961) Shearing of nerve fibres as a cause of brain damage due to head injury: A pathological study of twenty cases. *Lancet* **2**: 443-448.

STREIT W.J. and GRAEBER MB (1993) Heterogeneity of microglial and perivascular cell populations: insights gained from the facial nucleus paradigm. *Glia* **7**: 68-74

STREIT W.J., GRAEBER M.B., KREUTZBERG G.W. (1988) Functional plasticity of microglia : a review. *Glia* **1**: 301-307.

STREIT W.J., MRAK R.E., and GRIFFIN W.S. (2004) Microglia and neuroinflammation: a pathological perspective. *J. Neuroinflammation.* **1**: 14-17.

SUGIMOTO T., FUKUDA Y., and WAKAKUWA K. (1984) Quantitative analysis of a cross-sectional area of the optic nerve and comparison between albino and pigmented rats. *Exp. Brain Res.* **54**: 266-274.

SUSALKA S.J., and PFISTER K.E. (2000) Cytoplasmic dynein subunit heterogeneity: Implications for axonal transport. *J. Neurocytol.* **29**: 819-829.

- SVENSSON M., and AIDSKOGIUS H. (1992) Evidence for activation of the complement cascade in the hypoglossal nucleus following peripheral nerve injury. *J. Neuroimmunol.* **40**: 99-109.
- TABB J.S., MLNEAUX B.J., COHEN D.L., KUZNETSOV S.A., and LANGFORD G.M. (1998) Transport of ER vesicles on actin filament neurons by myosin V. *J. Cell Sci.* **111**: 3221-3234.
- TAKAGISHI Y., ODA S., HAYASAKA S., KEKKER-OHNO K., SHIKATA T., and INOUE M. (1996) The dilute-lethal(d(1)) gene attacks a ca^{2+} store in the dendritic spine of purkinje cells in mice. *Neurosci. Lett.* **215**: 169-172.
- TEASDALE G.M., and JENNET B. (1974) Assessment of coma and impaired consciousness. *Lancet* **2**: 81-84.
- TEASDALE G.M., MAAS A., IANNOTTI F., OHMAN J., and UNTERBER G.A. (1999) Challenges in translating the efficacy of neuroprotective agents in experimental models into knowledge of clinical benefits in head injured patients. *J. Acta Neurochir. Supp.* **73**: 111-116.
- THOMALLA G., GLAUCHE V., WEILLER C., and ROTHER J. (2005) Time course of Wallerian degeneration after ischemic stroke revealed by diffuse tensor imaging. *J. Neurol. Neurosurg. Psychiatry* **76**: 266-268.
- THOMPSON H.J., LIFSHITZ J., MARKLUND N., GRADY M.S., GRAHAM D.I., HOVDA D.A., and McINTOSH T.K. (2005) Lateral fluid percussion brain injury: A 15-year review and evaluation. *J. Neurotrauma* **22**: 42-75.
- THURMAN D.J., ALVERSON C.A., and DUNN K.A. (1999) Traumatic brain injury in United States: a public health perspective. *J. Head Trauma Rehabil.* **14**: 602-615.

- TOMEI G., SPAGNOLI D., DUCATI A., LANDI A., VILLANI R., FUMAGALLI G., and GENNARELLI T. (1990) Morphology and neurophysiology of focal axonal injury experimentally induced in the guinea pig optic nerve. *Acta Neuropathol.* **80**: 506-513.
- TOMLINSON B.E. (1970) Brain-stem lesions after head injury. *J. Clin. Pathol. Supp* **4**: 154-165.
- TRAPP B.D, ANDREWS S.B., WONG A., O'CONNELL M., and GRIFFIN J.W. (1989) Co-localization of the myelin-associated glycoprotein and the microfilament components, F-actin and spectrin, in Schwann cells of myelinated nerve fibres. *J. Neurocytol.* **18**: 47-60.
- TUKER R.P., BINDER L.I., VIREECKC., HEMMING S B.A., and MATUS A.I.(1998) The sequential appearance of low and high-molecular-weight forms of MAP2 in the developing cerebellum. *J.Neurosci.* **8**: 4503-4534.
- TYNAN S.H., GEE M.A., and VALLEE R.B. (2000) Distinct but overlapping sites within the cytoplasmic dynein heavy chain for dimerization and for intermediate chain and light intermediate chain binding. *J. Biol. Chem.* **275**: 32769-32774.
- VALE R.D., REESE T.S., and SHEETS M.P. (1985) Identification of a novel force-generating protein, kinesin, involved in microtubule-based motility. *Cell* **42**: 39-50.
- VALE R.D. (2003) The molecular motor toolbox for intercellular transport. *Cell* **112**: 467-480.
- VALLEE R.B., WALL J.S., PASCHAL B.M., and SHPETNER H.S. (1988) Microtubule-associated protein 1C from brain is two-headed cytosolic dynein. *Nature* **332**: 561-563.
- VERNOS I., VAUGHAN K.T., and GELFAND V.I. (2003) Dynactin is required for bidirectional organelle transport. *J. Cell Biol.* **160**: 297-301.
- VIAL J.D. (1958) The early changes in the axoplasm during Wallerian degeneration. *J. Biophysic. Biochem. Cytol.* **4**: 551-555.

VIANCOUR T.A., and KREITER N.A. (1993) Vesicular fast axonal transport rates in young and old rat axons. *Brain Res.* **628**: 209-217.

VINSON M., RAUSCH O., MAYCOX P.R., PRINJHA R.K., CHAPMAN D., MORROW R., HARPER A.J., DINGWALL C., WALSH F.S., BURBIDGE S.A., and RIDDELL D.R. (2003) Lipid rafts mediate the interaction between myelin-associated glycoprotein (MAG) on myelin and MAG-receptors on neurons. *Mol. Cell Neurosci.* **22**: 344-352.

WAGNER O.I., LIFSHITZ J., JANMEY P.A., LINDEN M., McINTOSH T.K., and LETERRIER L.F. (2003) Mechanisms of mitochondria- neurofilament interactions. *J. Neurosci.* **23**: 9046-9058.

WAINWRIGHT N.J., and McLEAN J. (1997) Axonal injury in falls. *J. Neurotrauma* **14**: 699-713.

WALLER A. (1850) Experiments on the section of glossopharyngeal and hypoglossal nerves of the frog and observations of the alternatives produced thereby in the structure of their primitive fibres. *Phil. Trans R. Soc. Lond.* **140** : 423-429.

WANG L., and BROWN A. (2001) Rapid intermittent movement of axonal neurofilaments observed by fluorescence photobleaching. *Mol. Biol. Cell* **12**: 3257-3267.

WANG L., and BROWN A. (2002) Rapid movement of microtubules in axons. *Curr. Biol.* **12**:1496-1501.

WANG L., HO C-L, SUN D., LIEM R.K.H., and BROWN A. (2000) Rapid movement of axonal neurofilaments interrupted by prolonged pauses. *Nature Cell Biol.* **2**: 137-141.

WANG M.S., WU Y., CULVER D.G., and GLASS J.D. (2000) Pathogenesis of axonal degeneration: Parallels between Wallerian degeneration and vincristine neuropathy. *J. Neuropathol. Exp. Neurol.* **59**: 599-606.

- WARDEN P., BAMBER N.L., HUAYING L., ESPOSITO A., AHMAD K.A., CHUNG H.Y., and XIAO M.X. (2001) Delayed glial cell death following Wallerian degeneration in white matter tracts after spinal cord dorsal column cordotomy in adult rats. *Exp. Neurology* **168**: 213-224.
- WATSON D. (1991) Regional variation in the abundance of axonal cytoskeletal proteins. *J. Neurosci. Res.* **30**: 226-231.
- WEGNER J.E., and MANNER P.J. (1976) *The Biology of the Guinea Pig*. Academic Press: New York.
- WEINBERGER R., SCHEVZOV G., JEFFREY P., GORDON K., HILL M., and GUNNING P. (1996) The molecular composition of neuronal microfilaments is spatially and temporally regulated. *J. Neurosci.* **16**: 238-252.
- WEISENBERG R.C. (1972) Microtubule formation in *vitro* in solutions containing low calcium concentrations. *Science* **117**: 1104-1105.
- WEISS D.G., LANGFORD G.M., SEITZ-TUTTER D., and MAIL W. (1991) Analysis of the gliding fishtailing and circling motions of native microtubules. *Acta Histochem. Suppl.* **41**: 81-105.
- WEN H., NAGELIUS E.A., AMIRY-MOGHADDAM M., AGRE P., OTTERSEN O.P. and NIELSEN S. (1999) Ontogeny of water transport in rat brain: postnatal expression of the aquaporin-4 water channel. *Eur. J. Neurosci.* **11**: 935
- WEST M.J. (1999) Stereological methods for estimating the total number of neurons and synapses: issues of precision and bias. *Trends in Neurosci.* **22**: 51-61.
- WILLIAMS R.W., and RAKIC P. (1988) Three-dimensional counting: an accurate and direct method to estimate numbers of cells in sectioned material. *J. Comp. Neurol.* **278**: 344-352.

- WILSON S., RAGHUPATHI R., SAATMAN E., MACKINNON M., McINTOSH T.K., and GRAHAM D.I. (2004) Continued in situ DNA fragmentation of microglia/ macrophages in white matter weeks and months after traumatic brain injury. *J. Neurotrauma* **21**: 239-250.
- WIRTHS O., MULTHAUP G., and BAYER T.A. (2004) A modified β -amyloid hypothesis: intraneuronal accumulation of the β -amyloid peptide – the first step of a fatal cascade. *J. Neurochem.* **91**: 513-520.
- WONG P.C., MARSZALEK J., CRAWFORD T.O., XU Z., HSICH S.T., GRIFFIN J.W., and CLEVELAND D.W. (1995) Increasing neurofilament subunit NF-M expression reduces axonal NF-H, inhibits radial growth, and results in neurofilamentous accumulation in motor neurons. *J. Cell Biol.* **130**: 1314-1322.
- XU Z., LIU W.S., and WILLARD M.B. (1992) Identification of six phosphorylation sites in the COOH-terminal tail region of the rat neurofilament protein. *M. J. Biol. Chem.* **267**: 4467-4471.
- XU Z., MARSZALEK J.R., LEE M.K., WONG P.C., FOLMER J., CRAWFORD T.O., HSIEH S.T., GRIFFIN J.W., and CLEVELAND D.W. (1996) Subunit composition of neurofilaments specifies axonal diameter. *J. Cell Biol.* **133**: 1061-1069.
- YANG Y., GERVAIS S.L., MOREST D.K., SOLIMENA M., and RASBAND M.N. (2004) β 1V spectrins are essential for membrane stability and the molecular organization of nodes of Ranvier. *J. Neurosci.* **24**: 7230-7240.
- YIN H.I., ALBRECHT J., and FATTOUM A. (1981) Identification of gelsolin, a ca^{+} -dependent regulatory protein of actin gelsol transformation. Its intercellular distribution in a variety of cells and tissue. *J. Cell Biol.* **91**: 901-906.

YIN X., CRAWFORD T.O., GRIFFIN J.W., TU P.H., LEE V.M.Y., LI C.M., RODER J., and TRAPP B.O. (1998) Myelin-associated glycoprotein is a myelin signal that modulates the caliber of myelinated axons. *J. Neurosci.* **18**: 1953-1962.

ZIMMERMAN R.A., LARISSA T., BILANIUK L.T., and GENNARELLI T.A. (1978) Computed tomography of shearing injuries of the cerebral white matter. *J. Radiology* **127**: 393-396.

APPENDIX
CHAPTER SEVEN
TABLES OF THE RAW DATA FOR
RESULTS OF EXPERIMENTS

Table 7. Raw data for the total cross sectional area (μm^2) of optic nerves of control, 1 week (n=3), 2 weeks (n=3) and three weeks (n=3) survival animals. (R. = right optic nerve; L. = left optic nerve).

Survival	RON	Mean diameter μm	Radius μm	R., Cross sectional area μm^2	L., Cross sectional area μm^2
Control	1	725	362.5	412991	412991
	2	650	332.5	347462.49	302028
	3	700	350	384999.99	306919.64
1 Week	1	700	350	384999.99	386428.57
	2	650	332.5	347462.49	385000
	3	700	350	384999	348999
2weeks	1	700	350	385000	306919
	2	650	325	331964	259776
	3	700	350	385000	282857
3 weeks	1	600	300	282857	331964
	2	650	325	331964	331964
	3	650	325	331964	306919

TABLES 8 - 11, 12-15, 16-19, 20-23 Raw data for the Number of Intact Axons within 0.5 μm wide bins for Controls (Tables 8-11), 1 week (Tables 11-14), 2 week (Tables 15-18) and 3 week (Tables 19-22) survival animals.

Table 8. Sham-control, animal one

Section	0-0.5 μm	0.51-1 μm	1-1.5 μm	1.51-2 μm	2-2.5 μm	2.51-3 μm	>3 μm	Total
1	8	76	83	98	41	9	3	318
2	6	69	109	114	25	6	0	329
3	18	85	96	103	20	16	3	341
4	15	97	77	96	24	8	2	319
5	2	105	81	101	34	5	0	328
6	11	97	61	97	12	15	5	298
7	14	127	100	112	23	6	2	384
8	12	106	88	108	56	15	3	388
9	6	102	94	97	43	15	3	360
10	11	110	96	114	27	5	0	363
Total, number in the sample	103	974	885	1040	305	100	21	3428
%	3.004	28.413	25.816	30.338	8.897	2.917	0.612	3.12
Total estimated number	3294	31145	28300	33255	9753	3197	672	109616

Estimated number of axons:

Total number of axons in the sample = 3428

Real magnification = 2400

Size of the area sampled = 12915.37 μm^2 .

Total transverse sectional area = 412991.06 μm^2 .

Estimated number of axons = $(412991.06 \div 12915.37) \times 3428 = 109616$ axons

Table 9. Sham-control, animal two

Section	0-0.5 μ m	0.51-1 μ m	1-1.5 μ m	1.51-2 μ	2-2.5 μ m	2.51-3 μ m	>3 μ m	Total
1	8	57	93	85	72	13	2	330
2	10	90	90	87	77	4	4	362
3	6	93	93	102	46	33	3	376
4	2	61	98	106	77	2	0	346
5	3	91	100	98	59	2	0	353
6	3	93	83	102	66	1	0	348
7	2	100	110	75	52	0	4	343
8	3	80	102	90	61	3	2	341
Total number in the sample	37	665	769	745	510	58	15	2799
%	1.3219	23.76	27.47	26.61	18.22	2.07	0.54	2.97
Total estimated number	1244	22365	25857	25053	17150	1950	507	94126

Total cross-sectional area = 347462.495762 μ m².

Total sample size = 10332.3 μ m².

Total number of axons in the sample = 2799

Total estimated number of axons in = (347462.49 + 10332.3) \times 2799

= 94126 axons

Table 10. Sham-Control, animal three

micrograph	0- 0.5 μ m	0.51- 1 μ m	1.1- 1.5 μ m	1.51- 2 μ m	2.1- 2.5 μ m	2.51- 3 μ m	>3 μ m	Total
1	8	84	86	79	64	6	0	327
2	9	60	93	86	61	2	3	314
3	7	85	86	76	50	2	0	306
4	7	66	94	65	62	2	0	296
5	3	82	82	90	77	1	0	335
6	6	52	70	73	71	5	1	278
7	3	60	93	86	53	1	4	300
8	6	80	101	89	64	1	2	343
9	5	75	70	88	65	1	1	305
10	7	80	81	89	68	0	0	325
Total number in the sample	61	724	856	821	635	21	11	3129
%	1.94	23.138	27.35	26.23	20.29	0.67	0.35	3.35
Total estimated number	1818	21582	25517	24473	18929	626	328	93273

Total cross sectional area = 384999 μ m².

Sample size = 12915.375 μ m².

Total number of axons in the sample = 3129

Estimated number of axons in this animal = (384999 \div 12915.375) \times 3129

= 93273

Table 11. The mean estimated number(n = 3), total (\pm SEM) and subgroups of intact axons in sham-controls

Sub-group	0-0.5 μ m	0.51-1.0 μ m	1.1-1.5 μ m	1.51-2.0 μ m	2.1-2.5 μ m	2.51-3.0 μ m	>3 μ m	Total
Animal one	3294	31145	28300	33255	9753	3197	672	109616
Animal two	1244	22365	25857	25053	17150	1950	507	94126
Animal three	1818	21582	25517	24473	18929	626	328	93273
Total Estimated	6356	75092	79674	82781	45832	5773	1507	297015
Mean estimated number of axons	2118 \pm 863.49	25031 \pm 4335.28	26558 \pm 1239.57	27594 \pm 4010.16	15277 \pm 3973.23	1924 \pm 1049.76	503 \pm 140.47	99005 \pm 7511.2
%	2.1392	25.28	26.82	27.87	15.43	1.94	0.5	

Table 12. One week survival, animal one

micrograph	0-0.5 μ m	0.51-1.0 μ m	1.1-1.5 μ m	1.51-2.0 μ m	2.1-2.5 μ m	2.51-3.0 μ m	>3 μ m	Total
1	4	71	84	79	8	11	1	258
2	2	65	58	80	18	8	2	233
3	3	76	60	77	19	12	0	247
4	2	89	69	70	12	11	0	253
5	1	77	75	73	40	23	1	290
6	4	75	86	60	16	13	1	255
7	2	59	79	69	24	21	2	256
8	2	60	78	52	29	16	1	238
9	5	69	87	65	28	10	0	264
10	3	88	71	62	29	9	0	262
Total axon in the sample	28	729	747	687	223	134	8	2556
%	1.09	28.52	29.22	26.87	8.72	5.24	0.31	3.35
Total estimated number	835	21729	22265	20477	6647	3994	238	76185

Total number of axons in the sample = 2556

Sample size = 12916.66

Cross-sectional area = 385000 μ m²

Total estimated axons in the area = (385000+12916.66) \times 2556
= 76185

Table 13. One week survival, animal two

Micrograph	0-0.5 μm	0.51-1 μm	1.1-1.5 μm	1.51-2 μm	2.1-2.5 μm	2.51-3 μm	>3 μm	Total
1	6	68	78	84	40	6	0	282
2	6	78	63	94	61	8	1	311
3	3	64	80	55	44	4	0	250
4	3	57	75	77	41	2	0	255
5	0	74	61	78	44	2	0	259
6	0	85	80	71	43	4	1	284
7	3	70	62	77	53	7	0	272
8	2	82	81	65	28	2	1	261
9	0	88	86	69	50	3	0	296
10	2	77	68	67	40	0	0	254
Total number of axons in the sample	25	743	734	737	444	38	3	2724
%	0.91	27.27	26.94	27.05	16.29	1.39	0.11	3.72
Total estimated axons	673	19988	19746	19827	11945	1023	81	73283

Total number of axons in the sample area = 2724

Size of the sample area = 12915.375 μm^2 .

Total cross section area = 347462.495 μm^2 .

Estimated number of axons = (347462.495 ÷ 12915.375

= 73283

Table 14. One week survival, animal three.

micrograph	0-0.5 μ m	0.51-1 μ m	1.1-1.5 μ m	1.51-2 μ m	2.1-2.5 μ m	2.51-3 μ m	>3 μ m	Total
1	10	45	70	80	35	5	0	245
2	09	55	65	85	60	9	1	284
3	08	39	73	50	45	2	0	217
4	05	57	68	75	50	3	0	258
5	03	49	55	80	35	4	0	226
6	08	59	83	72	38	6	0	266
7	12	61	63	75	50	5	0	266
8	19	40	75	66	31	4	1	236
9	11	49	80	65	45	3	2	255
10	12	57	72	70	46	6	1	264
Total number in the sample	97	511	704	718	435	47	6	2518
%	3.8	20.3	27.9	28.5	17.2	1.86	0.2	
Total estimated number	2892	15232	20986	21403	12967	1401	179	75060

Total estimated number of axons in the sample = 2518

Area of the sample = 12915.37 μ m²

Cross section area = 385000 μ m²

Total estimated number of axons = (835000+12915.37) \times 2518
=75060

Table 15. One week survival: Mean estimated number (n = 3), total (\pm SEM) and subgroups of intact axons

	0-0.5 μ m	0.51-1 μ m	1.1-1.5 μ m	1.51-2 μ m	2.1-2.5 μ m	2.51-3 μ m	>3 μ m	Total
Animal one	835	21729	22265	20477	6647	3994	238	76185
Animal two	673	19988	19746	19827	11945	1023	81	73283
Animal three	2892	15232	20986	21403	12967	1401	179	75060
Total estimated	4400	56949	85262	52707	31559	6814	501	224528
Mean estimated number of axons	1466.7 \pm 1010.0	18983 \pm 2745.93	20999 \pm 1028.4	20569 \pm 646.67	10522.67 \pm 2771.53	2139 \pm 1320.49	167 \pm 64.75	74845.7 \pm 1194.6
%	1.96	25.36	28.05	27.48	14	2.8	0.22	

Table 16. Two weeks survival, animal one

micrograph	0- .5 μ m	.51- 1 μ m	1- 1.5 μ m	1.51- 2 μ m	2- 2.5 μ m	2.51- 3 μ m	>3 μ m	Total no of axons
1	2	34	58	63	40	0	0	197
2	0	58	78	50	13	0	0	199
3	0	61	69	51	43	0	0	224
4	0	40	36	35	50	25	0	186
5	3	68	69	44	49	2	0	235
6	0	60	56	49	35	4	0	204
7	0	63	54	86	42	2	0	247
8	2	63	84	70	36	2	0	257
9	0	40	50	55	48	2	0	195
10	0	41	49	34	30	1	0	155
Total number in the sample	7	528	603	537	386	38	0	2099
%	0.33	25.15	28.72	25.58	18.38	1.81	0	3.35
Total estimated number	209	15739	17970	16008	11506	1133	0	62569

Total number of axons in the sample = 2099

Sample size = 12915.375 μ m².

Total cross section area = 385000 μ m².

Total estimated number of axons = (385000 ÷ 12915.375) × 2099

= 62569

Table 17. Two weeks survival, animal two

Micrograph	0- 0.5 μm	0.51- 1 μm	1- 1.5 μm	1.51- 2 μm	2- 2.5 μm	2.51- 3 μm	>3 μm	Total
1	0	63	79	76	58	0	0	276
2	2	73	61	85	65	0	0	286
3	0	65	68	61	60	3	0	257
4	2	74	67	73	49	0	0	265
5	0	65	64	73	40	4	0	246
6	2	89	64	61	57	0	0	273
7	0	50	62	46	70	2	0	230
8	0	60	68	60	48	0	0	236
Total number in the sample	6	539	533	535	447	9	0	2069
%	0.28	26.05	25.76	25.85	21.6	0.43	0	3.11
Total estimated number of axons	193	17317	17125	17189	14361	289	0	66474

Total number of axons in the sample = 2069

Sample size = 10332.3 μm^2 .

Total cross section area = 331964 μm^2 .

Total estimated number of axons = $(331964 \div 10332.3) \times 2069$

= 66474

Table 18. Two weeks survival, animal three

micrograph	0-0.5 μ m	0.51-1 μ m	1-1.5 μ m	1.51-2 μ m	2-2.5 μ m	2.51-3 μ m	>3 μ m	Total
1	2	70	105	69	57	0	0	303
2	0	62	58	72	34	0	0	226
3	0	56	70	32	42	0	0	200
4	0	62	46	71	27	0	0	206
5	0	34	52	59	20	0	0	165
6	0	46	68	77	49	0	0	240
7	1	52	78	87	51	1	0	270
8	3	69	105	69	57	0	0	303
Total number in the sample	6	451	582	536	337	1	0	1913
%	0.31	23.57	30.42	28.01	17.61	0.05	0	2.68
Total estimated number	224	16805	21686	19972	12557	37	0	71281

Total number of axons in the sample = 1913

Size of the sampled area = 10332.3 μ m².

Total cross section area = 385000 μ m².

Total estimated number of axons = (385000 + 10332.3) \times 1913

= 71281

Table 19. Two weeks survival (n =3): Mean estimated number, total (\pm SEM) and subgroups or bins of intact axons

	0-0.5 μ m	0.51-1 μ m	1.1-1.5 μ m	1.51-2 μ m	2.1-2.5 μ m	2.51-3 μ m	>3 μ m	Total
Animal one	209	15739	17970	16008	11605	1133	0	62569
Animal two	193	17317	17125	17189	14361	289	0	66474
Animal three	224	16805	21686	19972	12557	37	0	71281
Total	626	49861	56781	53169	38523	1459	0	200324
Mean estimated	208.67 \pm 12.65	16620 \pm 657.31	18927 \pm 1981.17	17723 \pm 1661.76	12841 \pm 1142.91	486 \pm 468.69	0	66774 \pm 3563.0
%	0.3	24.88	28.34	26.54	19.23	0.72	0	

Table 20. Three weeks survival, animal one

micrograph	0-0.5 μm	0.51-1 μm	1.1-1.5 μm	1.51-2 μm	2.1-2.5 μm	2.51-3 μm	>3 μm	Total
1	0	93	59	61	30	0	0	243
2	0	73	80	63	42	0	0	258
3	2	75	81	60	28	2	0	248
4	0	80	50	52	33	6	0	221
5	0	82	75	68	61	35	0	321
6	0	32	50	50	40	6	0	178
7	0	75	80	58	52	3	0	268
8	0	86	47	53	41	10	0	237
Total number in the sample	2	596	522	465	327	62	0	1974
%	0.1	30.1	26.44	23.55	16.56	3.1	0	3.58
Total estimated number	56	16638	14572	12980	9129	1731	0	55106

Total number of axons in the sample = 1974

Sample size = 10132.3 μm^2 .

Total cross sectional area = 282857.14 μm^2 .

Total estimated number of axons = (282857.14 + 10132.3) \times 1974

= 55106

Table 21. Three weeks survival, animal two

micrograph	0-0.5 μm	0.51-1 μm	1.1-1.5 μm	1.51-2 μm	2.1-2.5 μm	2.51-3 μm	>3 μm	Total
1	0	39	41	69	35	5	0	189
2	0	44	65	33	4	0	0	146
3	0	55	48	49	14	0	0	166
4	2	68	76	50	20	8	0	224
5	0	91	52	35	18	0	0	196
6	1	72	54	60	44	9	0	240
7	0	62	80	78	36	0	0	256
8	0	52	50	46	40	12	0	200
Total estimated	3	483	466	420	211	34	0	1617
%	0.18	29.87	28.8	25.97	13.04	2.1	0	3.05
Total estimated number	99	15824	15267	13761	6913	1113	0	52977

Total number of axons in the sample = 1617

Sample area = 10132.3 μm^2 .

Total cross sectional area = 331964 μm^2 .

Total estimated number of axons = (331964 ÷ 10132.3) × 1617

= 52977

Table 22. Three weeks survival, animal three

micrograph	0-0.5 μ m	0.51-1 μ m	1.1-1.5 μ m	1.51-2 μ m	2.1-2.5 μ m	2.51-3 μ m	>3 μ m	Total
1	0	83	117	57	35	0	0	292
2	2	73	50	13	11	0	0	149
3	0	64	47	53	22	0	0	186
4	0	61	64	50	30	3	0	208
5	0	60	75	70	50	10	0	265
6	0	58	63	50	35	5	0	211
7	0	61	90	30	30	15	0	226
8	3	94	77	60	30	0	0	264
Total number in the sample	5	554	583	383	243	33	0	1801
%	0.27	30.76	32.37	21.26	13.49	1.83	0	
Total estimated number axons	160	18151	19101	12549	7962	1081	0	59006

Total number of axons in the sample =1801

Sample size = 10132.3 μ m².

Total cross-sectional area =331964 μ m².

Total estimated number of axons = (331964 ÷10132.3) ×1801

= 59006

Table 23. Three weeks survival (n = 3): Mean estimated number, total (\pm SEM) and subgroups or bins of intact axons

	0-.5 μ m	0.51-1 μ m	1.1-1.5 μ m	1.51-2 μ m	2.1-2.5 μ m	2.51-3 μ m	>3 μ m	Total
Animal one	56	16638	14572	12980	9129	1731	0	55106
Animal two	99	15824	15267	13761	6913	1113	0	52977
Animal three	160	18151	19101	12549	7962	1081	0	59006
Total	315	50613	48940	39290	24004	3925	0	167089
Mean estimated	105 \pm 42.66	16872 \pm 964.17	16313.3 \pm 1991.49	13096.6 \pm 501.62	8001.3 \pm 905.1	1308.3 \pm 299.15	0	55696.3 \pm 2496.5
%	0.18	30.29	29.28	23.51	14.36	2.34	0	

Table 24. The mean estimated (n = 3), total and sub-groups in sham-control and one week, two weeks, and three weeks survivals.

Survival	0-0.5 μ m	0.51-1 μ m	1.1-1.5 μ m	1.51-2 μ m	2.1-2.5 μ m	2.51-3 μ m	>3 μ m	Total
Control	2118	25031	26558	27594	15277	1924	503	99005
%								
One week	754	20859	21005	20152	9296	2509	159	74734
%	1.0	27.91		26.96	12.43	3.35	0.21	
Two weeks	208	16620	18927	17723	12841	486	0	66774
%	0.3	24.88	28.34	26.54	19.23	0.72	0	
Three weeks	105	16872	16312	13096	8001	1308	0	55696
%	0.18	30.29	29.28	23.51	14.36	2.34	0	

Table 25. Number of axons (injured and intact) in each sample

Section	1	2	3	4	5	6	7	8	9	10	Total axons in the sample
W1 A1	322	303	299	310	293	311	293	330	316	340	3117
A2	344	392	400	394	319	332	390	350	309	438	3289
A3	343	319	299	334	290	298	297	292	284	376	3132
W2 A1	266	304	251	346	259	293	282	319	338	/	2658
A2	307	319	321	363	301	322	361	349	/	/	2643
A3	300	320	290	340	305	304	310	332	/	/	2480
W3 A1	350	345	355	331	346	325	337	325	/	/	2714
A2	400	400	269	300	304	310	300	303	/	/	2586
A3	386	260	318	242	345	240	325	350	/	/	2466

Table 26. Total estimated number of axons (normal + injured) (n = 3) at one, two and three weeks survivals.

Survival	Total in sample (N+I)	Sample area μm^2	Cross-sectional area μm^2	Total estimated (Normal+I)	Total estimated normal	Total estimated injured
W1 A1	3117	12916.66	385000	92906	76185	16721
A2	3289	12915.375	347452.49	91171	73283	17888
A3	3132	12915.37	385000	93363	75060	18303
W2 A1	2658	12915.375	385000	85500	62569	22931
A2	2643	10332.3	331964	84816	66474	18342
A3	2480	10332.3	385000	91291	71281	20010
W3 A1	2715	10132.3	282857.14	75765	55106	20659
A2	2586	10132.3	331964	84724	52977	31747
A3	2466	10132.3	331964	80793	59006	21787

Table 27. Estimated mean cross-sectional area of the number of axons within 0.5 μm wide bins in each experimental group. Each value is the total cross-sectional area in μm^2

Sub-group	0.0-0.5 μm	0.51-1.0 μm	1.01-1.5 μm	1.51-2.0 μm	2.01-2.5 μm	2.51-3.0 μm	>3.01 μm	Total	% of whole nerve
Control	149.77	9636.7	35264.6	66396.8	63496.6	11432.1	4046.9	190423.6	49.8
1 Week	103.7	8389.6	27883.2	49493.3	43733.1	12709.6	1343.6	143656.2	37.6
2 Weeks	14.7	7345.3	25131.9	42645.2	53371.7	2887.7	0	131396.6	34.4
3 Weeks	7.4	7456.7	21661.3	31513.1	33256.2	7773.7	0	101668.5	26.6